JANUARY 2021 M.Sc. in Textile Engineering NİMET KÖLEOĞLU

REPUBLIC OF TURKEY

GAZIANTEP UNIVERSITY

GRADUATE SCHOOL OF NATURAL & APPLIED SCIENCES

INVESTIGATION OF THE EFFECT OF COLOUR MASTERBATCH ADDITION ON THE PHYSICAL, MECHANICAL AND THERMAL PROPERTIES OF RECYCLED POLYETHYLENE TEREPTHALATE FIBERS

M.Sc. THESIS

IN

TEXTILE ENGINEERING

BY

NİMET KÖLEOĞLU

JANUARY 2021

INVESTIGATION OF THE EFFECT OF COLOUR MASTERBATCH ADDITION ON THE PHYSICAL, MECHANICAL AND THERMAL PROPERTIES OF RECYCLED POLYETHYLENE TEREPTHALATE FIBERS

M.Sc. Thesis

in

Textile Engineering

Gaziantep University

Supervisor

Assoc. Prof. Dr. Mehmet DAŞDEMİR

by

Nimet KÖLEOĞLU

January 2021

I hereby declare that all information in this document has been obtained and presented in accordance with academic rules and ethical conduct. I also declare that, as required by these rules and conduct, I have fully cited and referenced all material and results that are not original to this work.

Nimet KÖLEOĞLU

ABSTRACT

INVESTIGATION OF THE EFFECT OF COLOUR MASTERBATCH ADDITION ON THE PHYSICAL, MECHANICAL AND THERMAL PROPERTIES OF RECYCLED POLYETHYLENE TEREPTHALATE FIBERS

KÖLEOĞLU, Nimet
M.Sc. in Textile Engineering
Supervisor: Assoc. Prof. Dr. Mehmet DAŞDEMİR
January 2021
92 pages

Polyethylene terephthalate (PET) is a recyclable thermoplastic polymer. However, after several recycling processes of PET, degraded PET (*d*-PET) waste is formed. In order to utilize this *d*-PET waste and discover new useful form for it, the formation of by-products from *d*-PET waste was studied. In this regard, thermal, molecular, structural and chemical analyzes of *d*-PET were initially compared with virgin fiber grade PET, recycled PET (r-PET) flake, and r-PET granules. In order to obtain new useful carbonized materials and chemicals from *d*-PET, carbonization was carried out and optimum processing parameters were determined. As a result, the carbonization material yield of over 20% and the chemical yield of over 17% were achieved from the carbonization of *d*-PET. With using different milling speeds and time particle sizes of the carbonized material were reduced to nanometer scale and recycled carbon powders (r-CPs) were obtained. Fully recycled colour masterbatch (frc-MB) composites were also formed by using this r-CPs in different ratios. Lastly, fully recycled and coloured PET (frc-PET) filaments and fibers were formed with using varying amounts of frc-MB. Physical, mechanical and morphological properties of frc-PET fibers were investigated. Fully recycled products of frc-MB and frc-PET fibers were successfully developed from the *d*-PET waste.

Key Words: Polyethylene Terephthalate, Fiber and Polymer, Waste, Recycling, Masterbatch

ÖZET

RENKLİ BOYA MASTERBATCHİ EKLENTİSİNİN GERİ DÖNÜŞÜM POLİETİLEN TEREFTALAT ELYAFININ FİZİKSEL, MEKANİKSEL VE TERMAL ÖZELLİKLERİNE ETKİSİNİN İNCELENMESİ

KÖLEOĞLU, Nimet
Yüksek Lisans Tezi, Tekstil Mühendisliği
Danışman: Doç. Dr. Mehmet DAŞDEMİR
Ocak 2021
92 Sayfa

Polietilen tereftalat (PET), geri dönüştürülebilir bir termoplastik polimerdir. PET'in birçok kere geri dönüştürülmesiyle, yapısı bozulmuş PET (*d*-PET) atıkları açığa çıkar. Bu atıkları kullanmak ve yeni faydalı formlarını keşfetmek için, *d*-PET atıklarından elde edilebilecek yeni yan ürünlerin oluşumu incelenmiştir. Bunun için öncelikle *d*-PET'in termal, moleküler, yapısal ve kimyasal analizleri başlangıçta virjin PET, geri dönüştürülmüş PET (r-PET) flake ve r-PET granüllerinin özellikleri ile karşılaştırılmıştır. *d*-PET atığından yeni, faydalı karbonize malzemeler ve kimyasallar elde etmek için karbonizasyon pprosesi gerçekleştirilmiş ve optimum proses parametreleri belirlenmiştir. Sonuç olarak, *d*-PET atığının karbonizasyonundan %20'nin üzerinde karbonlaşmış malzeme ve %17'nin üzerinde kimyasal elde edilmiştir. Farklı öğütme hızları ve süresiyle karbonize malzemenin partikül boyutları nanometre ölçeğine indirgenmiş ve geri dönüştürülmüş karbon tozları (r-CP'ler) elde edilmiştir. Tamamen geri dönüştürülmüş renkli masterbatch (frc-MB) kompozitler, bu r-CP'lerin farklı oranlarda eklenmesiyle oluşturulmuştur. Son olarak, farklı miktarlarda frc-MB kullanılarak tamamen geri dönüştürülmüş ve renkli PET (frc-PET) elyaf ve filamentler oluşturulmuştur. frc-PET elyafının fiziksel, mekanik ve morfolojik özellikleri araştırılmıştır. Sonuçta, *d*-PET atıklarından tamamen geri dönüştürülmüş frc-MB ve frc-PET elyafı başarıyla geliştirilmiştir.

Anahtar Kelimeler: Polietilen Tereftalat, Elyaf ve Polimer, Atık, Geri Dönüşüm, Masterbatch

"Dedicated to my teachers and my family"

ACKNOWLEDGEMENTS

I would first like to thank my thesis advisor Assoc. Prof. Dr. Mehmet DAŞDEMİR. He has always guided my studies, did not withhold information, suggestions, and assistance at every stage of my research, and contributed to my growth and development with his vast ideas not only in professional terms but also in human relations. He consistently allowed this paper to be my own work but steered me in the right direction whenever he thought I needed it. Assoc. Prof. Dr. DAŞDEMİR convincingly guided and encouraged me to be professional and do the right thing even when the road got tough.

I am grateful to Assoc. Prof. Dr. Hatice Kübra KAYNAK and Assoc. Prof. Dr. Tuba GÜRKAYNAK ALTINÇEKİÇ for all their support and helpful recommendations.

I am most sincerely thankful to my mother, Sevgi KÖLEOĞLU, my father, Fatih KÖLEOĞLU for they believe me and of course to my brothers Mustafa KÖLEOĞLU and Sait KÖLEOĞLU for their helps. Also, I would like to thank you my sister Süheyla ÖZER ÇİFTÇİ for listening and guiding me my whole life.

I am sincerely thankful to my friends especially Özge BERK, Mücahit BAYTEKİN, and Muhammed YILDIZ for listening, offering me advice, and supporting me through this entire process. Also I would like to my colleague Eyüp Ali SATIL for his friendship and patience.

I would like to thank GAMA Recycle Elyaf ve İplik San. A.Ş. for its financial and infrastructural supports in this study.

This study was supported by the Scientific and Technological Research Council of Turkey (TÜBİTAK-TEYDEB-3181005). Therefore, I would like to thank TUBITAK for providing financial support to this study.

TABLE OF CONTENTS

Page

LIST OF TABLES

Page

LIST OF FIGURES

Page

LIST OF ABBREVIATIONS

ABS	Acrylonitrile Butadiene Styrene
Ar	Argon
CO_2	Carbondioxide
DC*	Saturation
DE*	Total Colour Daviations
DH*	Colour Hue Differences
DL*	Lightness
DMT	Dimethylenephthalate
***d*-PET**	Degraded Polyethylene Terephtalate Waste
DSC	Differential Scanning Calorimetry
ED-XRF	Energy Dispersive - X-Ray Spectroscopy
ED-XRF	Energy Dispersive X-Ray Fluorescence Spectrometer
FRCF	Fully Recycled Coloured Filaments
RMB	Fully Recycled Coloured Masterbatch
FTIR	Fourier Transform Infrared Spectroscopy
GC-MS	Gas Chromatography - Mass Spectrometry
HDPE	High Density Polyethylene
He	Helium
IV	Intrinsic Viscosity
LDPE	Low Density Polyethylene
MEG	Mono Ethylene Glycol
M_W	Molecular Weight
N_2	Nitrogen
NaOH	Sodium Hydroxide
O_2	Oxygen
PA's	Polyamides
PC	Polycarbonate
PET	Polyethylene Terephthalate

PP	Polypropylene
PS	Polystyrene
PTA	Terephthalic Acid
PVC	Polyvinyl Chloride
r-PET Flake	Recycled Polyethylene Terephtalate Bottles and Packaging Waste
r-PET granules	Recycled Polyethylene Terephtalate Textile Waste
SEM-EDX	Scanning Electron Microscopy Energy Dispersive X-ray Spectroscopy
T_g	Glass Transition Point
TGA	Thermogravimetric analysis
T_{mi}	Initial Melting Temperature
T_{mf}	Final Melting Temperature
T_{mp}	Melting Pick Temperature

CHAPTER I

INTRODUCTION

1.1 Introduction

Plastic materials have become indispensable in our daily life. Especially, its use is increasing day by day in the textile and packaging industries. The most preferred plastic in these sectors is polyethylene terephthalate (PET) polymer (Niksiar et al., 2015; Malik et al., 2017; Lee et al., 2017; Frida, 2018). A serious increase has been observed in the production and in the use of PET in recent years. When the increase is so high, the waste rate of this material in the environment also increases in terms of volume. If the plastic waste is not recycled, it can be subjected to land-filled or incinerated. This leads to air pollution, soil pollution and health problems (Chattopadhyay et al., 2015). Fortunately, polyethylene terephthalate polymer is an easily recyclable material. The thermoplastic property of PET waste is used to remelting the PET waste and transform it into new products (Frida, 2018). The recycled PET can then be recycled again. However, during the recycling of PET wastes, they are exposed to high heat treatments several times. A certain part of this PET polymer, which is subjected to high heat treatments, loses its usefull polymeric properties and it is degraded. The degraded PET polymer wastes are returned to the environment as waste, since they cannot be recycled and have no other uses.

Pyrolysis is the process of thermal degradation of the polymer. Plastic materials can be converted into usefull products by the pyrolysis process. In the pyrolysis process, long chain polymers transform with heat into smaller, less complex molecules. In this way, it can be divided into different products and the products obtained can be used as raw materials in other sectors. Three main products emerge during pyrolysis: oil, gas and carbonized material (Niksiar et al., 2015; Anuar Sharuddin et al., 2016).

Pyrolysis is a method commonly used for recycling waste polymeric materials. However, it is generally used in thermal recycling of long-chain polymers (Anuar Sharuddin et al., 2016). There are no studies on recycling of short chain length PET (degraded PET), which is the waste of waste. This study investigates the possibility of forming new recycled composite materials by using the carbonized material obtained by degraded PET. Also, this study focuses on obtaining fully recycled PET filaments and fibers including new recycled composite masterbatch. Thus, degraded polymeric materials, which are the waste of waste, can be recycled and reused without land-filling the earth or harming the environment.

1.2 Objective of the Study

In this study, it is aimed to recycle and reuse the degraded PET polymer, which is the waste of waste, to obtain carbon powders in nano or micron sizes from the degraded PET, to form recycled masterbatch composites from these carbon powders, to produce fully recycled coloured PET filaments including different ratios of this recycled composite colour masterbatch, and to investigate the effect of recycled colour masterbatch addition on the physical, mechanical and thermal properties of the recycled PET fibers.

1.3 Structure of the Thesis

Chapter 1 introduces background, aims and significance of this study. Chapter 2 presents the literature review about the study. This chapter discusses the details of solid wastes, plastics, PET polymer, the recycling methods of PET polymer, the degraded PET polymer, the pyrolysis method, and the factors affecting the pyrolysis. Chapter 3 focuses on a challenging and a novel study which is about obtaining carbon powder and by-products from the degraded PET waste. Chapter 4 includes the study of forming fully recycled and coloured PET filaments and investigating the effect of recycled colour masterbatch addition on the physical and mechanical properties of the recycled PET fibers. Finally, the conclusions of this study are given in Chapter 5.

CHAPTER 2

LITERATURE REVIEW

2.1 Solid Waste

The global adverse impacts of solid waste are increasing sharply day by day. The most important parameters affecting this situation are innovations in economic and developments in technology. With these developments, the amounts of municipal and industrial solid wastes have increased a lot. Solid wastes are generally classified according to their sources as residential (e.g., plastics, paper, textile, leather, household dangerous wastes, e-wastes), industrial (e.g., housekeeping wastes, packaging, food wastes, construction and demolition materials), commercial (e.g., paper, cardboard, plastics, wood, food wastes, glass, metals), institutional (e.g., plastics, wood, food wastes, glass, metals, special wastes, hazardous wastes, e-wastes), construction and demolition (e.g., wood, steel, concrete, dirt), process (e.g., industrial process wastes, scrap materials, off-specification products, slag), medical (e.g., infection wastes, dangerous wastes, pharmaceutical waste), agricultural (e.g., spoiled food wastes, hazardous wastes such as pesticides), and municipal (e.g., street sweepings; landscape and tree trimmings) (Hoornweg et al., 2012).

The main problem is the collecting of solid waste. In the most of countries solid waste is collected irregularly. Solid waste management must be regulated in order to solve this problem. The first step is to collect the wastes from the source in the right way. The solid waste is collected in some countries with several ways such as house-to-house, with community bins, curbside pick-up, self delivered, contracted or delegated services. The main issue to be considered here is that the waste is not separated at its source. Because, the degree of source separation not only influences the total amount of material recycled and also affects the quality of secondary materials (Hoornweg et al., 2012).

Types of waste compositions are paper, plastic, metal, glass, wood, special wastes, organic wastes and others (e.g., disposable diapers, textiles, carpets) (Thurston County Waste Composition Study 2008 – 2009). Organic wastes (food and green) have the largest waste category with 44% waste rate. Recyclable wastes (e.g., plastic, paper and cardboard, metal, and glass) are following the organic wastes with 38% waste rate (Figure 2.1) (Kaza, et al., 2018).

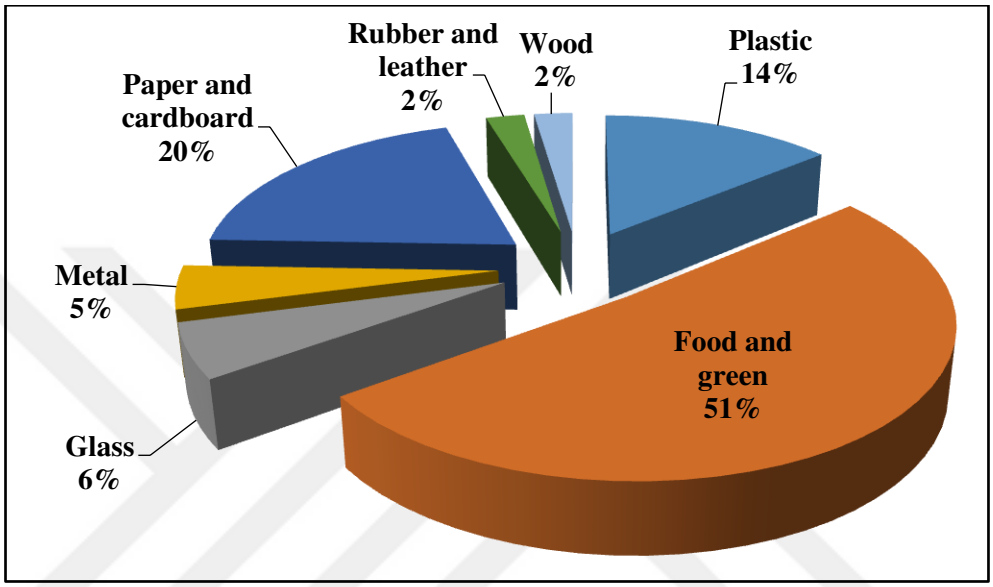

Figure 2.1 Global waste composition (Kaza, et al., 2018)

Composting, incineration, controlled landfill, landfill (unspecified), sanitary landfill (with landfill gas collection), open dump, recycling are the way of waste disposal. The most preferred method among these is open dump. However, the most significant way of waste disposal is recycling. Recyclable wastes which have waste rate percentage of 38%, can participate in the recycling cycle with different types of recycling methods (Hoornweg et al. 2012; Kaza, Silpa, et al., 2018).

2.2 Plastics

The first industrial production and usage of synthetic polymers (plastic) took place in in the firt part of 1900s (Al-Salem et al., 2009; Brydson, 1999). A significant increase in the use of plastics has been observed since these years. Plastics have number of usage areas such as construction, electrical and electronic applications, packaging, textiles, transport, medical appliances in our daily lifes. The increase in usage areas directly affects the consumption of the plastics. Unfortunately, plastics do not disappear on its own at short-term in nature and this situation causes some

environmental issues. It is important that plastics are non-renewable raw materials. The products that we obtain from non-renewable raw materials are commonly used in short-lived products (Pivnenko et al., 2016). These problems can be solved by recycling. By this way, these plastics can be turned into usable new products again.

Plastics are basically divided into two groups which are thermoplastics and thermosets (Al-Sabagh et al., 2016; Aydin, 2004). Thermoplastics comprise to the total plastic consumption by 80% (Al-Salem et al., 2009). Some of the most produced and consumed thermoplastics are polyethylene terephthalate (PET), high density polyethylene (HDPE), low density polyethylene (LDPE), polyvinyl chloride (PVC), polypropylene (PP), polystyrene (PS), polyamides (PAs), acrylonitrile butadiene styrene (ABS), and polycarbonate (PC) (Eyerer, 2010).

2.3 Polyethylene Terephthalate (PET)

Compounds formed by an acid and an alcohol are called esters. PET is a long chain polymer that is generally formed by polycondensation of an alcohol and a carboxylic acid (Mangut et al., 2008; Tortora et al., 1997). Alcohol and acids used in the polymerization of PET are ethylene glycol and terephtalic acid or dimethyl ester, respectively (Tortora et al., 1997; Al-Sabagh et al., 2016). The chemical structure of PET polymer can be seen in Figure 2.2.

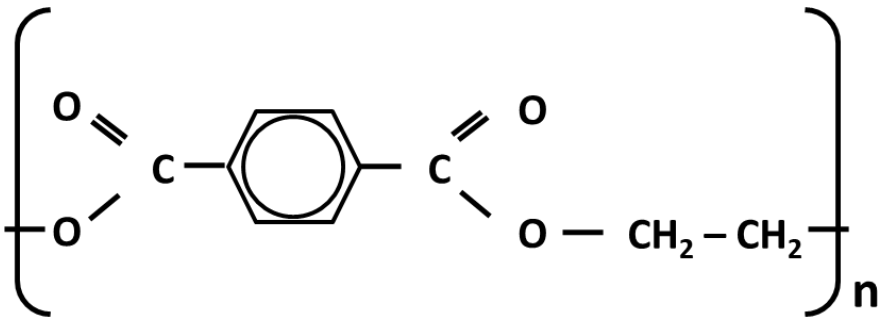

Figure 2.2 Chemical structure of PET

Depending on the chemical compounds used in the polymerization, PET can be formed with two different ways. When ethylene glycol and dimethyl teraftalate are used as starting materials, these two materials are placed in a boiler and are started to be heated in which ester exchange takes place (at 210 °C) and methyl alcohol is collected with coolant. After the materials are heated up to 270-280 °C with a

catalyst, they are allowed to react for several hours. Finally, the PET polymer forms into light coloured macromolecules. They are then cooled and converted into strips or rods. They are typically cut into 4x4 mm chips and are dried (Mangut et al., 2008). Alternatively, ethylene glycol and terephthalic acid can be used as starting materials. The process flow is the same as the one mentioned above. However, different from the polymerization of the first sets of starting materials, in the reaction of the ethylene glycol and terephthalic acid yields water as by-product (Mangut et al., 2008).

In order to produce filaments or staple fibers melt spinning method is used. In this method, crystallized and dried PET chips are melted at 260-280 °C. During this process, the contact of the polymer with air is prevented for protecting the polymer to be oxidized. The molten PET polymer is extruded through the spinnerers. Molten polymer is carried to spin pack by increasing their pressure with melt pump. Molten polymeric streams are ejected from the spinneret which has small holes. The molten polymeric streams are coolled and are solidified. Thus, filaments are formed. These filaments are stretched and drawn before they are wound onto the bobbins. If filaments are converted into staple fibers, firstly undrawn filaments will be brought together as tow form and then the tow will be drawn, crimped, finished, and cut into defined lengths (e.g. 38, 52, 64, 96, 128, 152 mm).

Spinneret's hole shape identifies the cross section of the PET fibers and filaments. It can be in different shapes including circular, trilobal, hollow or other. The specific gravity of PET is around 1.38 g/cm^3 which is comperatively higher than the other synthetic polymers such as PE, PP, and PA. PET is considered to be high strength fiber. The strength of PET fiber varies between 47-56 cN/tex. PET contains 0.4% humidity under standard ambient conditions. Due to the low moisture content, static electricity problem occurs. Some physical and chemical properties of PET are given in Table 2.1.

Table 2.1 Physical and chemical properties of PET (Tayyar et al., 2010)

Property	Test Method	Value
Molecular weight	-	192 g/mol
Average molecular weight (MW)	-	30000-80000 g/mol
Density	-	1.38-1.41 g/cm^3
Glass transition temperature	DSC	69-115 °C
Peak melting temperature	DSC	265 °C
Breaking force	Tensile	50 MPa
Tensile strength	-	1700 MPa
The lowest stress value that can be deformed	Tensile	4%
Impact resistance	ASTM D256-86	90 J/m
Water absorption (after 24 hours)	-	0.4-0.5%

PET is suitable to be converted into various forms such as film, filament, staple fiber, composites, packages. Therefore, it can be used in many sectors including textile (e.g. cloth, curtain, upholsery fabric), packaging (e.g. PET bottles, containers), automotive industry (e.g. upholsery fabric, air bag), medical application (e.g. suture) (Camlibel, 2018; Mangut et al., 2008).

PET is not a toxic material. On the other hand, the biggest problem related to PET is that it is not biodegradable. But, it can be easily recycled to various products thanks to its thermoplastic character. All materials made up of PET can be easily recycled if they consists only PET.

2.4 Recycling of Polyethylene Terephthalate (PET)

Conversion of the components into other products or energy by physical, chemical or biochemical methods by using the characteristics of the wastes is called “Recycling”. Recycling is the most convenient way to benefit from waste and prevent environmental problems (Tayyar et al., 2010). The environmental impacts of plastic wastes are increasingly attracting attention. Plastics are a major source of environmental problems when disposed as waste (Sevencan et al., 2007). The use of

PET is increasing day by day due to its usefull physical and chemical properties. Due to these properties, they are frequently used not only in clothing but also in PET bottles and packaging. Therefore, there is a vast amount of production and usage of PET products which unfortunately causes the existence of great deal of PET waste over time. It becomes necessary to reduce the environmental impact caused by PET waste. Recycling is the most accurate and economical way to decrease environmental impact of PET waste and to reduce the consumption of virgin PET obtained from limited natural source of petroleum products.

Recycling basically takes place in three different ways. The first is the reuse of PET waste. For instance, PET including clothes that are not used can be given to others. The second way is taking advantage of physical or mechanical recycling in which PET waste is washed, grinded, melted and reshaped. The third way is applying chemical recycling (Malik et al., 2017; Al-Sabagh et al, 2016; Navarro et al., 2008).

2.4.1 Chemical Recycling of PET

Chemical recycling is used to convert plastic materials into smaller molecules that are suitable for use as raw materials for the production of new petrochemicals and plastics (Al Salem et al., 2009; Çelikgöğüs, 2016). There are different recycling processes for the chemical reprocessing of PET waste such as aminolysis, ammonolysis, methanolysis, hydrolysis, glycolysis and saponification (Figure 2.3) (Al Salem et al., 2009; Jankauskaite et al., 2008; Tayyar et al., 2010; Nickles et al., 2004).

2.4.1.1 Aminolysis

Aminolysis is defined as the depolymerization of PET waste using different amines. Aminolysis of PET proceeds under the influence of amine and terephthalamide. (Jankauskaite et al., 2008). The products which are obtained from the chemical recycling of PET waste are especially used in the epoxy and urethane resin industry. However, aminolysis has not widespread commercial application (Tayyar et al., 2010; Jankauskaite et al., 2008; Malik et al., 2017).

2.4.1.2 Ammonolysis

Ammonolysis is usually carried out in an ethylene glycol medium using anhydrous ammonia. Diamines from teraftalamid are used to obtain various polyamides (Tayyar et al., 2010).

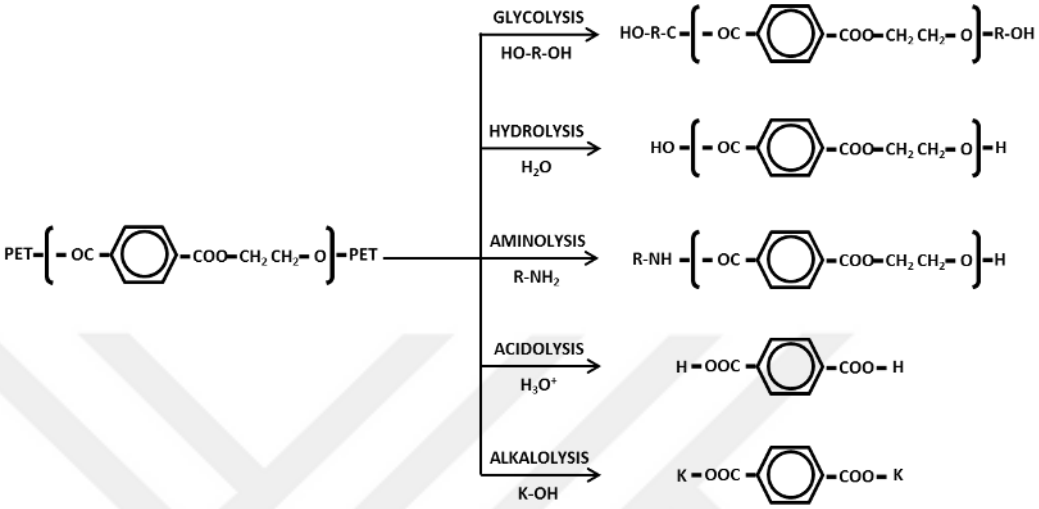

Figure 2.3 Some chemical recycling routes of PET

2.4.1.3 Methanolysis

PET waste is processed with methanol at 200 °C under pressure. This process causes the molecule to be depolymerized. Products of this process are dimethylenephthalate and ethyleneglycol. DMT is purified by distillation and then it is crystallizated and can be for PET production again. Purified ethylene glycol can be used in various applications such as antifreeze and PET production (Tayyar et al., 2010; Jankauskaite et al., 2008; Malik et al., 2017).

2.4.1.4 Hydrolysis

PET waste is hydrolyzed by water and acid or base. Thus, ethylene glycol is obtained with terephthalic acid from PET wastes. The reaction takes place in a neutral environment. Ethylene glycol and terephthalic acid must be purified before reuse. Commercial hydrolysis has not found much application compared to glycolysis and methanolization (Tayyar et al., 2010; Jankauskaite et al., 2008; Malik et al., 2017).

2.4.1.5 Glycolysis

Glycolysis reaction is the moleculer degradation of PET polymer with glycols. This degradation usually takes place with catalysts. To obtain oligomeric diols and polyols, PET and PET wastes can be depolymerized by glycolysis (Jankauskaite et al., 2008).

2.4.1.6 Saponification

PET waste is hydrolyzed with alkali. Two systems have been developed commercially of this chemical recycling method. These are Recopet (France) and Unpet (USA). Recopet PET is a multi-stage process where vials are soaped and filtered. The dyes are extracted before terephthalic acid precipitates. In addition, ethyleneglycol is extracted with sodium sulfate. In Unpet, ethylene glycol and disodium terephthalate are obtained end of the process (Tayyar et al., 2010).

2.4.2 Mechanical (Physical) Recycling of PET

2.4.2.1 Mechanical Recycling of PET Bottles and Packaging Wastes

18% of the total polymers produced in the worldwide is PET. More than 60% of the produced PET is used in PET bottles, packaging and in the production of synthetic fibers (Sulyman et al., 2016). PET bottles and packaging wastes are suitable for mechanical recycling. A typical mechanical recycling of PET has five steps which are (i) collecting PET wastes, (ii) removing contaminants and foreign materials from PET waste, (iii) crushing and washing of PET waste, (iv) drying PET flakes, and (v) extruding PET flakes into filaments or other plastic forms. The schematic representation of mechanical recycling of PET wastes is shown in Figure 2.4.

2.4.2.1.1 Collecting PET Wastes

When PET wastes are thrown to the trash, they remain in nature for many years without rotting, rust, dissolution and biodegradation. Firstly, PET wastes must be collected for recycling process. The collection containers in which PET bottles and packaging materials are collected, the deposit system, and the taxation system are some important ways of collecting PET wastes for recycling process (Sevencan et al., 2007). PET wastes can be grouped in two classes as process wastes and wastes after use. Process wastes are caused by the deburring of the materials produced or the

production defect during production in plastic factories and manufacturing plants. PET wastes after use can be classified according to wastes of their sectors such as urban wastes (supermarkets, shopping malls and household wastes etc.), packaging, agriculture, automotive, construction, electric, and electronics. At the same time, PET wastes intended to be recycled can be obtained from sources such as wastes produced in industrial facilities, commercial centers, used in agriculture, municipal dumps and used in homes (Tayyar et al., 2010). PET wastes collected from these centers are baled.

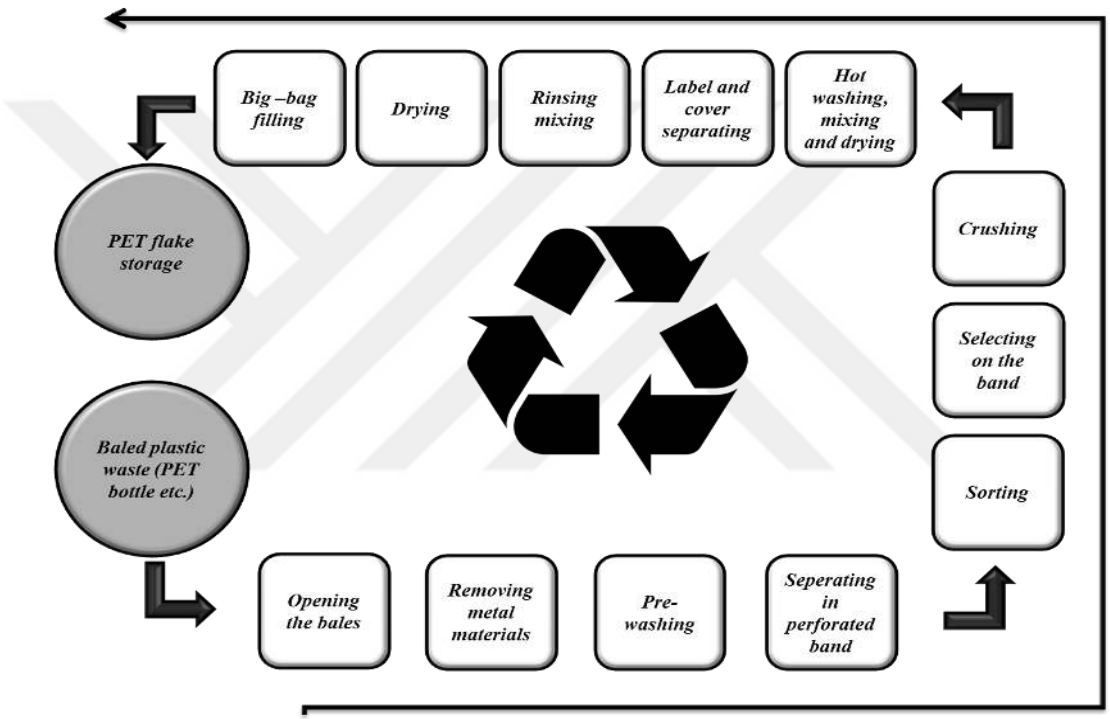

Figure 2.4 Schematic representation of mechanical recycling of PET wastes

2.4.2.1.2 Removing Contaminants and Foreign Materials

The most crucial step of recycling process is the removal of contaminants from PET wastes. PET wastes' bales which include foreign materials are opened and are passed through electromagnetic field. By this way, steel and aluminum materials are separated from PET wastes. The foreign plastics such as HDPE, PVC are manually separated on the separation band according to their ID codes. HDPE and PVC are separated from PET wastes with the help of visible light and X-ray, respectively (Awaja et al., 2005; Sevencan et al., 2007).

2.4.2.1.3 Crushing and Washing of PET Waste

After removing contaminants and foreign materials, PET wastes are crushed to reduce particle size. PET wastes are passed through graded knives. After crushing process the particle size of the PET wastes is approximately 10-15 mm. Thus, PET wastes take the form of PET flake. In the following stages, PET flakes are washed with 2% sodium hydroxide (NaOH) solution at 80-90 °C and then they are rinsed with cold water (Awaja et al., 2005; Al-Sabagh et al., 2016).

2.4.2.1.4 Drying PET Flakes

The crucial step of PET waste recycling includes drying of the PET flakes. The moisture on the PET flake must be completely removed. The reason for this is to prevent hydrolytic degradation. PET flakes are dried at a temperature between 140 °C and 170 °C for 3 to 7 hours to prevent degredation. To work with PET flakes without degradation, it should contain less than 50 ppm of moisture (Awaja et al., 2005; Tayyar et al., 2010).

2.4.2.1.5 Melting PET flakes

PET flakes can be processed with a method similar to virgin PET production which is the conventional melting process. PET flakes can be mixed with virgin PET if it is desired. The extrusion temperature of PET flakes is between 265 °C and 280 °C (Awaja et al., 2005).

2.4.2.2 Mechanical Recycling of PET Textile Wastes

The production of synthetic fibers is increasing day by day. In parallel, textile products produced from these synthetic fibers are also increasing. These textile products which are produced from synthetic fibers and natural fibers remain waste in the environment unless they are recycled. Approximately 80% of textile wastes include synthetic fibers and remaining includes natural fibers. In addition to selling, donating, or reconceive of used textile products, waste textiles which are made of synthetic fibers can be converted into granular form (Büyükaslan et al., 2015; Çelikgöğüs, 2016).

A granulating machine is used to recycle the textile wastes which include synthetic fibers or textiles. In this machine, waste textiles are shredded, melted, filtered and

brought into granule form. Degraded PET (*d*-PET) polymer is thrown out by the machine during this process. This *d*-PET polymer is not suitable for reusing.

2.5 Degradation of PET

2.5.1 Oxidation

Oxidative degradation is a very common degradation type in polymers. Oxidation in the extruder occurs at high temperatures. Thus, degradation becomes thermo-oxidative degradation. In oxidative degradation, polymer degradation begins with the formation of free radicals. Free radicals show an excellent affinity for reacting with oxygen, and when they react with oxygen, unstable peroxy radicals are formed. The peroxy radicals formed remove neighboring unstable hydrogen. Free radicals and unstable hydroxy peroxides are formed. This results in an autocatalytic process, which means that once the reaction begins, it replicates by itself. The process stops when the reactive chemical groups are reproduced (Altun et al., 2003). The final result of the oxidation reaction is carbon and hydrogen in organic material. This materials turn into carbon dioxide and water (Altun et al., 2003).

2.5.2 Thermal Degradation

During heating, PET may be exposed to degradation due to high temperature, long heating time, and the presence of catalysts or oxidizing agents. Heat affects a polymer molecule in two ways. Firstly, kinetic energy exceeds intermolecular forces, and the polymer becomes a high viscosity fluid mass. By this way solid polymer softens and eventually melts which is expected to cause no change in the chemical structure. Secondly, molecular chains break off and some unwanted changes occur in the chemical structure of the chains. PET can be degraded in two ways as intra-molecular thermal distortion and chain end thermal distortion. After the process, even if the original PET has recovered at the desired level, a decrease in molecular weight is observed due to thermal decomposition (Altun et al., 2003).

2.5.3 Hydrolytic Degradation

The degree of drying in PET polymer is very important during the extrusion of PET granules. If they are not dried at expected level, they may be subject to hydrolytic degradation which causes hydrolysis at high temperatures and at high pressure

resulting in breaking PET polymer into terephthalic acid (PTA) and mono ethylene glycol (MEG) (Altun et al., 2003).

2.5.4. Mechanical Degradation

Mechanical degradation refers to molecular divisions induced during mechanical stresses. During melting of PET polymer in an extruder, mechanical stresses occur. All factors that increase polymer to wall friction during the process and initiate the activity of free radicals produced by this effect induce mechanical degradation. Mechanical degradation in PET polymer melts always occur by thermal degradation and possibly by chemical degradation due to high temperatures in the melt (Altun et al., 2003).

2.6 Pyrolysis

Organic bonds of large molecule polymers are broken by the effect of high heat. Pyrolysis process occurs in an inert atmosphere, under vacuum, in the existence of reducing or oxidizing agents, with or without catalysts (Uzun et al., 2014, Çelikgöğüs, 2016; Kar, 2008; Açıkgöz, 2001). During this disintegration, chains or bonds break occur in the structure of polymeric materials. Thus, a large number of reactive radicals are formed. These reactive radicals react to stabilize (Çelikgöğüs, 2016). As a result of this reaction, a solid product rich with carbon, a liquid product called tar or pyrolytic oil, and a gas product with high thermal value are released (Uzun et al., 2014, Çelikgöğüs, 2016).

Pyrolysis, also defined as heating or partial combustion, is generally used in the production of secondary fuels and chemical products. Wastes which are difficult and expensive to store, can be converted into transportable and storable products by pyrolysis (Uzun et al., 2014; Kar, 2008). Different reactions occur as the temperature increases during pyrolysis. These reactions are given in Table 2.2 (Uzun et al., 2014).

There are different pyrolysis methods varied according to the time, heating rate and maximum temperature used in the method. The first of then is the carbonization method. In the carbonization method, the product to be pyrolyzed is processed at a very low heating rate and a long residence time (24 hours). A maximum temperature

of 400 °C is used and activated charcoal is obtained as the main product (Açıkgöz, 2001; Kar, 2008).

In the traditional pyrolysis method, biofuel, activated coal and gas are obtained. In this method, the heating rate is low and the residence time is short which is between 5 minutes and 30 minutes at the highest temperature of up to 600 °C (Açıkgöz, 2001; Kar, 2008).

In the fast pyrolysis method, the heating rate is slightly higher than the traditional pyrolysis method. The residence time varies between 30 minutes and 5 hours at highest temperature of the process is up to 650 °C. Biofuel emerges as the main product (Açıkgöz, 2001; Kar, 2008).

Flash pyrolysis method is divided into two groups according to end products obtained which are liquid and gas. In the flash-liquid pyrolysis method, biofuel is released. In the flash-gas pyrolysis method, chemical substances and fuel gas are released. Flash pyrolysis usually takes place at atmospheric pressure. The residence time of both methods takes a maximum of 1 hour. Heating rates are high. In addition, in both pyrolysis methods, a maximum temperature of 650 °C is used (Açıkgöz, 2001; Kar, 2008).

In the ultra-pyrolysis method, the residence time is about 30 minutes. The heat rate is very high and the maximum temperature used is 1000 °C. Chemicals and fuel are obtained as the main products (Açıkgöz, 2001; Kar, 2008).

In some cases, pyrolysis takes place under vacuum. The pyrolysis residence time under vacuum varies between 2 hours and 30 hours. The heating rate is moderate and a maximum temperature of 400 °C is used. At the end of the process, biofuel is obtained as the main product (Açıkgöz, 2001; Kar, 2008).

In the hydropyrolysis method, a high heating rate is used with a maximum temperature of 500 °C. The residence time for the process is about 10 hours. Biofuels and chemicals are obtained as a result of the process. Hydropyrolysis often takes place at a pressure of 20 MPa (Açıkgöz, 2001; Kar, 2008).

The methane pyrolysis method lasts a maximum of 10 hours, just like the hydrolysis method. The heating rate is also high. Temperature of 700 °C is used. Chemical substances are obtained as a result of the process (Açıkgöz, 2001; Kar, 2008).

Table 2.2 Events occurring at different temperatures during pyrolysis (Uzun et al., 2014)

Temperature (°C)	Happening
100-120	Absolute drying
120-150	The deoxidation, desulfurization, decomposition of body water
250	The depolymerization, decomposition of hydrogen and sulfur
340	Disintegration and degradation of bonds of aliphatic compounds, the formation of methane and hydrocarbons
380	Carbonization stage
400	The disintegration of bonds of C-N and C-O compounds
400-420	The transformation of all substances into pyrolysis liquid and tar
600	Craking of all materials to heat resistant materials
>600	Formation of aromates and ethylenes

2.6.1 Parameters Affecting the Pyrolysis

2.6.1.1 Effects of Heating Rate and Temperature

The most important parameters affecting pyrolysis are the heating rate and the temperature. Volatile products yield increases substantially in slow pyrolysis. In slow pyrolysis, volatile products remain too much in the reaction medium due to the low heating rate and the long stay of the material inside. As a result, secondary and tertiary products released (Açıkgöz, 2001; Kar, 2008; Çelikgöğüs, 2010). Depending on the structure of the plastic broken down with pyrolysis method, the product distribution (solid, liquid, gas) obtained as a result of the breakdown varies (Çelikgöğüs, 2010).

The thermogravimetric analysis of waste tires revealed that the thermal degradation of waste tires starts at 200 °C (Kar, 2011). This means that the pyrolysis of waste tires starts at 200 °C. At approximately 500 °C, the pyrolysis of waste tires ends. In

the pyrolysis of waste tires, when the temperature was raised, a liquid product was obtained at about 400 °C. Liquid product efficiency reaches maximum value at 500 °C (İlkılıç and Aydın, 2011). As the temperature increases, the char efficiency obtained from the pyrolysis of waste tires decreases (Kar, 2011; İlkılıç and Aydın, 2011). The gas product efficiency continues to increase as the temperature increases (Dogan et al., 2017; Shah et al., 2009; İlkılıç and Aydın, 2011; Kar, 2011). Not only in the pyrolysis of waste tires, but also in the pyrolysis of PS plastic waste, a decrease in the amount of char and an increase in the amounts of liquid and gas products were observed when the temperature was raised (Çelikgöğüs, 2010).

2.6.1.2 Effect of Type of Catalyst

Catalysts are substances that increase the speed of approaching equilibrium in a chemical reaction. Catalyst-free reactions generally take place at very low speed. In some cases the catalyst not only accelerates the reaction but also increases the product efficiency. Metals (Fe, Ni, Pt, Pd, Cu, Ag), oxides (Al_2O_3, SiO_2, MgO, SiO_2-Al_2O_3, Zeolites), and sulfides (NiO, ZnO, CuO, Cr_2O_3, MoS_2) are used as catalysts (Çelikgöğüs, 2010).

When SiO_2, Al_2O_3 and SiO_2/Al_2O_3 catalysts were used in the pyrolysis of tire wastes, an increase in the amount of final products was observed. In the experiment carried out in the temperature range of 300-400 °C, Al_2O_3 catalyst increased the amount of gas product by 20.9%. SiO_2 catalyst increased the amount of obtained liquid product by 28.2% (Shah et al., 2009). In the pyrolysis made with waste plastics using a zeolite catalyst, waste plastics turned into gas and liquid form at a rate of 90-98%. The amount of gas product released as a result of pyrolysis varied between 20-55%. The amount of liquid products released varied between 32-70% (Scott et al., 1990).

2.6.1.3 Effect of Atmospheric Gases

The pyrolysis atmosphere is one of the important parameters that has a considerable impact on the yields and compositions of the pyrolysis products. Pyrolysis process generally takes place under assistant gases such as nitrogen (N_2), helium (He), argon (Ar), oxygen (O_2), carbon dioxide (CO_2). The assistant gas quickly removes the released pyrolysis products and prevents the occurrence of secondary reactions (Kar, 2008). Pyrolysis of waste PET bottles was carried out in N_2 and CO_2 atmospheres

(Lee et al., 2017). The final product quantities obtained from this pyrolysis experiment were compared. In the pyrolysis in CO_2 atmosphere, thermal separation accelerated compared to the pyrolysis in N_2 atmosphere. In addition, more gas by-product was obtained in the CO_2 atmosphere. However, the total amount of carbonized material and pyrolysis oil obtained in CO_2 environment decreased (Figures 2.5 and 2.6).

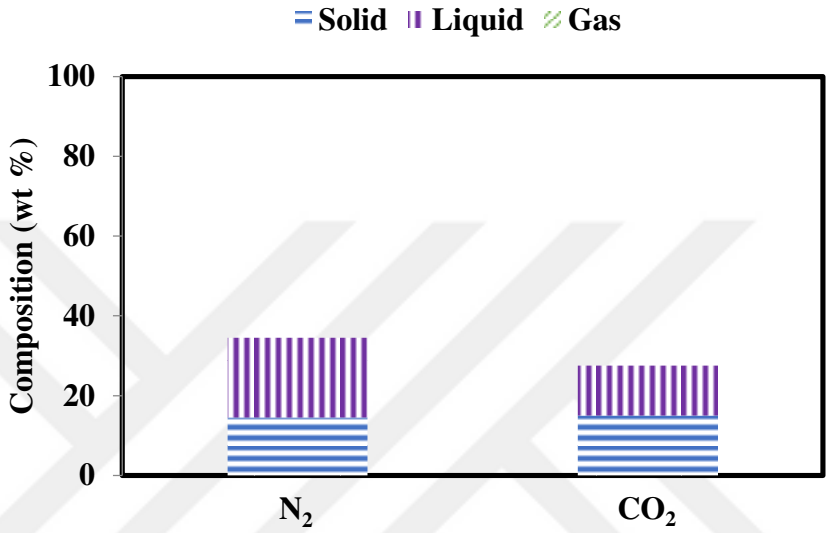

Figure 2.5 Mass balance of pyrolytic products of PET waste under N_2 and CO_2 atmospheres (Lee et al., 2017)

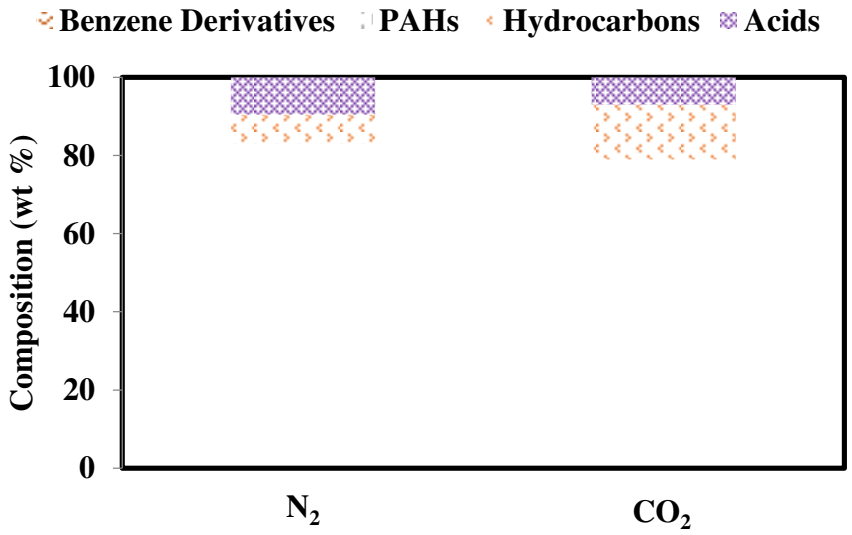

Figure 2.6 Compositions of chemical compounds in the gas by-product obtained by the pyrolysis of PET wastes under N_2 and CO_2 atmospheres (Lee et al., 2017)

2.6.1.4 Effect of Types of Reactor

Reactor type used in the pyrolysis can affect the residence time, heat transfer and efficiency of the reaction. Batch, semi-batch, fluidized bed, fixed-bed, conical spouted bed, microwave reactors are some of the reactor types used in the pyrolysis (Anuar Sharuddin et al., 2016).

Batch reactor is a closed system. During the process there is no inflow or outflow of any product. But semi-batch reactor permits to inflow or outflow of product. Pyrolysis temperature range in batch reactor or semi-batch reactor is in between 300 °C and 800 °C. The design of the fixed-bed reactor is not complex. The catalyst that is used in the fixed-bed reactor packed in a bed. This reactor is generally used for secondary pyrolysis. In the fixed-bed reactor, reaching the surface area of the catalyst is limited. In fluidized bed reactor has a distributer plate. The catalyst in fluidized bed reactor sits on the distributer plate. The fluidizing gas passes through the distributer plate and the particles are carried in a fluid state. The conical spouted bed reactor is provides good mixing ability. This reactor suitable for the materials that has large particle size. The most recently developed reactor type in pyrolysis systems is the reactor working with microwaves. Different from conventional pyrolysis system, microwave radiation provides fast heating, high production speed, and low production costs (Anuar Sharuddin et al., 2016).

2.7 Pyrolysis of PET

In the literature there are some studies for the pyrolysis of PET (Dogan et al., 2017; Shah et al., 2009; Terakado et al., 2004; Lee et al., 2017; Anuar Sharuddin et al., 2016; Cepeliogullar and Putun, 2013; Heikkinen et al, 2004). When the waste tires and PET material were pyrolyzed together, the most significant parameter affecting the pyrolysis was found to be the temperature (Dogan et al., 2017). In this study, the pyrolysis of the PET materials did not occur since the temperature of the pyrolysis was kept low (200-350 °C). The pyrolysis temperature values of 350 °C (Dogan et

al., 2017) and 400 °C (Shah et al., 2009) resulted in the gasification of waste tires, though there was no gasification observed for PET at those temperatures.

In one study, the pyrolysis was carried out using PET and various metal oxide mixtures with or without the acid-treatment. Metal oxides of Fe_2O_3, ZnO and Nd_2O_3 were used in the pyrolysis. As a result of this study it was found that, catalysts not only increased the amount of obtained final products, but also improved the properties of final products. These catalysts caused changes on the surface morphology of the final carbonized char product. Porous structures were formed on the carbonized materials with these catalysts (Figure 2.7). These porous structures were varied according to the type of metal oxides used and acid treatment applied (Terakado et al., 2004).

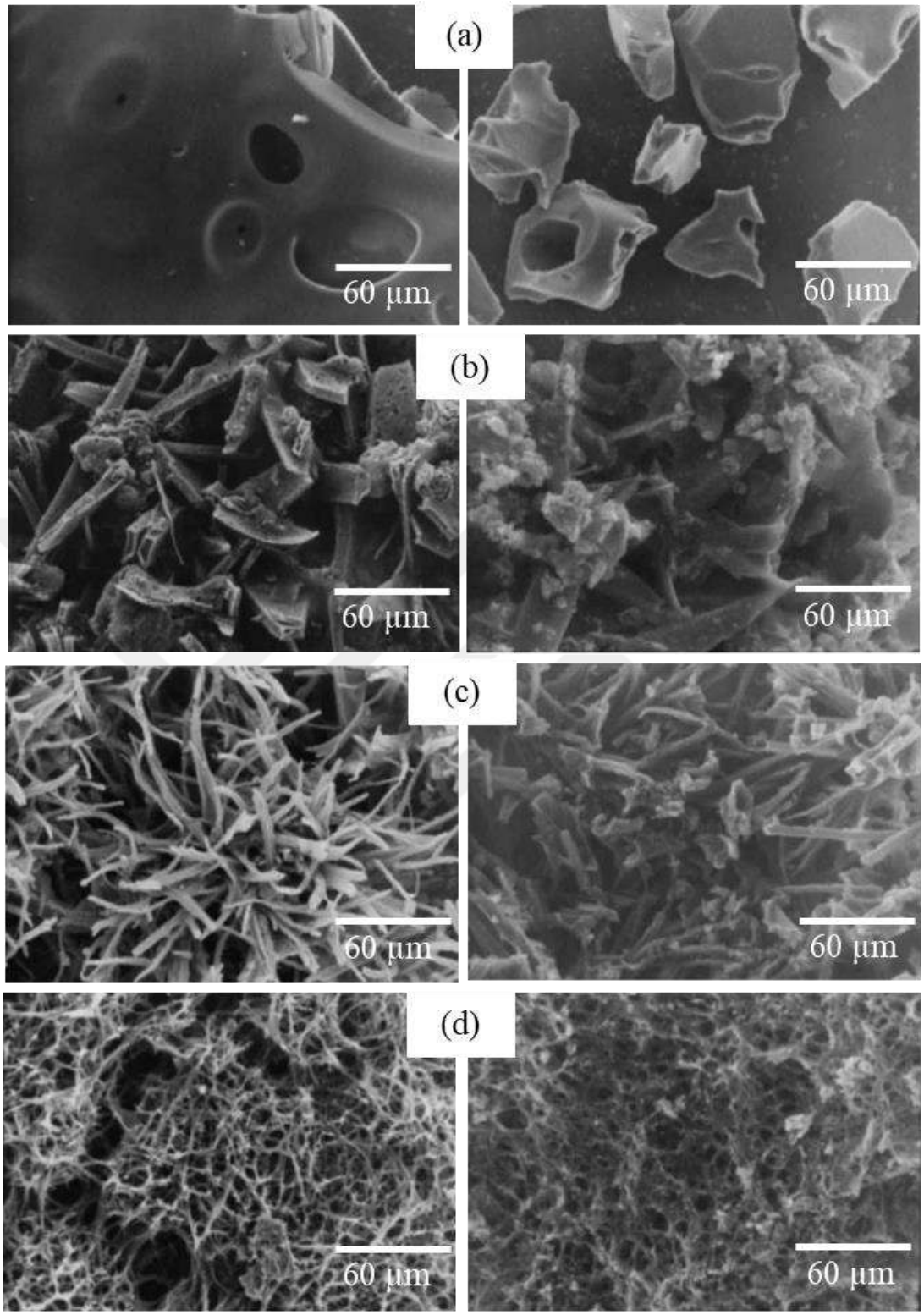

Figure 2.7 SEM images of the pyrolysed carbonized products of: (a) PET; (b) PET - Fe_2O_3; (c) PET - ZnO; and (d) PET - Nd_2O_3 with (right) or without (left) acid-treatments (Terakado et al., 2004)

2.7.1 By-Products of the PET Pyrolysis

2.7.1.1 Pyrolytic Oil

The analysis of pyrolytic oils obtained from the pyrolysis process can be done by using Fourier Transform Infrared Spectroscopy (FTIR) and Gas Chromatography - Mass Spectrometry (GC-MS) (Lee et al., 2017). 1-propanone, benzoic acid, biphenyl, 4-ethylbenzoic acid, diphenylmethane, 4-vinylbenzoic acid, fluorene, benzophenone, 4-acetylbenzoic acid, anthracene, biphenyl-4-carboxylic acid, 1-butanone, and m-terphenyl were chemical compounds obtained from the analysis of pyrolytic oil by-product of PET pyrolysis (Anuar Sharuddin et al., 2016). It was found that approximately 50% of the pyrolitic oil by-product of PET pyrolysis consisted of benzoic acid (Lee et al., 2017).

2.7.1.2 Carbonized Material

Depending on the residence time, heating rate and temperature, changes were observed in the types and amounts of by-products obtained from PET pyrolysis (Heikkinen et al, 2004). PET waste, which was subjected to the pyrolysis process using long residence time and low heating rate yielded more amount of carbonized material (Heikkinen et al, 2004). Compared to PP and PE wastes, less amount of carbonized material was obtained from PET wastes (Anuar Sharuddin et al., 2016). It was suggested that carbonized materials obtained from plastic wastes can be used in the production of activated carbon (Anuar Sharuddin et al., 2016).

2.7.1.3 Gas

The type of gas released from the pyrolysis process varied according to the pyrolysis material (Anuar Sharuddin et al., 2016). The main gas compounds released during the pyrolysis of HDPE, LDPE, PP, and PS materials were determined as hydrogen, methane, ethane, ethane, propane, propene, and butane. In the PET pyrolysis, carbon dioxide and carbon monoxide gases were released in addition to these gases. In the PET pyrolysis, as the pyrolysis temperature increased, an increase in the amount of gas by-product was observed (Dogan et al., 2017; Shah et al., 2009).I was suggested that pyrolysis gas can be used to generate electricity or to directly heat pyrolysis boilers (Anuar Sharuddin et al., 2016).

2.8 Characterization of PET Polymer and By-Products of PET Pyrolysis

2.8.1 Thermal Analysis

Thermogravimetric analysis (TGA) method is used for the thermal analysis of polymeric materials. This analysis is generally used for the determination of the thermal stability, thermal degredation, oxidation, combustion, and thermogravimetric kinetics (Coats and Redfern, 1963; Liu and Yu, 2005). There are three different TGA techniques which are isothermal or static thermogravimetry, quasistatic thermogravimetry, and dynamic thermogravimetry (Loganathan et al., 2017). In isothermal or static thermogravimetry technique, sample weight is used as a function of time at constant temperature. In quasistatic thermogravimetry, the sample is heated until the sample mass reaches stability and then next heating cycle is applied. In dynamic thermogravimetry, the sample is heated in an environment whose temperature varies linearly.

The initial temperature of the decomposition of PET polymer and its wastes, the temperature range at which decomposition takes place, and the amount of different polymeric and other materials contained in degraded PET can be analyzed by TGA. ASTM E2550-17 (Standard Test Method for Thermal Stability by Thermogravimetry) test standard is used for this analysis.

Another thermal analysis technique for determining the thermal properties of polymers is Differential Scanning Calorimetry (DSC). There are two different types of DSC which are heat-flux DSC and power differential DSC. In the heat-flux DSC, two sample cells are prepared. While one of the sample cells contains the polymeric sample, another one does not contain any sample and is kept empty as a reference. After preparing the sample cells, they are placed into two identical sample holders in DSC machine. The difference in the amount of heat flow at raising temperature is measured in the analysis and is plotted against the temperature and time.

Glass transition temperature, melting temperature range, melting peaks, and crystallinity of PET polymer can be determined with DSC. ASTM D3418-15 (Standard Test Method for Transition Temperatures and Enthalpies of Fusion and Crystallization of Polymers by Differential Scanning Calorimetry) test standard can be used for the DSC analysis.

2.8.2 Molecular and Structural Analysis

The determination of the viscosity of a polymer solution gives information about the molecular weight and molecular weight distribution of polymers. ASTM D 4603 (Standard Test Method for Determining Inherent Viscosity of PET) is the standard test method applied for measuring the viscosity of PET polymer. In order to measure the intrinsic viscosity of PET polymer, a polymer solution is prepared at a concentration of 0.5 wt.% with 60 wt.%/40 wt.% phenol/1,1,2,2-tetrachloroethane solvents mix. The polymer solution is heated at 100 °C until the PET polymer is fully dissolved. After the polymer solution is cooled to 30 °C, it is placed into Ubbelohde viscometer tube. The polymer solution is waited inside the Ubbelohde viscometer tube for 15 minutes at 30 °C. The polymer solution is vacuumed on to the top of the tube and is then released to flow in the tube from two marked places. The transition time for the flow between two marked spots is measured. This test is performed for both polymer solution and the solvents with three replicates and the average transition times for polymer solution (t_1) and the solvent (t_0) are reported. Intrinsic viscosity is then calculated by substituting them in Equation 2.1.

$$\text{Viscocity } (\eta) = \frac{\sqrt{1+1.4\left(\frac{t-t_0}{t_0}\right)} - 1}{0.35} \qquad (2.1)$$

Using the Mark-Houwink equation (Equation 2.2), the average molecular weights by weight (M_w) (Equation 2.3) and number (M_n) (Equation 2.4) and the polydispersity index (PDI) (Equation 2.5) are calculated from the intrinsic viscosity value (η).

$$(\eta) = K * M^a \qquad (2.2)$$

$$\eta = 3.72 * 10^{-4} * (M_n)^{0.73} \qquad (2.3)$$

$$\eta = 4.68 * 10^{-4} * (M_w)^{0.68} \qquad (2.4)$$

$$PDI = M_w / M_n \qquad (2.5)$$

2.8.3 Chemical Characterization

FTIR is used in the analysis of solid and liquid samples using special reflection techniques in areas where high sensitivity is required (Faix, 1992). Infrared spectroscopy is the most widely used technique to characterize organic and inorganic materials. FTIR analysis takes place in the spectral range of 4000 to 50 cm $^{-1}$. The state of the bonds in the structure and the analysis of the bonding sites can be analyzed by FTIR. Also, introducing several FTIR spectrums to the library of the FTIR machines allows us to identify the chemical compounds and polymers. In FTIR analysis, ASTM E1252-98 (Standard Practice for General Techniques for Obtaining Infrared Spectra for Qualitative Analysis) test method is used.

2.8.4 Elemental Analysis

Elemental analysis of a material can be done with Energy Dispersive - X-Ray Spectroscopy (ED-XRF) and Scanning Electron Microscopy Energy Dispersive X-ray Spectroscopy (SEM-EDX). XRF analyzers are generally classified by wavelength or energy distribution for X-ray line detection and analysis. The wavelength distribution is divided according to the wavelengths of the X-ray lines, which can be realized by crystals (crystal dispersion), diffraction (diffraction dispersion) or spatial (geometric) distribution. In energy distribution, separation of X-ray lines relies on photon energies (Kalnicky and Singhvi, 2001). SEM is a method for high resolution imaging of surfaces. Just as light microscopy uses visible light, SEM uses electrons for imaging. SEM has more advantages over light microscopy. The first of these is SEM, which has a much higher resolution (>100,000X). It also includes up to 100 times greater depth of field than a light microscope. Qualitative and quantitative chemical analysis information is also obtained with SEM using EDX. The EDX technique detects x-rays emitted from the sample to characterize the basic composition of the material being analyzed (SEM-EDX, 2020). While SEM-EDX can be used for the elemental analysis of chemical compounds, ED-XRF can be used to determine the type and weight percentages of inorganic and foreign compounds in PET polymers. ASTM E1508-12a (Standard Guide for Quantitative Analysis by Energy-Dispersive Spectroscopy) test standard can be used for both analyzes.

2.8.5 Colour Analysis

The colour measurement and colour specifications can be based on the CIE system. This system was originally created in 1931, but despite this, new additions and corrections have been made in the basic structure and principles. The CIE system is based on experimental observations rather than colour perception theories. In colour measurement, light source, observer and surface are always taken into consideration (Yesil, 2010).

Although X, Y and Z tristimulus values can express colour numerically, they do not provide information about colour. In order to make a more easily understandable definition of colour, CIE defined a system called the CIELab system with three coordinates L*, a* and b* calculated from X, Y and Z tristimulus values (Figure 2.8) (Yesil, 2010).

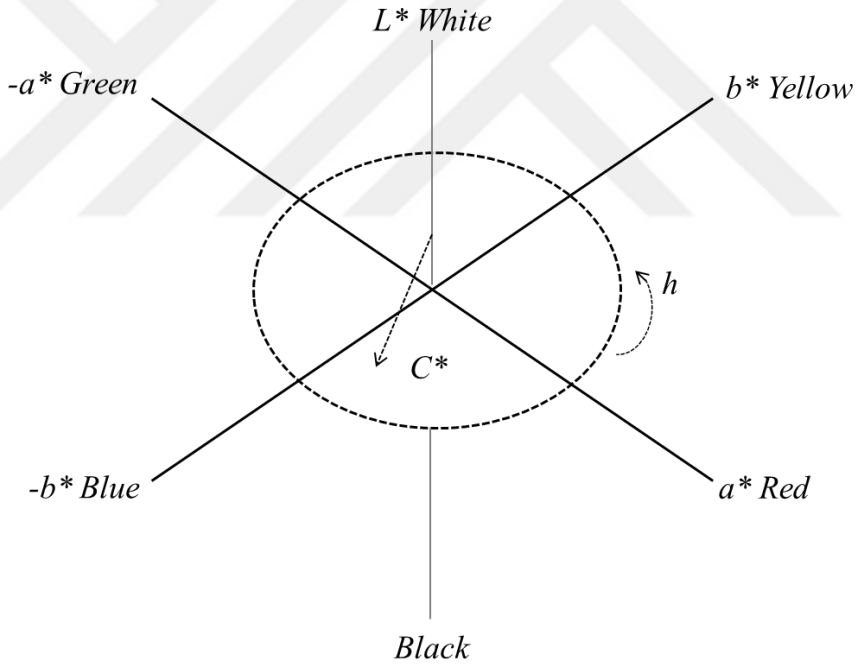

Figure 2.8 CIELab colour space (Acar, 2009)

In CIELab colour space, a* and b* axes make right angles to each other and intersect at the neutral point (Figure 2.8). The third axis L* is a measure of lightness/darkness (brightness) and is perpendicular to the plane formed by a* and b* axes. It intersects this plane at the neutral point. Different shades of the same colour are located on a line extending outward from the neutral point within the plane formed by a* and b* axes. The rotation angle "h" (in degrees), which increases from red to yellow, is a

measure of the colour. For example, h=0° corresponds to a red hue, h=90° to a yellow hue, h=270° to a blue hue. A point away from the neutral point denotes chroma (C*), which is a measure of the vividness (saturation) of a colour at a given luminance (L* value). A colour can be determined either by L*, a* and b* coordinates or with the help of L*, C* and h values. The values of L* range from 0 for black to 100 for white (Acar, 2009). A circle drawn around the neutral point (a*=b*=0) defines a colour circle with constant chroma, and the angle h (in degrees), starting from red, is a measure of the colour (Yesil, 2010). ASTM D3265-17a (Standard Test Method for Carbon Black—Tint Strength) test standard is used for colour analyzes.

CHAPTER 3

INVESTIGATION OF THE FORMATION OF USEFUL BY-PRODUCTS FROM DEGRADED POLYETHYLENE TEREPHTALATE (PET) WASTE

3.1 Introduction

Thermoplastics have been a part of our industrial and social life especially for the last 50 years. They are widely used in every field and every sector. They are also used in the production of many materials including fibers, filaments, films, packaging products, medical products, electronics, automotive parts etc. One of the most widely used thermoplastics is polyethylene terephthalate (PET). PET is highly preferred because of its unique thermal, chemical, and mechanical properties. PET production and usages have steadily increased since it was discovered (Achilias et al., 2010; Dogan et al., 2017; Karayannidis and Achilias, 2007).

PET bottle and packaging wastes have a very short period of use, so they are trashed to the environment as a waste in a short time. Since this cycle takes place rapidly, the amount of waste increases (Achilias et al., 2010; Lee et al., 2017). In addition, PET wastes which are not biodegradable remain in the nature for long time (Niksiar et al., 2015; Achilias et al., 2010; Bratek et al; 2013; Lee et al., 2017; Esfandiari et al., 2011; Altun, 2012). According to the PET consumption by end-use worldwide in 2016, PET bottles had the highest share of 26.3% (Figure 3.1) (Statista, 2020).

Plastic wastes comprises about 5-9 wt.% and 15-20 v.% of all total wastes (Dogan et al., 2017) . It was estimated that 5% of these plastic wastes are PET wastes including mostly PET bottles and packaging products (Dogan et al., 2017). The important point here is that PET is a fully recyclable thermoplastic polymer and these PET wastes can be recyclable to reduce the amount of PET waste in the nature. Three different

routes can be followed to recycle these high volume PET wastes. They are reusing, physical or mechanical recycling, and chemical recycling (Malik et al., 2017; Al-Sabagh et al, 2016; Navarro et al., 2008; Nickles and Farahat, 2004).

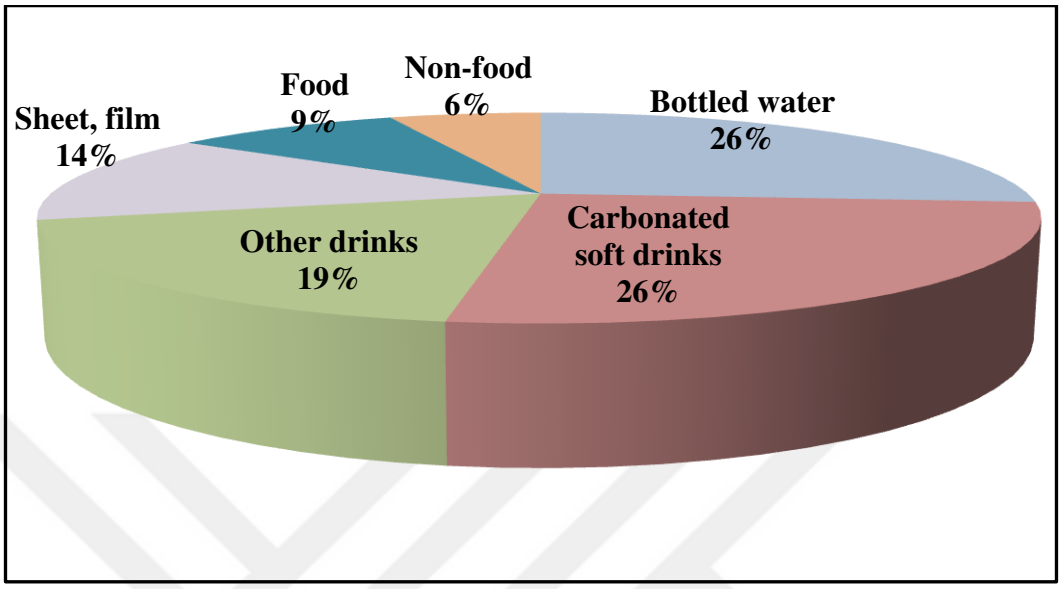

Figure 3.1 PET consumption by end-use worldwide in 2016 (Satista, 2020)

In addition to bottles and packaging products, filaments, fibers and yarns are also produced from PET polymer. These products are then converted into textile products. While filament and yarns are transformed into textile products, textile wastes come into existence especially at the ready-made garment production. These wastes can be recycled by using physical recycling methods (Kaplan et al., 2019; Kaplan, 2020). If textile wastes consist of solely PET component, they can be converted into agglomerates. For conversion, first of all, these wastes are transferred to the agglomer fornation part of a special machine with a brand name of Starlinger recoStar (Starlinger, 2020). Agglomeration part of this machine consists of blades and nozzles in a cauldron. The waste textiles coming here are shredded by rotating blades at a certain speed and are heated. If the temperature increases too much, it is reduced to the desired temperature with the help of water coming from nozzles. Dust and gases released here are evacuated with the help of vacuum. Waste textiles softened in the aggregation section are fed into an extruder for melting. The melted waste is filtered to remove foreign materials on or in textiles. The melt that does not pass through the filter is thrown out of the discharge part of the machine. This melt thrown out is a *degraded* PET (*d*-PET) waste. The *d*-PET waste that is the waste of recycled PET (r-PET) polymer has no usage area. r-PET melt, which is removed

from foreign substances, is cooled and cut into granule form with the help of rotating knives. In this way, *r-PET granules* are obtained from PET based textile waste.

PET bottle and packaging wastes are fed into the feeding machine to be turned into r-PET flake form. For this, it is first transmitted to optical separators to separate the foreign polymeric (non-PET) wastes and metals from PET bottle and packaging wastes (Kaplan et al., 2019; Kaplan, 2020). Remained non-PET materials, aluminum cans and metal wastes are also manually separated on a conveyor belt by workers. After the separation is made, it is brought to the desired part sizes with the help of the blades in the crushing machine and transferred to the washing line. In the first pool of the washing line, the foreign substances on the PET wastes are washed and cleaned. In addition, they are washed with chemical agents to remove the labels and adhesives on the PET wastes. After chemical washing, it is washed again to remove the excess chemical. The lower density caps and labels are separated from PET wastes. Polipropylene (PP) and polyethylene (PE) have lower density than PET polymer. Taking advantage of this density difference, these materials are separated from each other. After the separation the materials are dried. These materials are called *r-PET flakes*. r-PET flakes are first crystallized and then transferred to the extrusion section.

In the extrusion section, r-PET granules and r-PET flakes can be mixed or in some cases they are mixed with *virgin fiber grade PET* (Kaplan et al., 2019; Kaplan, 2020). These materials are then melted in the extruder. They are conveyed to the spinneret by increasing the flow pressure with the help of the melt pump. The polymer melts coming out of the spinneret are converted into filaments upon cooling. The filaments on which the finishing chemical is applied on are subjected to heat and tension in the drawing section in order to improve molecular orientation and crystallization. They are then crimped, dried, and cut, respectively. Afterwards, these filaments become r-PET fibers.

PET wastes can be recycled several times. However, during the recycling process, some part of PET polymer degrades. This degraded part is not suitable for the recycling process again. In order to recycle these degraded PET polymers, pyrolysis or carbonization can be a suitable method. However, there is not any study on the pyrolysis or carbonization of *d*-PET wastes in the literature. These *d*-PET wastes are

released to the environment as waste. In order to reduce these *d*-PET wastes and discover new usefull forms, the formation of useful by-products from *d*-PET wastes was studied here.

3.2 Materials and Methods

3.2.1 Materials

r-PET flakes were obtained from recycled post-consumer bottles. The PET bottle wastes were 12 mm x 12 mm size. r-PET granule was obtained from recycled PET-based clothing wastes. *d*-PET was taken from the waste generated when recycling waste textiles into r-PET granule. Virgin fiber grade PET, r-PET flakes, r-PET granules, and *d*-PET were supplied from GAMA Recycle Elyaf ve İplik San. A.Ş..

Phenol and 1,1,2,2 tetrachloroethane were used for the measurement of the intrinsic viscosity (IV) of samples. The phenol (C_6H_6O, CAS No: 106-95-2) was purchased from Daejung. The 1,1,2,2 tetrachloroethane ($C_2H_2Cl_4$, CAS No: 79-34-5) was purchased from Sigma Aldrich.

3.2.2 Thermal Analyses

Thermogravimetric analysis (TGA) of the virgin fiber grade PET r-PET flakes, r-PET granules, and *d*-PET were performed using a SHIMADZU TGA-50. The decomposition temperatures and the total weight lost of the virgin fiber grade PET and *d*-PET were determined with the TGA. During TGA analysis, samples were heated from 25 °C to 650 °C with a heating rate of 10 °C/min. TGA was used at atmospheric pressure with a nitrogen flow of 50 ml/min. For the determination of the thermal stability and degradation ASTM E2550-17 (Standard Test Method for Thermal Stability by Thermogravimetry) standard was followed for analysis.

Thermal analysis was carried out for virgin fiber grade PET, r-PET flakes, r-PET granule, and *d*-PET by means of differential scanning calorimetry (DSC). SHIMADZU DSC-60 Plus was used for thermal analysis of all samples (Figure 3.2). The glass transition temperature (T_g), melting temperature range and peak melting temperature (T_m) of all samples were determined by DSC device. Samples were heated from 25 °C to 290 °C with a heating rate of 10 °C/min at atmospheric pressure with a nitrogen flow of 50 ml/min. ASTM D3418-15 (Standard Test Method

for Transition Temperatures and Enthalpies of Fusion and Crystallization of Polymers by Differential Scanning Calorimetry) standard was followed for analysis.

Figure 3.2 SHIMADZU DSC-60 Plus differential scanning calorimeter

3.2.3 Molecular and Structural Analyses

The intrinsic viscosity of the samples was determined. For the determination a polymer solution was prepared. For the solvent mix a concentration of 0.5 wt.% with 60 wt.%/40 wt.% phenol/1,1,2,2-tetrachloroethane was used. Virgin fiber grade PET, r-PET flakes, r-PET granule, and *d*-PET were cut into small particles. 0.125 ± 0.0001 g sample was added into the prepared solution. The mixture was stirred at 100 °C until the sample was fully dissolved. The prepared solution was cooled to 30 °C. After cooling, the solution was put into the ubbelohde viscometer tube in the IV device (Figure 3.3). The solution was kept 15 minutes at 30 °C in the ubbelohde viscometer tube. The solution was vacuumed on to the top of the tube and was then released to flow in the tube from two marked places. The transition time for the flow between two marked spots was measured. This test was performed for both polymer solution and the solvents with three replicates and the average transition times for polymer solution (t_1) and the solvent (t_0) are reported. The intrinsic viscosity was calculated by using Equation 3.1. The intrinsict viscosity of virgin fiber grade PET, r-PET flakes, r-PET granule, and *d*-PET were determined according to the standart methods ASTM D4603 (Standard Test Method for Determining Inherent Viscosity of PET by Glass Capillary Viscometer).

$$\text{Viscocity } (\eta) = \frac{\sqrt{1+1.4\left(\frac{t-t_0}{t_0}\right)} - 1}{0.35} \qquad (2.1)$$

Using the Mark-Houwink equation (Equation 2.2), the average molecular weights by weight (M_w) (Equation 2.3) and number (M_n) (Equation 2.4) and the polydispersity index (PDI) (Equation 2.5) are calculated from the intrinsic viscosity value (η).

$$(\eta) = K * M^a \qquad (2.2)$$

$$\eta = 3.72 * 10^{-4} * (M_n)^{0.73} \qquad (2.3)$$

$$\eta = 4.68 * 10^{-4} * (M_w)^{0.68} \qquad (2.4)$$

$$PDI = M_w / M_n \qquad (2.5)$$

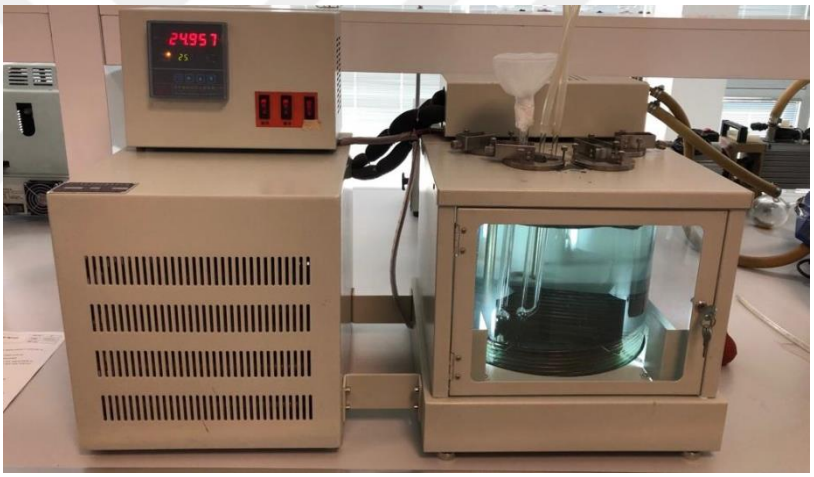

Figure 3.3 Intrinsic viscosity measurement device

3.2.4 Chemical and Elementel Analyses

The chemical structure of the virgin fiber grade PET, r-PET flakes, r-PET granule, and *d*-PET was characterized with Fourier Transform Infrared Spectroscopy (FTIR). Based on the ASTM E1252 (Standard Practice for General Techniques for Obtaining Infrared Spectra for Qualitative Analysis) standard, measurements were taken. Samples were analyzed in the 400-4000 cm^{-1} band range and 2 cm^{-1} resolution. Spectra were obtained by using SHIMADZU IRAffinity-1S spectrometer with (ATR) setup (Figure 3.4). Samples were placed on the diamond crystal of the ATR

which was previously cleaned with alcohol. Samples were firmly clamped and measurements were taken to obtain the infrared spectrums of the samples.

Figure 3.4 SHIMADZU IRAffinity-1S Fourier-transform infrared spectrometer

Energy Dispersive X-Ray Fluorescence Spectrometer (ED-XRF) was used to determine the elementel composition of *d*-PET and the type and weight percentages of foreign elements (Figure 3.5). For ED-XRF analysis, the samples were placed between 5 μm thick PP film. Measurements were taken under vacuum. Organic and inorganic materials in the samples were also analyzed with detailed measurement. For the analysis, ASTM E1508-12a (Standard Guide for Quantitative Analysis by Energy-Dispersive Spectroscopy) testing standard was used. The carbon content of carbonized material was determined by Scanning Electron Microscopy-Energy Dispersive X-Ray Analyzer (SEM-EDX) with JEOL JSM-6390.

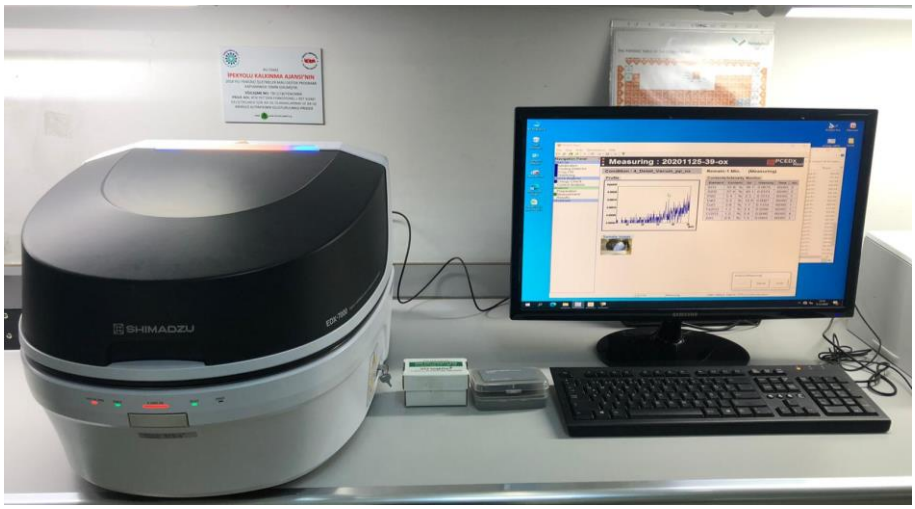

Figure 3.5 SHIMADZU EDX-7000 energy dispersive X-ray fluorescence (ED-XRF) spectrometer

3.2.5 Carbonization

r-PET flake and *d*-PET of different sizes (10 mm and 30 mm) were used in carbonization experiments. Carbonization experiments were carried out at various temperatures at Protherm Furnaces-PC 442 atmosphere controlled high temperature furnace (Figure 3.6). Ceramic and metalic plates were used as sample holder in the furnace. Carbonization temperatures were varied between 450 ºC and 600 ºC. Two heating rates were used as 5 ºC/min and 10 ºC/min. Residence time in furnace was varied between 1 hour and 2 hours. The nitrogen (N_2) and oxygen (O_2) gas of various flow rates were supplied into the furnace seperately at different stages of the carbonization processes. The detailed parameters of the conducted carbonization experiments are given in Table 3.4

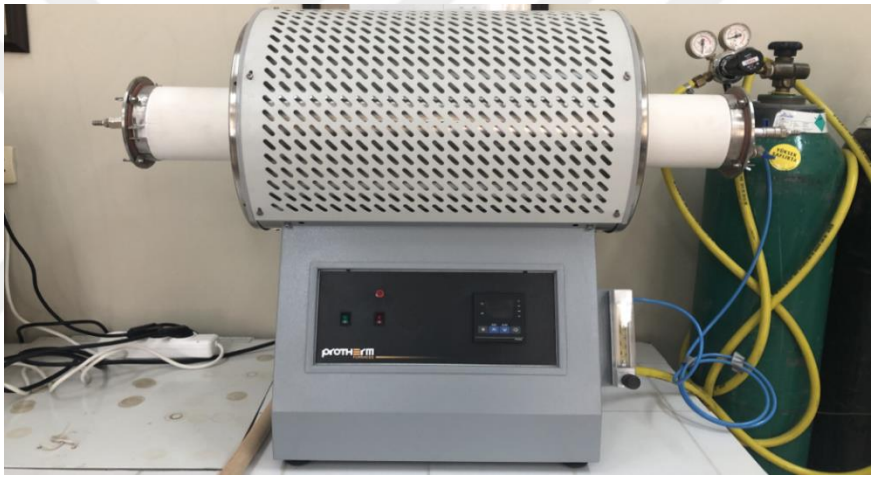

Figure 3.6 Atmosphere controlled furnace used in the carbonization

Table 3.1 Parameters of the conducted carbonization experiments

Sample	Sample Size (mm)	Heating Rate, HR (°C/min)	Carbonization Temperature, T_c (°C)	Residence Time in Carbonization, t_r (min)	Auxiliary Gas	Gas Flow Rate, FR (L/h)
d-PET	10	5	500	60	N_2	100
d-PET	30	5	500	60	N_2	100
d-PET	10	5	500	60	N_2	50
d-PET	10	5	500	60	O_2	100
d-PET	10	5	500	120	N_2	100
d-PET	10	10	450	60	N_2	100
d-PET	10	10	500	60	N_2	100
d-PET	10	10	600	60	N_2	100

3.2.6 Milling

In order to reduce the particle sizes of the carbonized materials obtained as a result of the carbonization experiments, milling was performed at different milling times and speeds in the RETSCH PM100 milling machine (Figure 3.7). Stainless steel balls of 5 mm diameter were used to mill the carbonized materials. While about one third of the milling cup was filled with stainless steel balls, other one third of the milling cup was filled with carbonized materials and the remaining was kept empty. The carbonized materials were milled from 5 min to 15 min with an interval of stopping at each minute, at milling speeds of 350 rpm, 400 rpm, and 450 rpm for completing the first cycle. For the second cycle, milled carbonized materials were remilled for 30 min with an interval of stopping at each minute, at milling speed of 600 rpm.

Figure 3.7 Retsch PM100 milling machine

3.2.7 Particle Size Analyses

Particle size distributions of carbonized materials, which were milled at different duration and speeds, were measured. MALVERN Zetasizer Nano ZS was used to determine the particle sizes of milled carbonized materials (Figure 3.8). 0.1% carbonized material was put into distilled water. The placed material was mixed and placed in the tub of the device. Particle size measurements were conducted for each sample taken from this tub. Three repeats were done for each sample at 25 °C. For measurements, refractive index value of carbon was entered as 2.41. Three measurements were taken for each prepared sample.

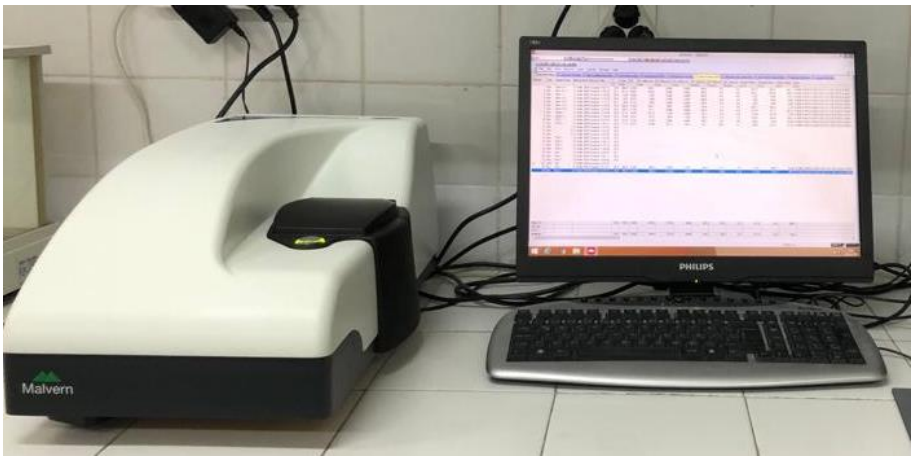

Figure 3.8 MALVERN zetasizer Nano ZS particle size analyser

3.2.8 Morphological Analysis

SEM images were taken for the carbonized materials. To take an image, carbonized materials were fixed with adhesive tape. Images of the samples were taken at 10 kV accelerating voltage with using JEOL JSM-6390.

3.3 Results and Discussions

3.3.1 Molecular and Structural Characterization of Virgin Fiber Grade PET, r-PET Flakes, r-PET Granule, and d-PET

Intrinsic viscosities (IV) of virgin fiber grade PET, r-PET flakes, r-PET granule, and *d*-PET were measured and results were calculated using Equation 3.1. According to results, while r-PET flake had the highest IV value of 0.81 dl/g, *d*-PET had the lowest IV value of 0.12 dl/g (Table 3.2). Our results are almost coherent to the values reported by Sanches et al. (2005) who found IVs of the fiber grade PET and r-PET flake as 0.67 dl/g and 0.77 dl/g, respectively. But, it needs to be considered that virgin bottle grade PET usually has higher IV values than the virgin fiber grade PET. When we investigated the effect of recycling on the IV properties of polymers, we found that recycling decreased the IV of the polymers. For instance, while the IV of the virgin fiber grade PET was 0.55, it reduced to 0.5 in r-PET granule as a result of additional thermal effect on recycling. When PET polymer is subjected to several recycling cycles, some portions can be degraded and as a result of this *d*-PET forms. It is therefore expected to have much lower viscosity in *d*-PET which is justified with our finding of 0.12 IV value. Oromiehie and Mamizadeh (2004) added different

proportions of r-PET flake into virgin bottle grade PET and reported that as the ratio of r-PET was increased, the IV of the blend decreased. In the literature, it was also concluded that IV decreased as a result of recycling (Sanches et al., 2005).

Table 3.2 Intrinsic viscosity values of virgin fiber grade PET, r-PET flakes, r-PET granule, and *d*-PET

	Intrinsic viscosity (dl/g)
Virgin fiber grade PET	0.55
r-PET flake	0.81
r-PET granule	0.5
***d*-PET**	0.12

Using the Mark-Houwink equation (Equation 3.2), M_w (Equation 3.3) and M_n (Equation 3.4) and PDI (Equation 3.5) values were calculated from the obtained IV values (η). We found that the *d*-PET sample had the lowest number and weight average molecular weights followed by r-PET granule, fiber grade PET, and r-PET flake (Table 3.3). It was determined that the molecular weight of *d*-PET reduced dramatically when it was degraded. The first reason for this situation is that *d*-PET was thermally processed many times in which the PET can be subjected to mechanical forces at high heat several times and can be oxidized during recycling if it was directly contacted to oxygen during recycling. Thus, chains of PET materials were damaged and chain scission and other degradation mechanisms occcured. As a result of this, the molecular weight of the PET could decrease. Oromiehie and Mamizadeh (2004) also reported that the recycling of PET reduced the melt viscosity and the average molecular weight as a result of hydrolytic chain scission and mechanical degradation undergone during recycling process.

Table 3.3 Number (M_n) and weight (M_w) average molecular weights and PDI values of virgin fiber grade PET, r-PET flakes, r-PET granule, and *d*-PET

	M_n (g/mol)	**M_w (g/mol)**	**PDI (g/mol)**
Fiber grade PET	21990	32720	1.49
r-PET flake	37370	57820	1.55
r-PET granule	19300	28440	1.47
***d*-PET**	2732	3487	1.28

3.3.2 Thermal Characterizations of Virgin Fiber Grade PET, r-PET flake, r-PET Granule, and d-PET

Initial (T_{mi}), final (T_{mf}) and peak (T_{mp}) melting temperatures and glass transition temperatures (T_g) of virgin fiber grade PET, r-PET flake, r-PET granule, and *d*-PET were determined by taking DSC thermograms (Figure 3.9 and Table 3.4). According to results, T_{mi}, T_{mp}, T_{mf} and T_g temperatures of r-PET flakes, r-PET granule, and *d*-PET were lower than those of virgin fiber grade PET. Also, Jiang et al (2019) reported that T_g and T_m of r-PET were found to be lower than those of virgin fiber grade PET. Among the recycled wastes, *d*-PET was found to have the lowest T_{mi}, T_{mp}, T_{mf} and T_g temperatures. Our molecular and structural characterization results also support the thermal characterization results obtained for *d*-PET in which the average molecular weight dramatically decreased (Table 3.3). This can be caused by several recycling cycles applied to PET before it degrades, since each recycling cycle can induce molecular chain damages. It is concluded that as the lengths of the molecular chains are shortened, $T_{mi,}$ T_{mp}, T_{mf} and T_g of *d*-PET reduce.

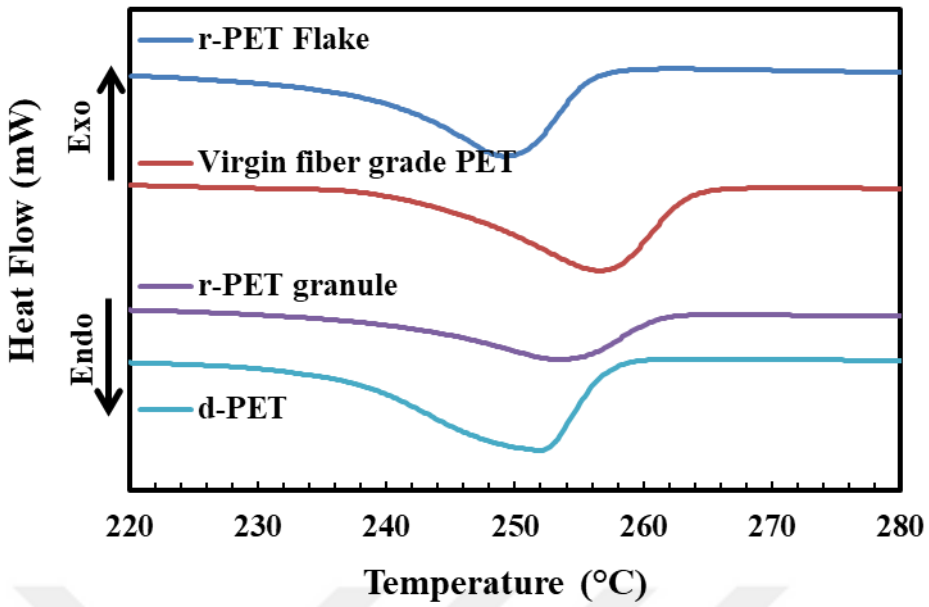

Figure 3.9 Melting thermograms of virgin fiber grade PET, r-PET flake, r-PET granule, and *d*-PET

Table 3.4 Melting and glass transition temperatures of virgin fiber grade PET, r-PET flake, r-PET granule, and *d*-PET

	T_{mi} (°C)	T_{mp} (°C)	T_{mf} (°C)	T_g (°C)
Virgin fiber grade PET	238,7	255,9	264,6	81,4
r-PET flake	233,2	249,1	257,6	78,8
r-PET granule	231,3	253,1	261,8	77,5
***d*-PET**	229,9	248,8	257,9	63,4

Degradation temperatures (1%, 10% and 50%) and total weight loss of virgin fiber grade PET, r-PET flakes, r-PET granule, and *d*-PET under incremental heating were analyzed with TGA. When results were analyzed, it can be said that as the temperature increased mass losses increased for all samples (Figure 3.10 and Table 3.5). According to the results, *d*-PET had the lowest decomposition temperatures at 1%, 10%, and 50% weight reduction compared to virgin fiber grade PET, r-PET flakes, r-PET granule. Also, total weight loss at 650 °C was the highest for *d*-PET which was followed by r-PET flake, r-PET granule, and virgin fiber grade PET. This can be ascended by oxidation and various mechanical forces applied on the polymer at high heat during repeated recycling processes. Jiang et al, (2019) also reported that

the initial decomposition temperature of r-PET was lower than that of virgin fiber grade PET. Similarly, in our study the initial decomposition temperature of r-PET granule was found to be lower than that of virgin fiber grade PET (Table 3.5).

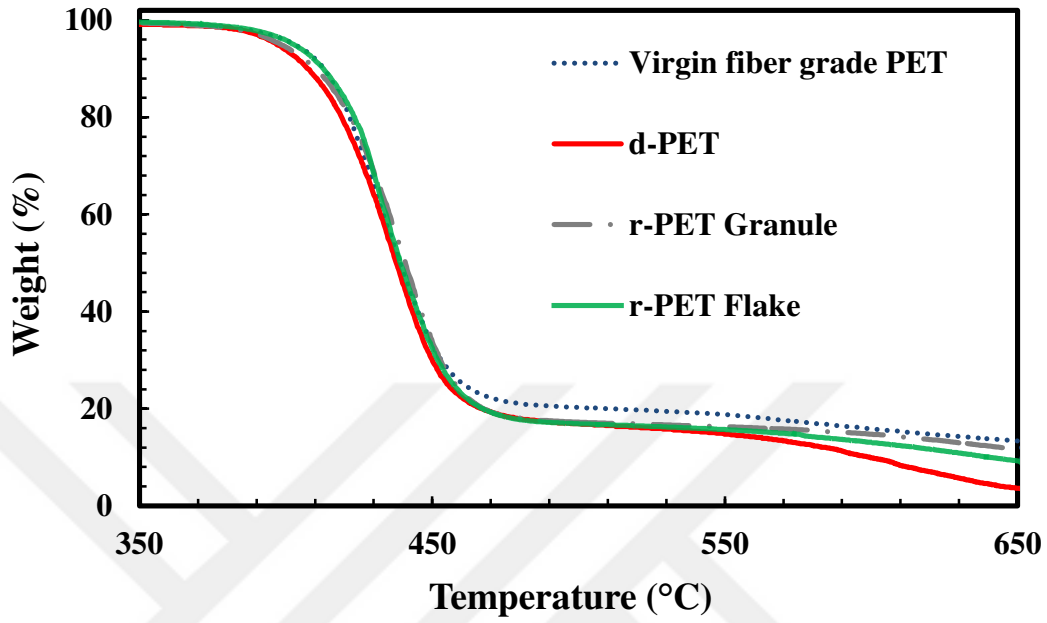

Figure 3.10 Degradation temperatures of samples

Table 3.5 Degradation temperatures and weight losses of virgin fiber grade PET, r-PET flakes, r-PET granule, and *d*-PET

	T_d (%1)	T_d (%10)	T_d (%50)	Total Weight Loss at 650 °C (%)
Virgin fiber grade PET	374,4	412,9	439,2	86,6
r-PET flake	374,8	412,9	439,0	90,7
r-PET granule	367,5	410,2	440,8	88,6
***d*-PET**	358,1	407,6	437,6	96,4

3.3.3 Chemical Characterization of Virgin Fiber Grade PET, r-PET Flakes, r-PET Granule, and d-PET

Bonds and bond strengths in the structures of virgin fiber grade PET, r-PET flakes, r-PET granule, and *d*-PET polymers were characterized by FTIR. FTIR spectra of the samples were compared with each other and standard PET polymer. A standard PET polymer has peaks around 720, 1094, 1241, and 1713 wavelengths (cm^{-1}) which correspond to aromatic CH out of plane bending (720 cm^{-1}), C-O stretching (1094

cm^{-1} and 1241 cm^{-1}), and C=O stretching (1713 cm^{-1}) (Jung et al., 2018). When Figure 3.11 is examined, all of the samples showed the characteristic PET peaks. FTIR analysis results of virgin fiber grade PET, r-PET flakes, r-PET granule, and *d*-PET polymers were very similar to each other and standard polyester and no significant differences were detected in terms of functional groups, and bonding sites. However, the percent transmittances of *d*-PET were much lower than those of other samples. This can be due to the fact that the lower frequencies in *d*-PET were obtained for the weaker bonds the atoms vibrate at (Master Organic Chemistry).

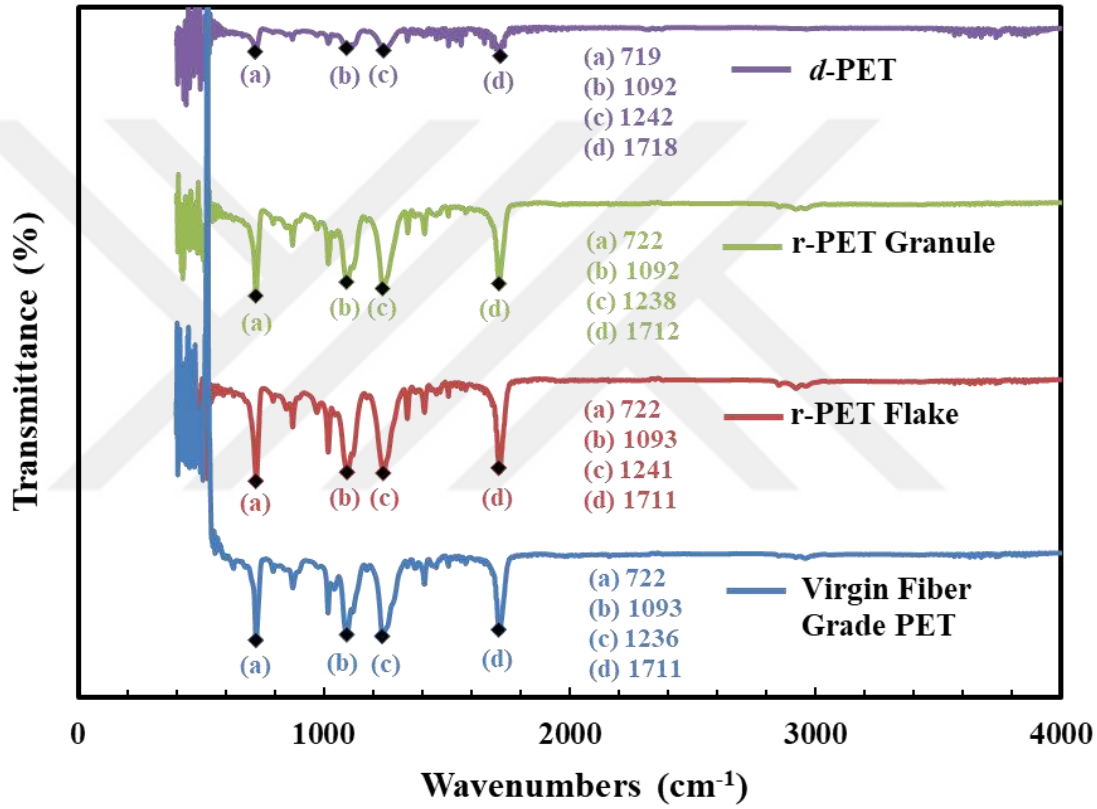

Figure 3.11 Comparative FTIR spectra of virgin fiber grade PET, r-PET flakes, r-PET granule, and *d*-PET

3.3.5 Carbonization Process Observation

10 mm *d*-PET samples were used in the carbonization trials. The sample was placed on a ceramic plate. N_2 gas was purged at the 100 L/h flow rate. The carbonization trial was performed from room temperature to carbonization temperature of 500 ºC with a heating rate of 5 ºC/min. The residence time at the maximum temperature (500 ºC) was set for 1 hour. After the trial, it was observed that there was no carbonized material left on the ceramic plate (Figure 3.12-a). Instead, carbonized

materials were around the plate. This happened because the ceramic plate had a porous structure which could let the molten material to flow into at melting temperatures. So it did not remain on the surface and entered inside the pores. Also, there was no constricted volume for the molten *d*-PET material to flow upon heating. This leaded us to design and use a metal tray (Figure 3.12-b). Following carbonization trial was performed under the same conditions with the metal plate. After the trial was completed, it was observed that there was carbonized material in the metal tray (Figure 3.12-c).

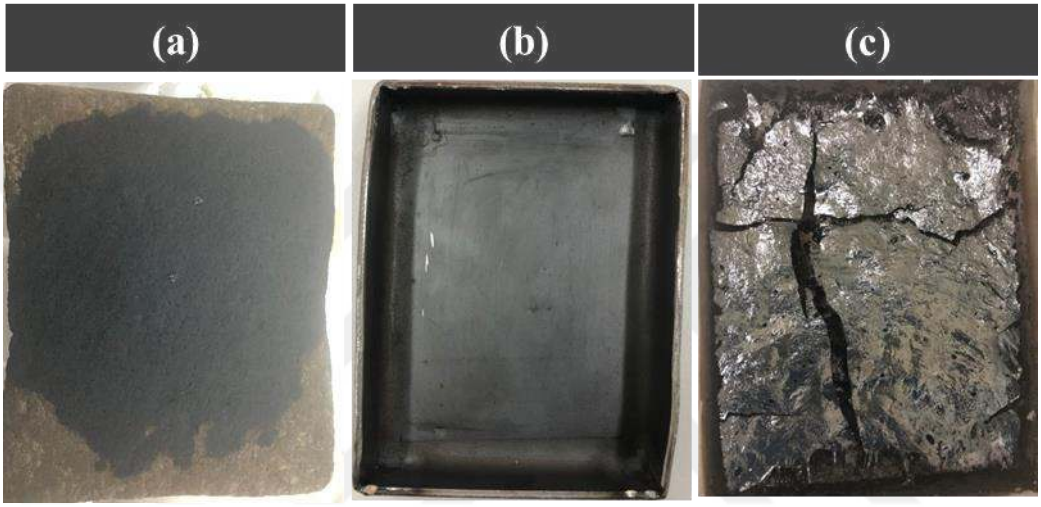

Figure 3.12 Pictures of ceramic plate (a) and metal tray before (b) and after (c) carbonization trials

3.3.6 Effect of Material Size on Carbonization Efficiency

In order to determine the effect of material size on the carbonization efficiency, experiments were carried out with 10 mm and 30 mm *d*-PET samples at the same carbonization process conditions (T_c= 500 °C, HR= 5 °C/min, t_r= 1 h, FR= 100 L/h, N_2 atmosphere). Carbonization experiments were successfully performed and both carbonized materials and chemicals were obtained as seen in Figure 3.13.

Figure 3.13 Carbonized materials and chemicals obtained from the carbonization of 10 mm and 30 mm *d*-PET

While carbonized material yields were found to be 20.6% and 22.5%, chemical yields were 17.3% and 14.3% for 10 mm and 30 mm *d*-PET, respectively (Table 3.6). As the size of the material increased, the amount of carbonized material increased and chemical yield decreased. This was due to the better dissipation of heat in small sized materials which induced easier gasification. Niksiar et al. (2015) claimed that material size has a slight effect on the kinetic parameters. However, our results indicated that material size had a nonnegligible effect on the kinetic parameter. When the total yields were compared, higher yield of 37.9% were obtained for 10 mm than 30 mm. Therefore, following experiments were carried out with 10 mm *d*-PET.

Table 3.6 The effect of particle size on the carbonized material and chemical yields

***d*-PET Particle Size (mm)**	**Carbonized Material Yield (%)**	**Chemical Yield (%)**	**Total Yield (%)**
10	20.6	17.3	37.9
30	22.5	14.3	36.8

3.3.7 Effects of Auxilary Gas Types and Gas Flow on Carbonization Efficiency

In order to determine the effect of auxiliary gas type on the carbonization efficiency, experiments were carried out with N_2 and O_2 atmospheres at the same carbonization process conditions (*d*-PET Size= 10 mm, T_c= 500 °C, HR= 5 °C/min, t_i= 1 h, FR= 100 L/h). Carbonization experiments were successfully performed at N_2 atmosphere (Figure 3.14). However, during the carbonization experiments by using O_2 gas atmosphere, it was observed that there was too much gas released from the system. Also, there was more gas odor in the laboratory. After the experiment, it was seen that the inside of the furnace was burned. Acccording to visual observations, the carbonized material obtained from O_2 gas came out in two different colours as brown and black (Figure 3.14). This was caused by O_2 gas which could partially induce oxidation and decomposition upon heating.

While carbonized material yields were found to be 4.4% and 20.6%, chemical yields were 13.4% and 17.3% for *d*-PET by using O_2 and N_2 auxilary gases, respectively (Table 3.7). Total percent yield results obtained from the carbonization under O_2 and N_2 auxilary gases showed a great deal of difference which was more than 20%. The reason for this could be the higher gasification under O_2 atmosphere. Lee et al. (2017) performed pyrolyses of waste PET bottles in N_2 and CO_2 atmospheres. In this study, percent yields obtained from these pyrolyses were compared and found to be 38% in N_2 and 28% in CO_2 atmospheres. The remaining by-products of the pyrolyses were the released gas which was higher in the pyrolysis under CO_2 atmosphere. He mentioned that in the pyrolysis under CO_2 atmosphere, thermal separation was accelerated compared to the pyrolysis under N_2 atmosphere, and therefore more gas by-products were obtained in CO_2 atmosphere.

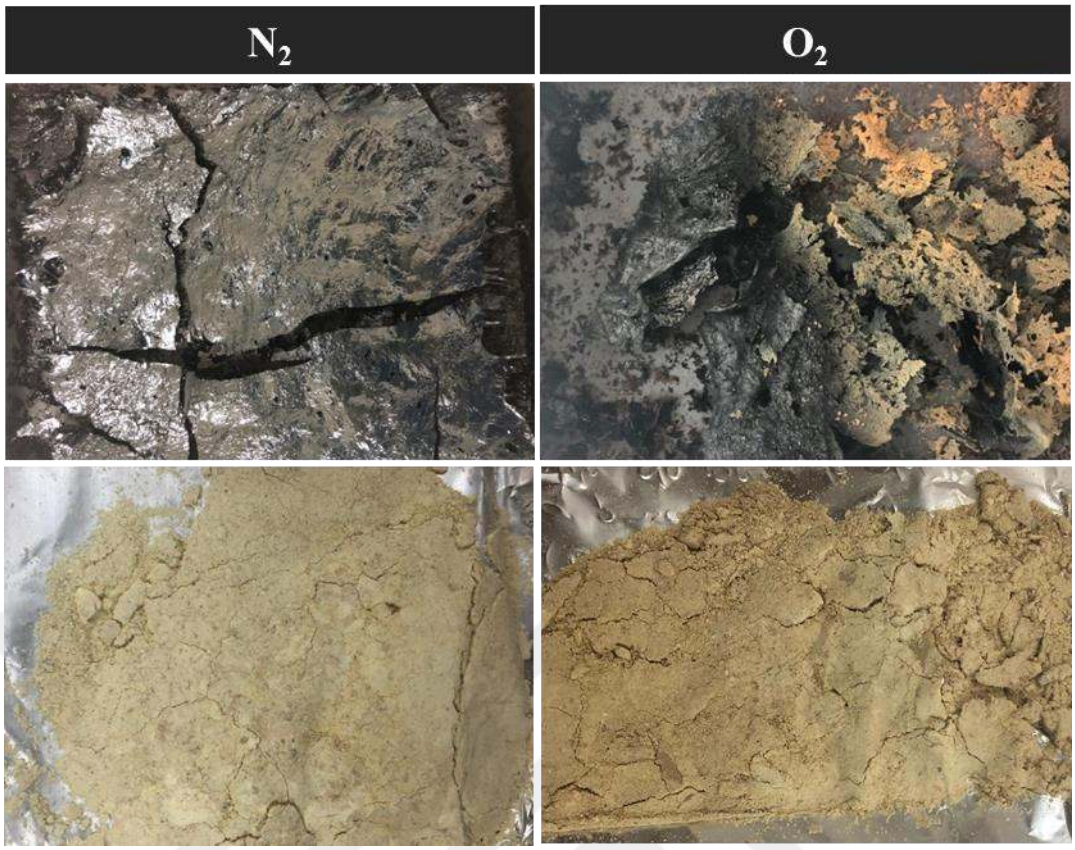

Figure 3.14 Carbonized materials and chemicals obtained from the carbonization of *d*-PET by using O_2 and N_2 auxilary gases

Table 3.7 The effect of auxiliary gas type on the carbonized material and chemical yields

Auxiliary Gas	Carbonized Material Yield (%)	Chemical Yield (%)	Total Yield (%)
O_2	4.4	13.4	17.8
N_2	20.6	17.3	37.9

In order to determine the effect of gas flow rate on the carbonization efficiency, experiments were carried out with 50 L/h and 100 L/h N_2 gas flow rate at the same carbonization process conditions (*d*-PET Size= 10 mm, T_c= 500 °C, HR= 5 °C/min, t_r= 1 h, N_2 atmosphere). Carbonization experiments were accomplished and both carbonized materials and chemicals were obtained as seen in Figure 3.15. Visual examinations revealed that carbonization at 50 L/h N_2 gas flow rate gave more brownish by-products. This was a sign of low blanketing with N_2 which was supposed to sweep away the O_2 from the heating zone of the furnace.

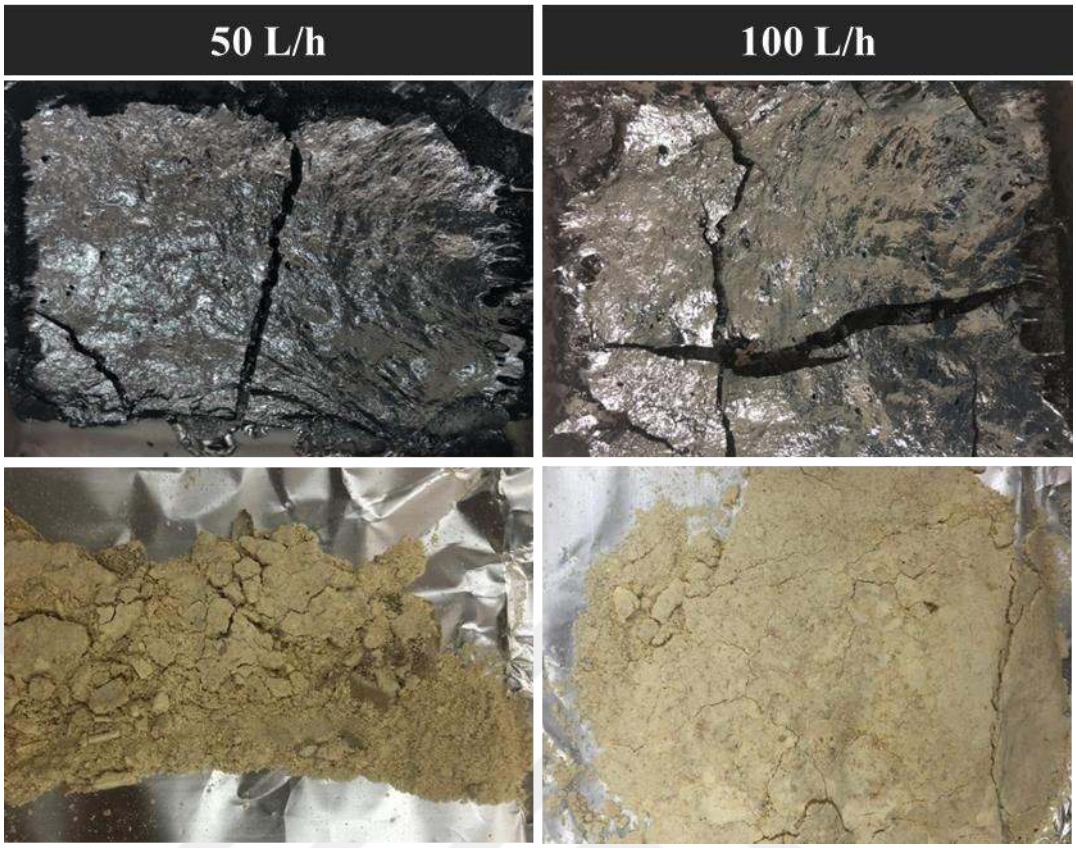

Figure 3.15 Carbonized materials and chemicals obtained from the carbonization of *d*-PET with different N_2 gas flow rates of 50 L/h and 100 L/h

While carbonized material yields were found to be 22.1% and 20.6%, chemical yields were 13.0% and 17.3% for *d*-PET with gas flow rates of 50 l/h and 100 l/h, respectively (Table 3.8). As the flow rate of the gas increased, the amount of carbonized material decreased and chemical yield increased. When the total yields were compared, higher yield of 37.9% were obtained for 100 L/h N_2 gas flow rate. This was due to the fact that 50 L/h N_2 gas flow rate was not sufficient enough to sweep away the O_2 from the the heating zone of the furnace which could cause more gasification. Thus, it was determined that 100 L/h N_2 gas flow provided more sufficient blanketing than 50 L/h N_2 gas flow.

Table 3.8 The effect of gas flow rate on the carbonized material and chemical yields

Gas Flow Rate, FR (L/h)	**Carbonized Material Yield (%)**	**Chemical Yield (%)**	**Total Yield (%)**
50	22.1	13	35.1
100	20.6	17.3	37.9

3.3.8 Effects of Residence Time and Heating Rate on Carbonization Efficiency

In order to determine the effect residence time on the carbonization efficiency, experiments were carried out at the residence times of 1 hour and 2 hours while other conditions were kept the same (*d*-PET Size= 10 mm, T_c= 500 °C, HR= 5 °C/min, FR= 100 L/h, N_2 atmosphere). Carbonization experiments were successfully performed and both carbonized materials and chemicals were obtained as seen in Figure 3.16.

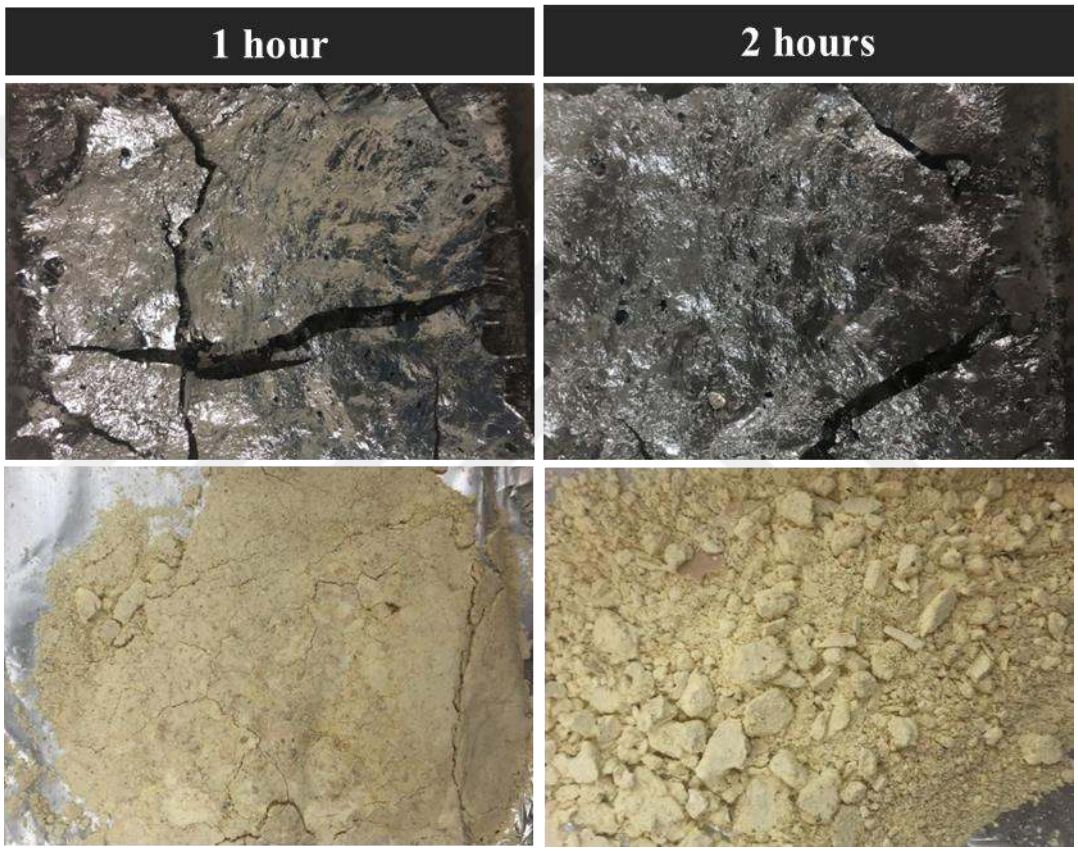

Figure 3.16 Carbonized materials and chemicals obtained from the carbonization of *d*-PET with 1 hour and 2 hours residence time

While carbonized material yields were found to be 20.6% and 19.1%, chemical yields were 17.3% and 18.6% for *d*-PET at residence times of 1 hour and 2 hours in carbonization, respectively (Table 3.9). As the residence time in carbonization increased, the amount of carbonized material reduced and chemical yield increased. When total yields were compared, there were not significant differences between 1 hour (37.9%) and 2 hours (37.7%) residence time. Generally, in the pyrolysis process using long residence time yields more amount of carbonized material (Heikkinen et

al, 2004). But such trend was not observed in our study. The reason could be that only 20 g of *d*-PET material was carbonized and for such amount the residence time of 1 hour might be enough. Therefore, following experiments were carried out by using 1 hour residence time.

Table 3.9 The effect of residence time on the carbonized material and chemical yields

Residence Time in Carbonization, t_r (min)	**Carbonized Material Yield (%)**	**Chemical Yield (%)**	**Total Yield (%)**
60	20.6	17.3	37.9
120	19.1	18.6	37.7

In order to determine the effect of heating rate on the carbonization efficiency, experiments were carried out at the heating rates of 5 °C/min and 10 °C/min while other conditions were kept the same (*d*-PET Size= 10 mm, T_c= 500 °C, t_r= 1 h, FR= 100 L/h, N_2 atmosphere). Carbonization experiments were successfully performed and both carbonized materials and chemicals were obtained as seen in Figure 3.17.

While carbonized material yields were found to be 20.6% and 21.6%, chemical yields were 17.3% and 17.7% for *d*-PET at heating rates of 5 °C/min and 10 °C/min, respectively (Table 3.10). As the heating rate increased, both carbonized material and chemical yields increased. When the total yields were compared, the higher yields of 39.3% were obtained for 10 °C/min heating rate. It was probably caused by the higher rate of gasification at higher heating rate which took more time to reach the temperature of carbonization. In order to obtain higher total yield following experiments were carried out at 10 °C/min heating rate.

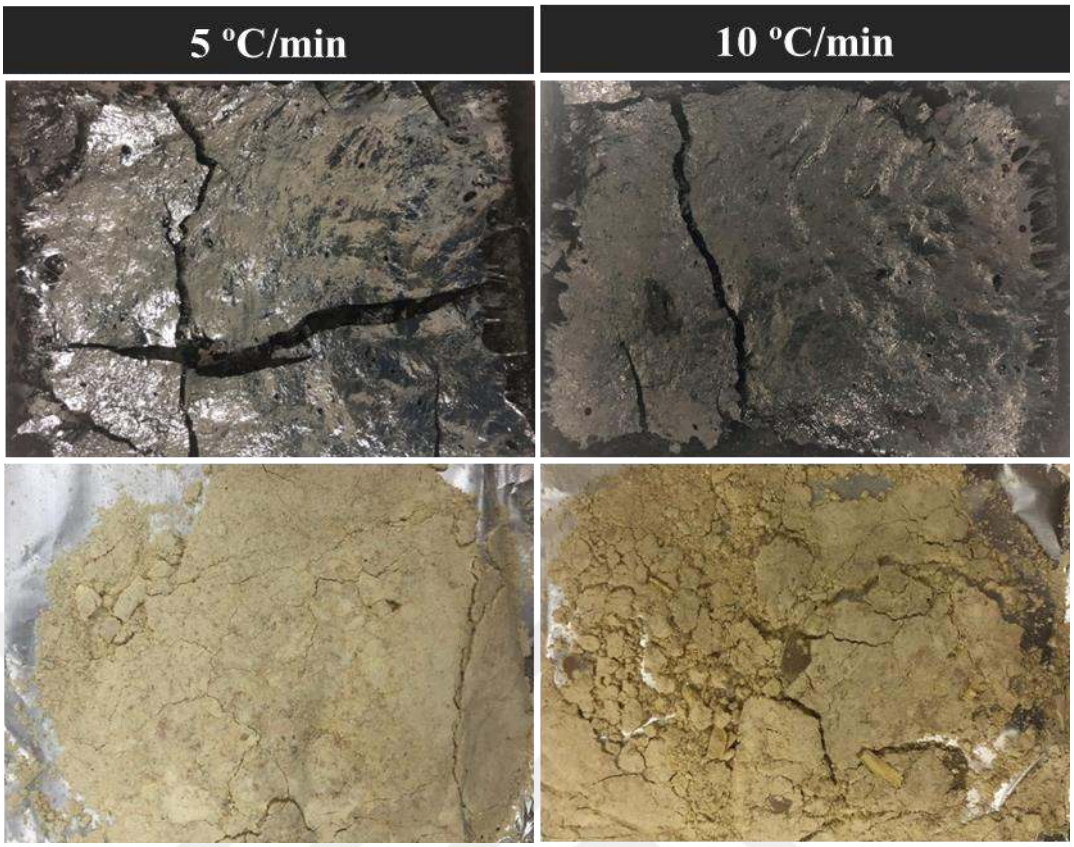

Figure 3.17 Carbonized materials and chemicals obtained from the carbonization of *d*-PET with 5 ºC/min and 10 ºC/min heating rates

Table 3.10 The effect of heating rate on the carbonized material and chemical yields

Heating Rate, HR (°C/min)	Carbonized Material Yield (%)	Chemical Yield (%)	Total Yield (%)
5	20.6	17.3	37.9
10	21.6	17.7	39.3

3.3.9 Effect of Carbonization Temperature on Carbonization Efficiency

In order to determine the effect carbonization temperature on the carbonization efficiency, experiments were carried out at the carbonization temperatures of 450 ºC, 500 ºC, and 600 ºC while other conditions were kept the same (*d*-PET Size= 10 mm, HR= 10 °C/min, t_r= 1 h, FR= 100 L/h, N_2 atmosphere). Carbonization experiments were successfully performed and both carbonized materials and chemicals were obtained at all carbonization temperatures as seen in Figure 3.18.

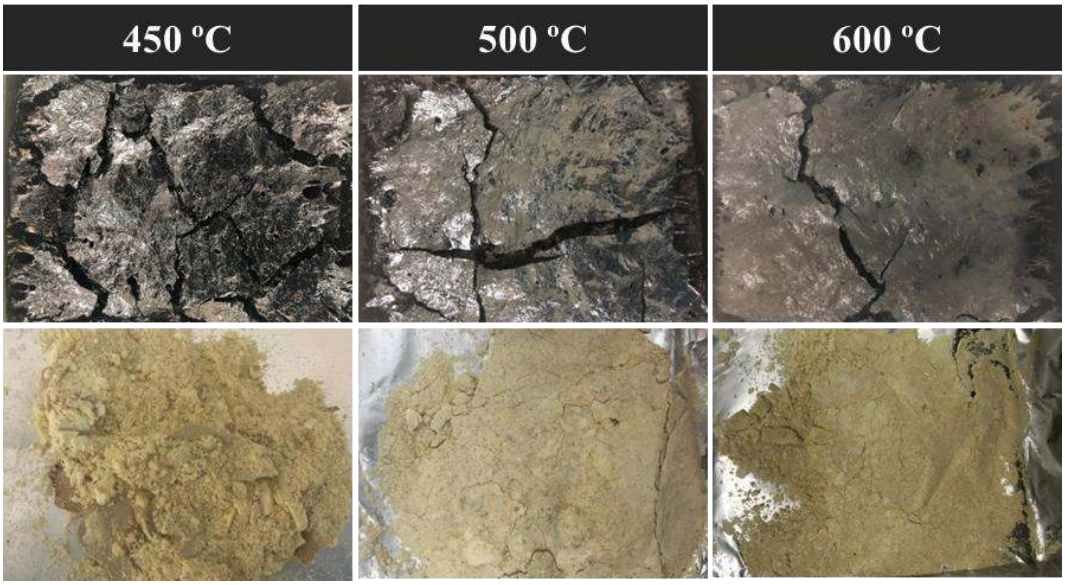

Figure 3.18 Carbonized materials and chemicals obtained from the carbonization of *d*-PET at different carbonization temperatures

While carbonized material yields were found to be 21.0%, 21.6%, and 20.4% chemical yields were 18.2%, 17.7%, and 15.7% for *d*-PET at carbonization temperatures of 450 °C, 500 °C, and 600 °C, respectively (Table 3.11). When the total yields were compared the highest total yield of 39.3% was obtained at 500 °C carbonization temperature. The carbonization temperature increase did not have much effect on the amount of carbonized material obtained after carbonization. However, the amount of chemicals obtained after carbonization reduced when the temperature was raised from 500 °C to 600 °C. The reason for this can be continuing gasification from the chemicals between 500 °C and 600 °C which could induce a reduction in the amount of chemicals and an increase in the amount of released gas. In other words, this was due to the gas phase transition of low molecular weight chemicals at higher temperatures. Our observations of continuing gas release between 500 °C and 600 °C also supported this justification. Dogan et al. (2017) and Shah et al. (2009) also reported that as the pyrolysis temperature increased, an increase in the amount of gas by-product was observed in the PET pyrolysis.

Table 3.11 The effect of carbonization temperature on the carbonized material and chemical yields

Carbonization Temperature, T_C (°C)	Carbonized Material Yield (%)	Chemical Yield (%)	Total Yield (%)
450	21	18.2	39,2
500	21.6	17.7	39,3
600	20.4	15.7	36,1

3.3.10 Chemical Analysis of Carbonization By-Products (Chemicals) of *d*-PET

The results of FTIR analysis of the chemicals collected from the furnace after the carbonization experiments under N_2 atmosphere were examined (Figure 3.19). According to the results, the wavelengths of the chemical obtained from *d*-PET wavelengths are 708 cm^{-1}, 933 cm^{-1}, 1291 cm^{-1}, and 1685 cm^{-1}. The wavelengths of standard benzoic acid has peaks around 707, 948, 1298, and 1684 wavelengths (cm^{-1}) which correspond to benzene ring (707 cm^{-1}), OH streching (948 cm^{-1}), OH stretching, and inplane bending (1298 cm^{-1}), and C=O stretching (1684 cm^{-1}) (Hayashi et al., 1966). Thus, it was determined that the chemicals obtained from the *d*-PET carbonization process under N_2 atmosphere were benzoic acid. Anuar Sharuddin et al. (2016) and Lee et al. (2017) conducted the pyrolysis of PET and chemicals obtained after pyrolyses were also found to be benzoic acid.

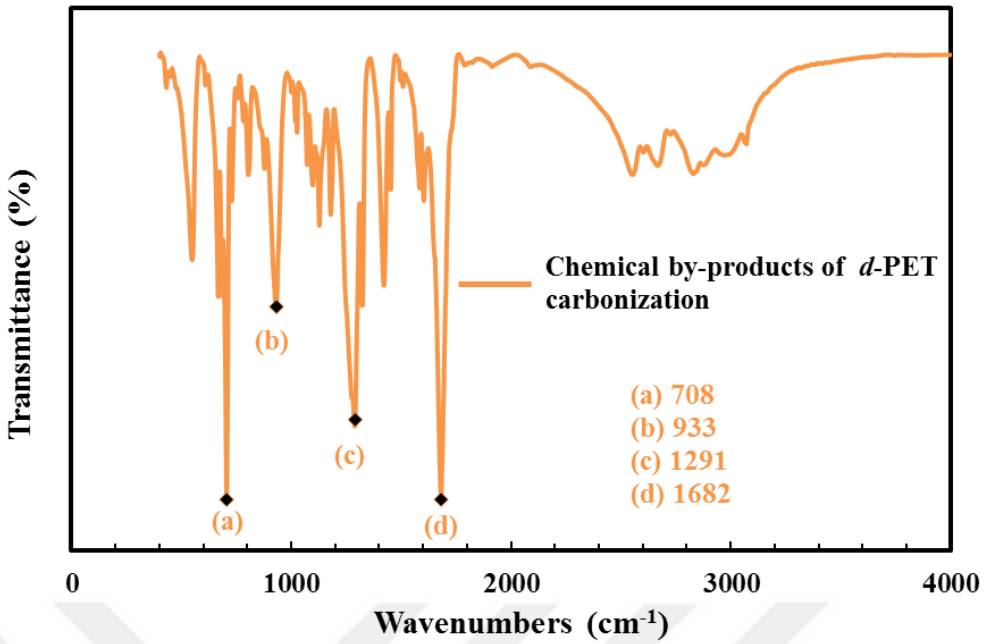

Figure 3.19 FTIR spectra of the chemicals collected from the furnace after *d*-PET carbonization

3.3.11 Elementel Analyses of *d*-PET and the Carbonized Materials Obtained From *d*-PET

XRF analysis of the *d*-PET was conducted to determine foreign inorganic materials inside the *d*-PET. According to results, *d*-PET contained Si, Ca, Ti, S, Sb, Cl, K, Fe, P, Al, and Cu elements (Table 3.12). During the manufacturing of PET fibers, some colour masterbatches are added and these masterbatches usually include Si, Ti, and Ca elements which were also detected in *d*-PET as expected. Sb and S elements can be encountered for the virgin PET polymerization. The existence of Cl, K, Fe, P, Al, and Cu elements can be originated from the recycling processes. This is because many foreign materials can be mixed with recycled polymers and these materials cannot be fully removed during recycling.

Table 3.12 XRF analysis result of *d*-PET

Element	Content (%)	Sigma, σ (wt. %)
Si	0.245	0.016
Ca	0.161	0.002
Ti	0.139	0.004
S	0.066	0.007
Sb	0.035	0.006
Cl	0.025	0.003
K	0.016	0.001
Fe	0.010	0.000
P	0.008	0.005
Al	0.006	0.005
Cu	0.004	0.003
Polymer	99.285	0.000

In order to identify and compare elementel compositions and percentages of the final carbonized materials obtained from r-PET flake and *d*-PET, analyses were carried out with carbonized samples processed at the same conditions (Sample Size= 10 mm, T_c= 500 °C, HR= 5 °C/min, tr= 1 h, FR= 100 L/h, N_2 atmosphere). Our results showed that the carbonization of the *d*-PET yielded higher carbon (C) percentage (99.12 wt%) than that of the r-PET (80.67 wt%) (Table 3.13). The reason for this can be caused from the differences in the molecular weights of the samples which was much lower for *d*-PET (M_n for *d*-PET= 2732 g/mol and M_n for r-PET= 37370 g/mol). Thus, it is expected to remove non-carbon elements (hydrogen and oxygen) easily and effectively from lower molecular weight precursor (Cuhadar, 2005). Unlike *d*-PET, other elements such as Si, P, S, K, and Ca were found in the carbonized materials obtained from the r-PET flake. The existence of these materials can be originated from the remaining foreign materials after the mechanical recycling and washing of the r-PET flakes.

Table 3.13 Elementel analysis results of the carbonized materials obtained from r-PET flake and *d*-PET

Sample Type		C	O	Si	P	S	K	Ca	Ti	Fe	Al	Cu
r-PET Flake	wt%	**80.67**	14.74	0.92	0.18	0.28	0.33	0.8	0.56	1.52	-	-
	σ	0.24	0.24	0.02	0.02	0.01	0.01	0.02	0.02	0.03	-	-
***d*-PET**	wt%	**99.12**	-	-	-	-	-	-	0.18	0.7	-	-
	σ	0.05	-	-	-	-	-	-	0.03	0.04	-	-

In order to identify and compare elementel compositions and percentages of the final carbonized materials obtained from different sizes of *d*-PET (10 mm and 30 mm), analyses were carried out with carbonized samples processed at the same conditions (T_c= 500 °C, HR= 5 °C/min, tr= 1 h, FR= 100 L/h, N_2 atmosphere). Our results showed that using 30 mm sample size yielded slightly higher C percentage (99.94 wt%) than using 10 mm sample size (99.12 wt%) for the carbonization of *d*-PET (Table 3.14). But it is important to point out that iron (Fe) percentage of 10 mm (0.7 wt%) was higher than that of 30 mm (0.06 wt%). The existence of Fe can be caused from the metal tray used in the carbonization or from the different spots of the *d*-PET materials used in the experiments. Note that during the experiments sometimes the carbonized materials were removed from the metal tray with scraping which might contaminate the carbonized sample. The existence of titanium (Ti) in the carbonized materials obtained from 10 mm *d*-PET was also arised from the different spots of the *d*-PET materials used in the experiments which can include colour masterbatches remainings of Si, Ti, and Ca. When Fe and Ti were omitted and non-existence of the oxygen (O) in the both 10 mm and 30 mm was considered, we can conclude that the sample size did not change the C percentage of the carbonized samples.

Table 3.14 Elementel analysis results of the carbonized materials obtained from 10 mm and 30 mm *d*-PET

***d*-PET Sample Size (mm)**		**C**	**O**	**Si**	**P**	**S**	**K**	**Ca**	**Ti**	**Fe**	**Al**	**Cu**
10	wt%	**99.12**	-	-	-	-	-	-	0.18	0.7	-	-
	σ	0.05	-	-	-	-	-	-	0.03	0.04	-	-
30	wt%	**99.94**	-	-	-	-	-	-	-	0.06	-	-
	σ	0.02	-	-	-	-	-	-	-	0.02	-	-

In order to identify and compare elementel compositions and percentages of the final carbonized materials obtained under different auxiliary gas atmosphere (N_2 and O_2), analyses were carried out with carbonized samples processed at the same conditions (Sample Size= 10 mm, T_c= 500 °C, HR= 5 °C/min, tr= 1 h, FR= 100 L/h). Our results showed that using N_2 auxilary gases for the carbonization yielded higher C percentage (99.12 wt%) than using O_2 auxilary gases (92.06 wt%) for the carbonization (Table 3.15). The existence of O in the carbonization products obtained under O_2 auxilary gas atmosphere was quite likely caused from the oxidation of the *d*-PET materials during the carbonization. As described before, existences of other elements (Si, K, Ti, and Fe) in the carbonized materials can be originated from the metal tray used in the carbonization (Fe) and the different spots of the *d*-PET materials used in the experiments (Si, K, and Ti).

Table 3.15 Elementel analysis results of the carbonized materials obtained from *d*-PET under O_2 and N_2 at atmospheres

Auxilary Gas Type		**C**	**O**	**Si**	**P**	**S**	**K**	**Ca**	**Ti**	**Fe**	**Al**	**Cu**
O_2	wt%	**92.06**	**7.52**	0.09	-	-	0.11	-	-	0.22	-	-
	σ	0.14	0.14	0.01	-	-	0.01	-	-	0.02	-	-
N_2	wt%	**99.12**	**-**	-	-	-	-	-	0.18	0.7	-	-
	σ	0.05	-	-	-	-	-	-	0.03	0.04	-	-

In order to identify and compare elementel compositions and percentages of the final carbonized materials obtained by using different flow rates (50 L/h and 100 L/h), analyses were carried out with carbonized samples processed at the same conditions

(*d*-PET Size= 10 mm, Tc= 500 °C, HR= 5 °C/min, tr= 1 h, N_2 atmosphere). Our results showed that using 50 L/h gas flow rate for the carbonization gave lower C percentage (75.73 wt%) than using 100 L/h gas flow rate (99.12 wt%) for the carbonization (Table 3.16). This was caused by the insufficient blanketing of N_2 inside the furnace at 50 L/h which could not swiped out the O_2 from the carbonization atmosphere and thereby oxidation took place. As described before, existences of other elements (Si, K, Ti, Fe, Al, Cu) in the carbonized materials can be originated from the metal tray used in the carbonization (Fe) and the different spots of the *d*-PET materials used in the experiments (Si, K, Ti, Al, and Cu) which may include the remainings from recycling or masterbatches.

Table 3.16 Elementel analysis results of the carbonized materials obtained from *d*-PET at gas flow rates of 50 L/h and 100 L/h

Gas Flow Rate (L/h)		**C**	**O**	**Si**	**P**	**S**	**K**	**Ca**	**Ti**	**Fe**	**Al**	**Cu**
50	wt%	**75.73**	**20.43**	1.19	-	-	0.5	-	0.08	0.7	1.25	0.11
	σ	0.23	0.23	0.02	-	-	0.01	-	0.01	0.03	0.02	0.03
100	wt%	**99.12**	**-**	-	-	-	-	-	0.18	0.7	-	-
	σ	0.05	-	-	-	-	-	-	0.03	0.04	-	-

In order to identify and compare elementel compositions and percentages of the final carbonized materials obtained by using different heating rates (5 °C/min and 10 °C/min), analyses were carried out with carbonized samples processed at the same conditions (*d*-PET Size= 10 mm, Tc= 500 °C, tr= 1 h, FR= 100 L/h, N_2 atmosphere). Our results showed that using 10 °C/min heating rate for the carbonization yielded slightly higher C percentage (99.56 wt%) than using 10 °C/min heating rate (99.12 wt%) for the carbonization (Table 3.17). However, when the percentages of other non-oxygen foreign elements (K, Ti, and Fe) which were considered as remainings from recycling (K), masterbatches (Ti), and metal tray (Fe) were excluded, there was no difference left between 5 °C/min and 10 °C/min heating rates.

Table 3.17 Elementel analysis results of the carbonized materials obtained from *d*-PET at carbonization heating rates of 5 °C/min and 10 °C/min

Heating Rate (°C/min)		C	O	Si	P	S	K	Ca	Ti	Fe	Al	Cu
5	wt%	**99.12**	-	-	-	-	-	-	0.18	0.7	-	-
	σ	0.05	-	-	-	-	-	-	0.03	0.04	-	-
10	wt%	**99.56**	-	-	-	-	0.08	-	0.09	0.27	-	-
	σ	0.03	-	-	-	-	0.01	-	0.01	0.02	-	-

3.3.12 Analysis of the Particle Size of the Milled Carbonized Materials

Carbonized materials obtained as a result of the carbonization process (*d*-PET Size= 10 mm, T_c= 500 °C, HR= 5 °C/min, t_r= 1 h, FR= 100 L/h, N_2 atmosphere) were milled at 400 rpm with different milling time of 5 minutes, 7.5 minutes, and 10 minutes. After milling process the particle sizes and size distributions were analyzed (Figure 3.20). According to the results of this analysis, the average smallest sized particles in the milled sample were measured as 610 nm at 5 minutes milling time, 530 nm at 7.5 minutes milling time and 200 nm at 10 minutes milling time. However, in addition to these low-sized carbon particles, it was observed that there were particles of approximately 5500 nm after 7.5 minutes and 10 minutes milling. Particle sizes show a wide size distribution. In addition, the device cannot measure over 10 μm. As a result of the physical measurements, it was found that there were particles over 10 μm.

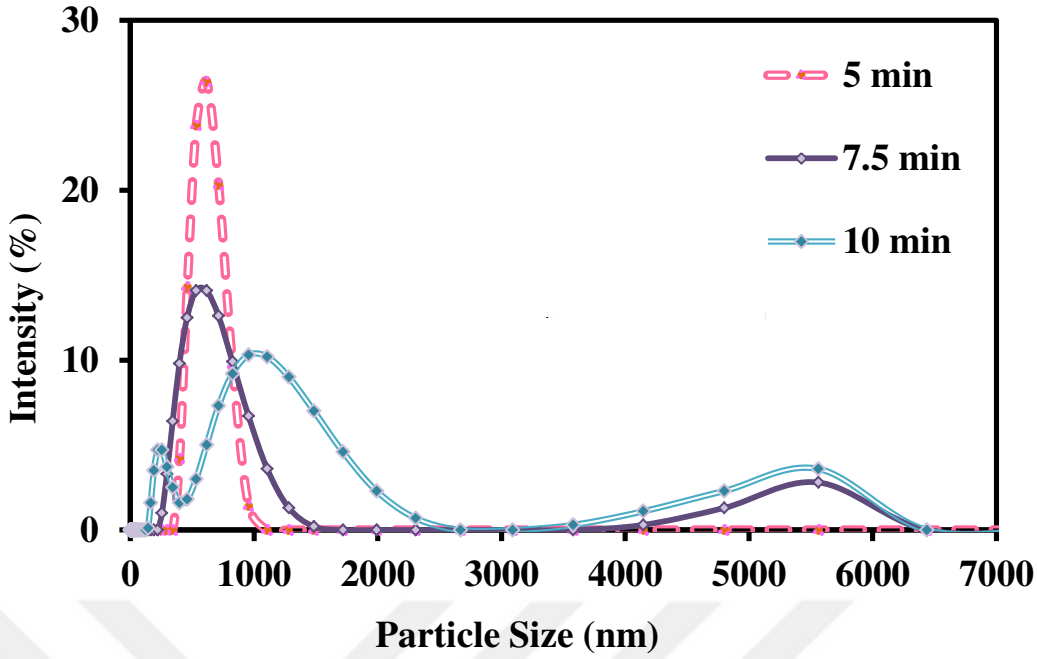

Figure 3.20 Size measurements of the carbonized particles after 5 min, 7.5 min and 10 min milling at 400 rpm

The carbonized materials obtained as a result of the carbonization process (*d*-PET Size= 10 mm, T_c= 500 °C, HR= 5 °C/min, t_r= 1 h, FR= 100 L/h, N_2 atmosphere) were milled for 10 min with different milling speeds of 350 rpm, 400 rpm, and 450 rpm. After milling process the particle sizes and size distributions were analyzed (Figure 3.21). According to the results of this analysis, the average smallest sized particles in the milled sample were measured as 250 nm at 350 rpm, 190 nm at 400 rpm and 160 nm at 450 rpm. In addition to the lowest-sized carbon particles, it was observed that there were particles with sizes around 800 nm and 5500 nm. Particle groups of 800 nm and 5500 nm particularly showed a wide size distribution. Since the device could not measure more than 10 µm, it could not be determined whether there were particles over 10 µm. However, in physical measurements, it was found that there were also particles over 10 µm.

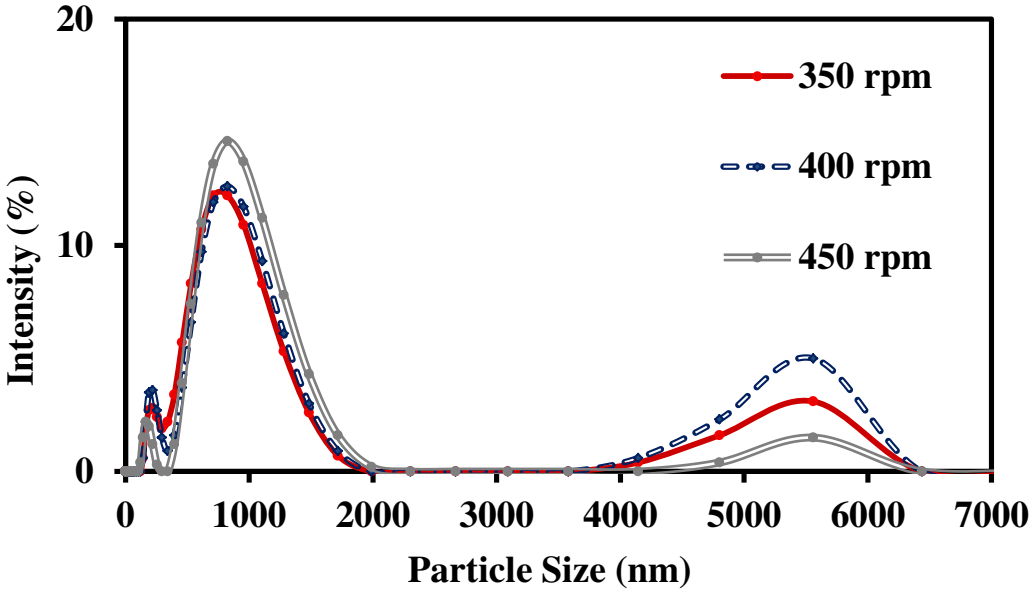

Figure 3.21 Size measurements of the carbonized particles milled at 350 rpm, 400 rpm, and 450 rpm for 10 min

Size distributions of the milled carbonized materials passed through the first milling cycle were examined and it was decided that the particle sizes were not small enough to use as a carbon powder in masterbatches. Therefore, the milled carbonized materials were subjected to the second milling. In the second milling, the carbonized materials were milled for 15 min at 450 rpm and for 30 min at 600 rpm (Figure 3.22). As seen in Figure 3.22 the volume of the carbonized particles milled for 30 min at 600 rpm was higher than the carbonized particles milled for 15 min at 450 rpm which was an indication of obtainining smaller-sized particles or powders.

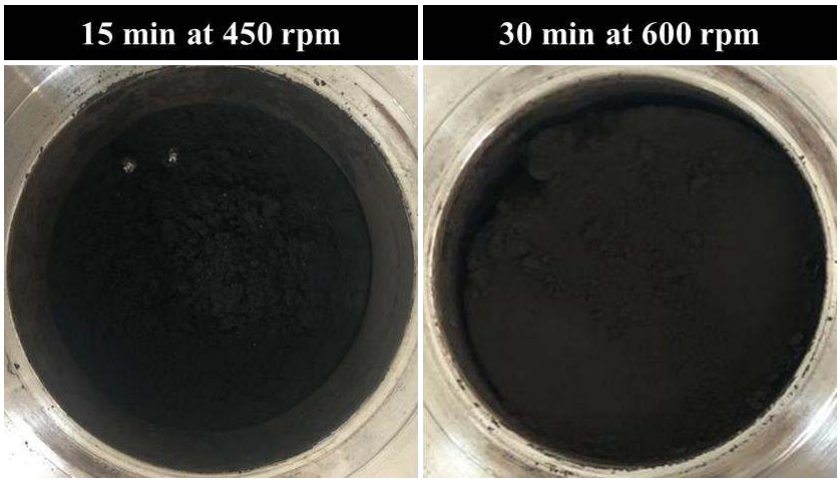

Figure 3.22 Pictures of the carbonized materials milled for 15 min at 450 rpm and for 30 min 600 rpm

After the second milling process the particle sizes and size distributions were analyzed. Size measurement results showed that the average particle size for the milled samples at 600 rpm for 30 min were 390 nm with a high intensity peak (Figure 3.23). Even though there were 190 nm particles for the milled samples at 450 rpm for 15 min, their intensity was so low and there were particles around 1000 nm and 5560 nm with much higher intensities.

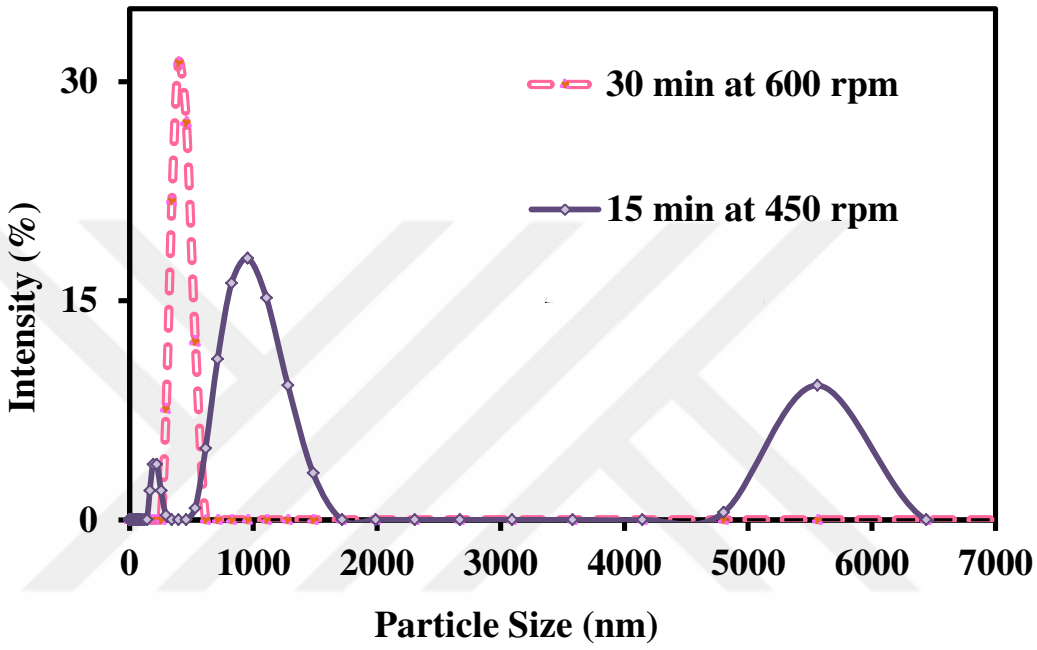

Figure 3.23 Size measurements of the carbonized particles milled at 450 rpm 15 for min and 600 rpm for 30 min (second milling)

SEM images of the milled carbonized materials obtained from the first (for 15 min at 450 rpm) and second milling (for 30 min at 600 rpm) were shown in Figure 3.24. SEM images clearly showed that there were variations in the particle sizes of the carbonized materials after the first milling. On the other hand, after the second milling the particle size distribution were successfully narrowed and average particles sizes were favorably reduced.

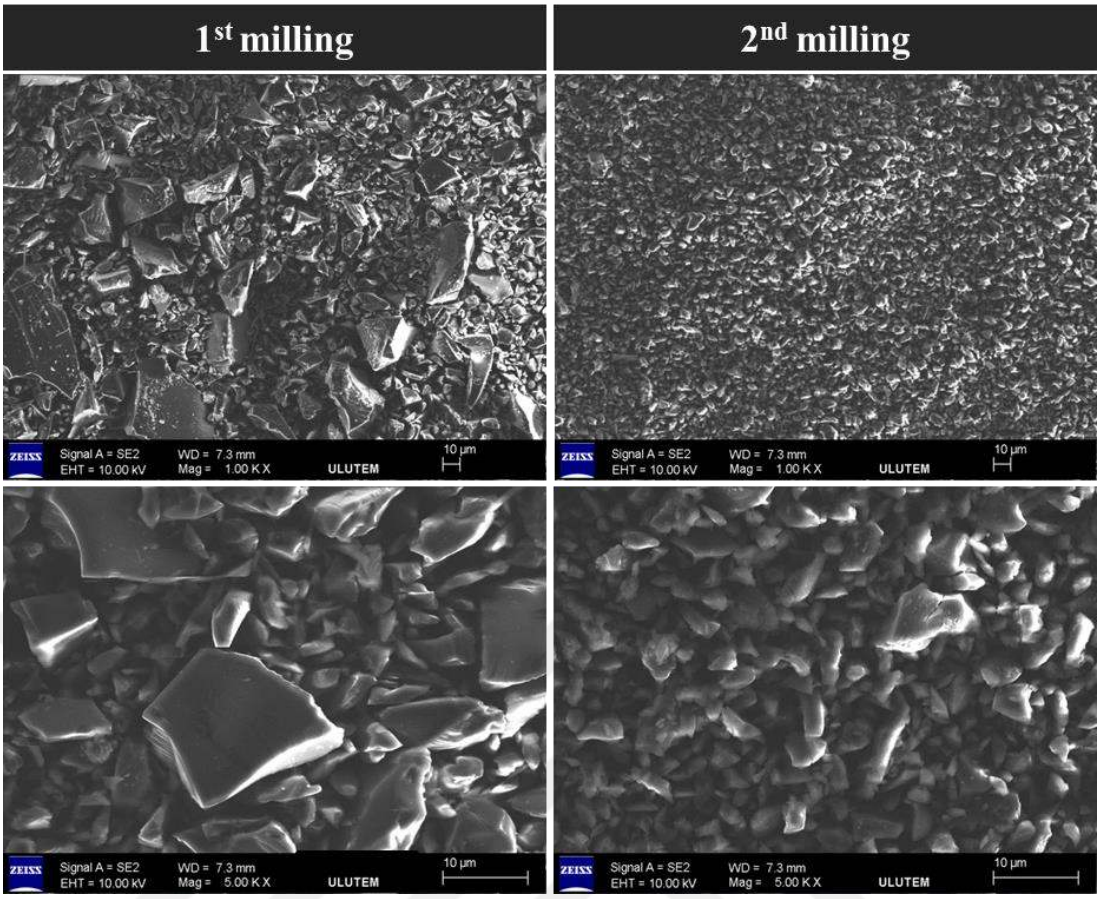

Figure 3.24 SEM images of the carbonized materials after the first (for 15 min at 450 rpm) and the second milling (for 30 min at 600 rpm)

CHAPTER 4

INVESTIGATION OF PHYSICAL AND MECHANICAL PROPERTIES OF FULLY RECYCLED FIBERS COLOURED WITH CARBON POWDER OBTAINED FROM DEGRADED PET (*d*-PET)

4.1 Introduction

Utilization rates of recyclable plastics have never caught up with new plastics made from virgin polymers. Currently, high proportions of plastics are being thrown away or disposed of. Polyethylene terephthalate (PET) is the most preferred polymeric raw for textiles, bottling, packaging indudtries. In textile industry, one of the most widely usage of PET polymer is filament or fiber formation. The demand for PET fiber has been increasing in recent years (Frida, 2018). This leads to an increase in the PET waste formation as a solid waste. Incineration of wastes can reduce the volume by 90% (Hoornweg et al., 2012). However, the incineration has negative effects on human health and the environment. It may be suitable for medical waste, but it should not be preferred for recyclable thermoplastic materials such as PET. PET is not a biodegradable material so it takes about several hundred years to be decomposed in the nature. On the other hand, when the used PET materials are collected properly, they can be recycled.

The PET can be recycled several times. However, after several recycling processes, some portions of the PET polymer can degrade due to severe mechanical and thermal treatments occurred especially in the existence of oxidation agents and environment. This degradation can affect the various properties of the PET such as chemical composition, chain conformation, molecular weight (M_W), M_W distribution, and crystallinity (Frida, 2018). The degraded PET (*d*-PET) polymer

cannot be used and therefore it is thrown away to the environment as a waste or is incinerated in burning ovens which unfortunately increases the released CO_2 emmision.

Some researches conducted studies to obtain energy and by-products from polymeric materials' waste using pyrolysis technique Anuar Sharuddin et al. (2016). As a result of the pyrolysis process, oil or chemical, gas and carbonized materials were obtained as by-products. Anuar Sharuddin et al. (2016) studied the pyrolysis of the PET bottle wastes and found that the amount of obtained by-products changed with processing conditions of the pyrolysis including heating rate, residence time, and temperature. Slow heating rate, low temperature, and long residence time in the pyrolysis process generally led an increase in the amount of the obtained carbonized materials from PET bottle waste.

In the literature, there was no study conducted on the pyrolysis or carbonization of the *d*-PET. Also, studies related with the pyrolysis of PET bottle wastes were limited and only focused on the formation of the oil or chemical, gas and carbonized materials (Sophonrat, 2019). These studies do not concentrate on the usage of these by-products in a useful medium. In this regard, our studies which were presented at Chapter 3 initially focused on the formation of the chemicals and carbonized materials from *d*-PET which is the waste of the waste. This part of the study focused on our efforts to use the recycled carbon powder (r-CP) obtained from the carbonized materials of *d*-PET in forming a fully recycled colour masterbatch (frc-MB) composites. This study also includes the formation of fully recycled and coloured PET fibers or filaments (frc-PET) containing only frc-MB composites and r-PET flakes. In this regard, initially ratios of the r-CP in frc-CMB were varied during the formation of frc-MBs and their colour analyses were carried out to determine the optimum r-CP addition. Secondly, frc-PET filaments were obtained at different loading of the frc-MB to r-PET matrix polymer. After frc-PET filaments were successfully formed, their colour and mechanical properties were investigated with respect to varying ratios of frc-MB in fibers.

4.2 Materials and Methods

4.2.1. Materials

r-PET flakes (12 mm x 12 mm), r-PET particles (average diameter < 2 mm) and r-CP (average diameter = 390 nm) obtained from *d*-PET were used in the study. While r-PET flakes and particles were supplied from GAMA Recycle Elyaf ve İplik San. A. Ş. (Gaziantep/TURKEY), r-CPs were formed from *d*-PET in the laboratory (see Chapter 3). Like *d*-PET, r-PET particles were the unused wastes of r-PET flakes.

4.2.2. Formation of Fully Recycled Colour Masterbatch (frc-MB) Composites

r-PET particles were used as matrix for preparing frc-MB composites. r-PET particles were initially dried for 6 hours at 145 °C. r-CPs and r-PET particals were dry mixed. Mixtures were then fed into a twin screw extruder (screw diameter = 21.7 mm; L/d = 40 mm). The extrusion blending was carried out with a temperature profile of 100 °C, 240 °C, 270 °C, 270 °C, 280 °C, and 280 °C, for the sequential heaters, respectively. The rotation speed of the twin screw extruder was set to 50 rpm. The feed rate was adjusted to be 75 g/min. r-CP ratios in r-PET matrix were 16.6 wt% and 30 wt%. The extruded materials were come out in the form of spaghetti. These extruded materials were quenched in a water bath and they were sliced into granules by cutter/shredder. Thus, frc-MB composites including 16.6 wt% and 30 wt% r-CPs were formed.

4.2.3. Preparion of Test Plate

Test plates were created by using a heat press machine. Temperature values of plates were set on 290 °C. During heat pressing, a non-stick wax paper was used to prevent polymeric materials from sticking to hot plates. After the frc-MB composites were placed between the plates, it was left for 5 minutes to soften. Then, three pressing steps were sequentially applied at 30 Bar for 5 seconds, 60 Bar for 5 seconds, 110 Bar for 5 seconds. After completing the first cycle of the heat pressing, the second cycle was applied with the same steps. The test plate taken from the hot press was then placed between the cold press plates in which test plates were cooled at pressure of 100 Bar for 60 seconds.

Figure 4.1 Twin screw extruder, water bath, and cutter/slicer used in the formation of frc-MB composites

4.2.4. Production of Fully Recycled and Coloured PET (frc-PET) Filaments

A laboratory type melt spinning machine (screw diameter = 25 mm; L/d = 32.5) was used to produce frc-PET filaments. r-PET flake and frc-MB composites were initially dried at 145 °C for 8 hours. The frc-MB composites and r-PET flakes were then dry mixed at frc-MB composite ratios of 0 wt% (control sample), 5 wt%, 10 wt% and 20 wt%. The mix was carefully fed to the hooper of the melt spinning machine .The melt spinning was carried out with a temperature profile of 130 °C, 270 °C, 285 °C, 285 °C, 290 °C, and 290 °C, for the sequential heaters of the extruders, respectively. While the extruder screw speed was set at 14 rpm, the molten polymer feed ratio was adjusted to be 100 g/min. Rotation speeds of godets were 600 rpm for Godet 1, 650 rpm for Godet 2, 1900 rpm for Godet 3, and 2050 rpm for Godet 4. Winder speed was set as 2090 rpm. Drawing godets of 2 and 3 were heated at 100 °C and 90 °C, respectively.

Figure 4.2 Laboratory type melt spinning machine used for the production of frc-PET filaments

4.2.5 Morphological Analysis

Cross-sectional and longitudinal images of frc-PET fibers were taken with the help of an optical microscope for morphological analysis. The frc-PET fiber samples were cut and placed in between slides to obtain longitudinal images at 10x magnification. In order to obtain cross-sectional images, frc-PET fiber samples and different coloured threads were placed together into a cross-section kit for providing a contrast in the images. frc-PET fibers and coloured threads out of the kit were then cut with a razor blade. The kit was placed under microscope lens and cross-sectional images were taken at 10x magnification.

4.2.6 Colour Difference Analysis

DATACOLOR 650 colour spectrophotometer was used for colour measurements of frc-MB test plates and frc-PET filaments (Figure 4.3). While frc-MB test plates were

directly used, frc-PET filaments were wound with uniform tension and the same thickness on cardboards for sampling in the colour analysis. Measurements were made according to the CIELab system under the D65 light source with a standard observation angle of 10°. Total colour difference between sample filaments was calculated with Equation 4.1 (Foisal, 2018; McGuire, 1992).

$$\Delta E^* = ((\Delta L^*)^2 + (\Delta a^*)^2 + (\Delta b^*)^2)^{0.5} \quad (4.1)$$

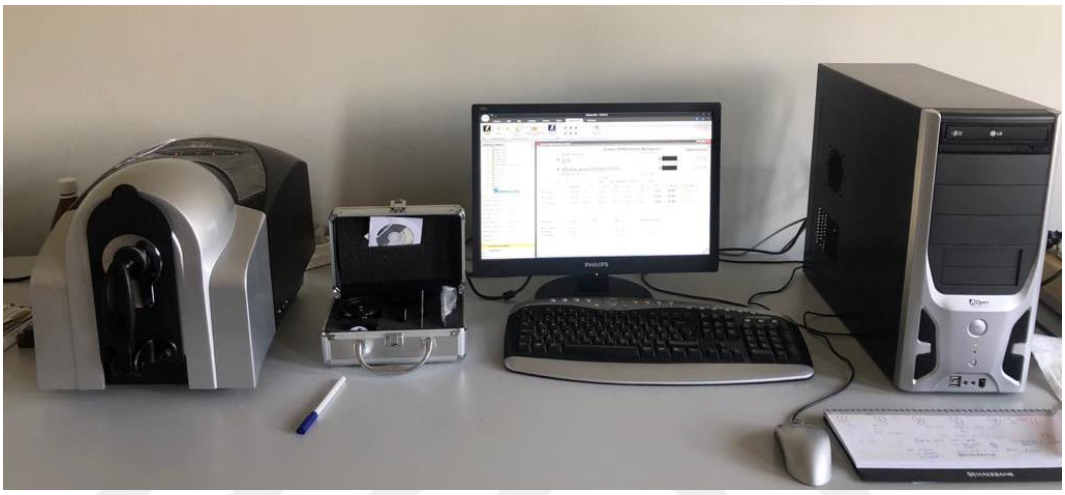

Figure 4.3 DATACOLOR 650

4.2.6 Testing of Mechanical Properties

Single-fiber tensile strength measurement device (Changzhou JinSong YG001B) was used to obtain tensile strength and elongation properties of frc-PET fiber samples. The filaments were cut to a length of 50 mm to obtain fibers. Before the tensile test the linear density (dtex) of the each fiber sample was measured. The dtex of the sample was entered into the device software. A single fiber was then attached to the clips. The fiber attached to the clips was placed in the clamping distance of 10 mm and the test was performed. From each sample, 20 single-fiber strength tests were done and the average of the results was calculated. ASTM D3822/D3822M-14 (Standard Test Method for Tensile Properties of Single Textile Fibers) testing standard was followed for the testing.

4.3 Results and Discussions

4.3.1 Effect of Recycled Carbon Powder (r-CP) Ratio on Colour Properties of Fully Recycled and Coloured Masterbatch (frc-MB) Composites

Colour properties of frc-MB composites containing 16.6 wt% and 30 wt% r-CPs (Figure 4.4) were characterized from the prepared test plates (Figure 4.5). In order to simplify the naming of these composites, frc-MB composites containing 16.6 wt% and 30 wt% r-CPs were refered as frc-MB-16.6 and frc-MB-30, respectively.

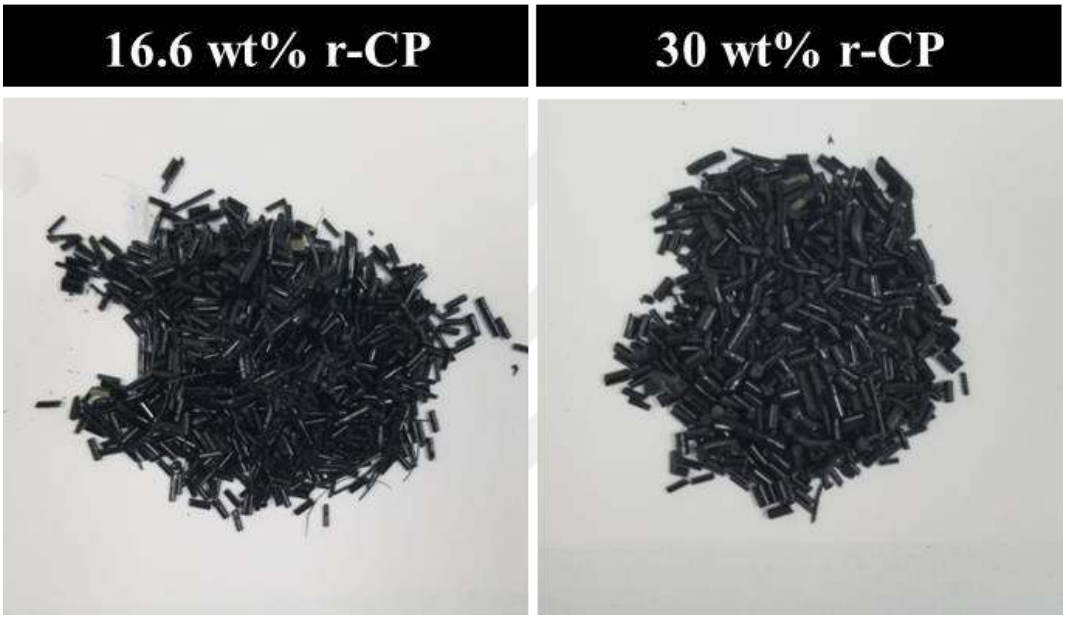

Figure 4.4 frc-MB composites containing 16.6 wt% and 30 wt% r-CPs

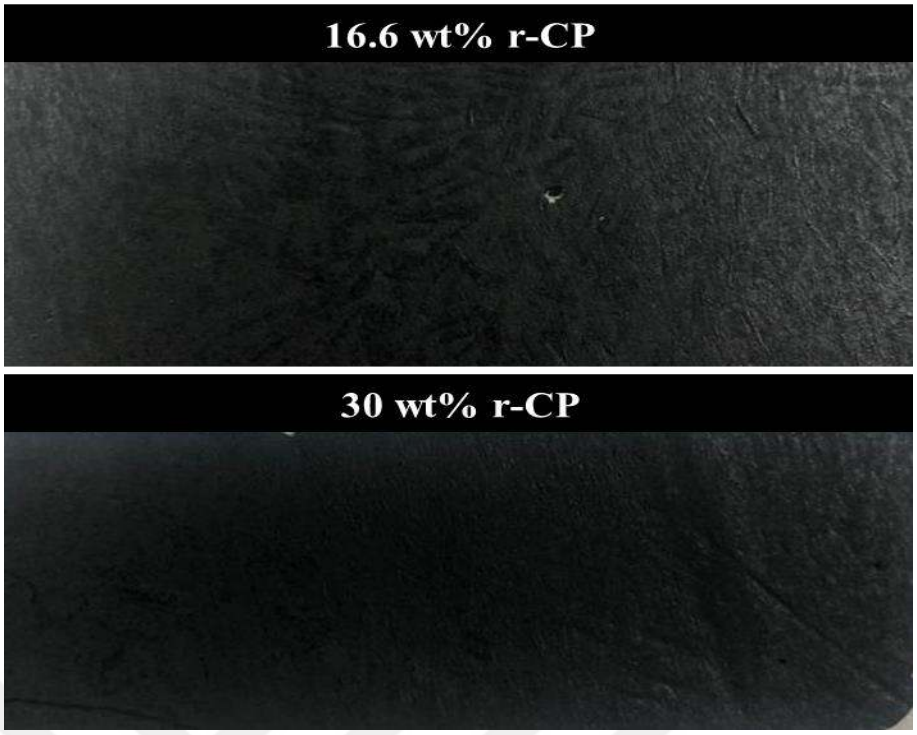

Figure 4.5 Test plates of frc-MB composites containing 16.6 wt% and 30 wt% r-CPs

The test plate of frc-MB-16.6 was used as the reference and measurements were taken against the reference test plate. The ΔE* value of test plates was calculated using Equaton 4.1. and found as 0.81. Ipek (2018) stated that when the ΔE* is smaller than one there is no serious colour difference between samples. Therefore, it can be said that there was no serious colour difference (ΔE*=0.81<1) between test plates of frc-MB-16.6 and frc-MB-30. According to the brightness results, brightness of frc-MB-16.6 (4.2) was found to be very close to that of frc-MB-30 (4.3) (Table 4.1). Despite the high carbon powder content of the frc-MB-30, there was no serious difference observed in ΔE* and brightness. During the masterbatch formation of frc-MB-30, we observed that molten polymer composites exiting from the outlet head of the extruder was not smooth and we had difficulties to maintain the flow of the molten polymeric streams to cooling zone and cutter. It was evaulated that the reason for this was the low percentage of polymer used as matrix. Colour analysis results and our observations were coherent to each other and pointed out the over-loading of r-CPs at frc-MB-30. Therefore, it was decided to use the frc-MB-16.6 for the following studies.

Table 4.1 Colour properties of frc-MB test plates

Sample Code	r-CP Ratio (wt%)	L*	a*	b*	Brightness
frc-MB-16.6	16.6	27	0.1	-1.12	4.2
frc-MB-30	30	26	0.1	-0.91	4.3

4.3.2 Effect of Fully Recycled and Coloured Masterbatch (frc-MB) Composites Ratio on Colour Properties of Fully Recycled PET (frc-PET) Filaments

Colour properties of frc-PET filaments containing 0 wt%, 5 wt%, 10 wt%, and 20 wt% frc-MB-16.6 (Figure 4.6) were characterized from the obtained filaments. In order to simplify the naming of these composites, frc-PET filaments containing 0 wt%, 5 wt%, 10 wt%, and 20 wt% frc-MB-16.6 were refered as frc-PET-0, frc-PET-5, frc-PET-10, and frc-PET-20, respectively.

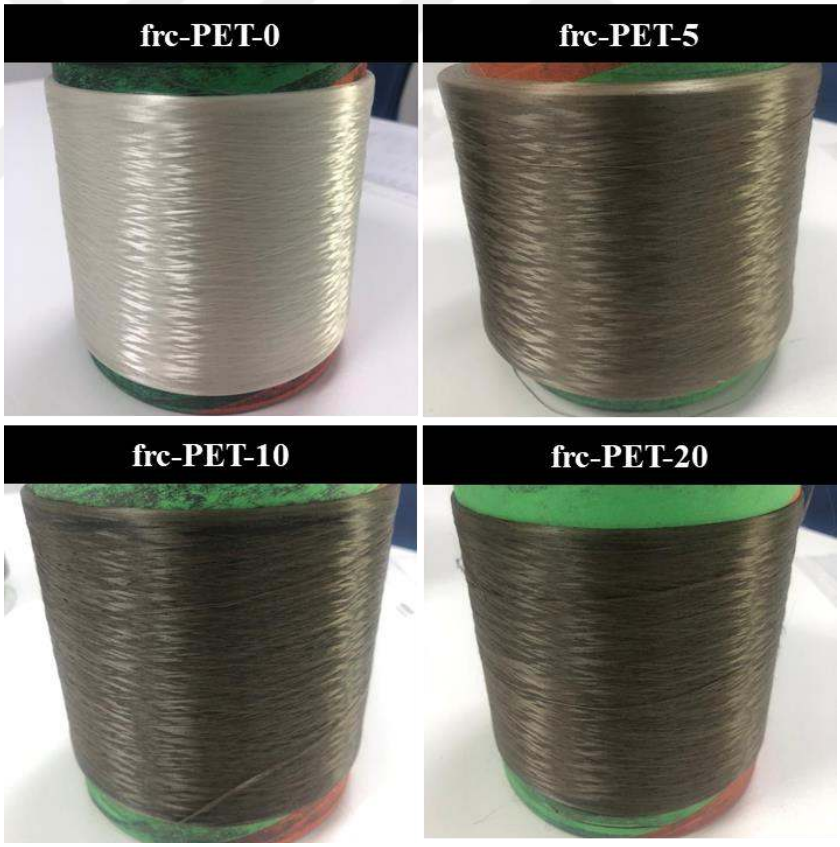

Figure 4.6 frc-PET filaments containing 0 wt%, 5 wt%, 10 wt%, and 20 wt% frc-MB-16.6

According to visual examination (Figure 4.6), the frc-PET-5 was darker than the frc-PET-0. Similarly, frc-PET-10 was more saturated than frc-PET-5. However, there

were not any difference observed for frc-PET-10 and frc-PET-20. In order to support visual evaluations colour measurements were also analyzed. The frc-PET-0 was used as the reference and colour measurements were taken against the reference. Colour strength difference, lightness differece (ΔL*), colour saturation difference (ΔC*), colour hue difference (ΔH*), total colour deviations (ΔE*), and brightness were obtained and given in Table 4.2.

Table 4.2 Colour properties of frc-PET filaments

Sample Code	frc-MB-16.6 (wt%)	r-CP Ratio (wt%)	Colour Stregth Diff.	ΔL*	ΔC*	ΔH*	ΔE*	Brightness Diff.
frc-PET-5	5	0.83	1893	-36.4	1.55	-3.08	13.81	14.3
frc-PET-10	10	1.66	4045	-17.22	0.72	-4.24	17.75	8.3
frc-PET-20	20	3.32	3930	-17.07	0.80	-4.26	17.61	7.9

It was found that the colour strength difference increased gradually from 1893 for frc-PET-5 to 4045 for frc-PET-10 and then remained almost the same at 3930 for frc-PET-20 (Table 4.2 and Figure 4.7). Lightness difference results (ΔL*) of frc-PET-10 (-17.22) and frc-PET-20 (-17.07) which found to be close to each other, were closer to zero more than that of frc-PET-5 (-36.4) (Table 4.2 and Figure 4.8). The closeness to zero means that the colour is darker (İpek, 2018).

A positive saturation difference (ΔC*) indicates that the sample has a higher saturation, and a negative saturation difference shows that the sample has a lower saturation. When the saturation difference is close to zero, it means that the sample is duller and grayer instead of being more pure and vivid (Xrite). When saturation difference (ΔC*) results were compared, it was found that frc-PET-5 (1.55) had higher saturation differences than frc-PET-10 (0.72) and frc-PET-20 (0.80) (Table 4.2 and Figure 4.9). It was expected to obtain lower numbers for higher r-CP loading which can change the colour saturation and make it duller. Brighthtness difference results also supported these findings since the lowest loading of r-CPs gave the highest brightness difference value meaning that brightness decreased compared to higher loading levels (Table 4.2 and Figure 4.10). When total colour deviation (ΔE*) results were compared, it was found that there was a very small difference (0.14) in between frc-PET-10 and frc-PET-20 (Table 4.2 and Figure

4.11). If this difference is smaller than one, it can be considered that there is no serious colour difference between samples (İpek, 2018). All the above mentioned results suggested us that the saturation of the filaments at r-CP ratio of 1.66 wt% was already occured.

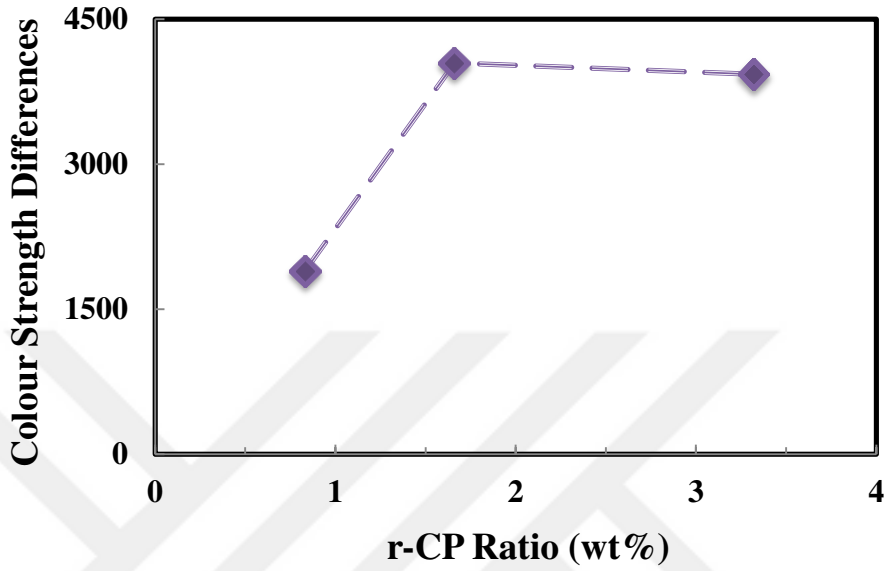

Figure 4.7 Colour strength difference of frc-PET filaments

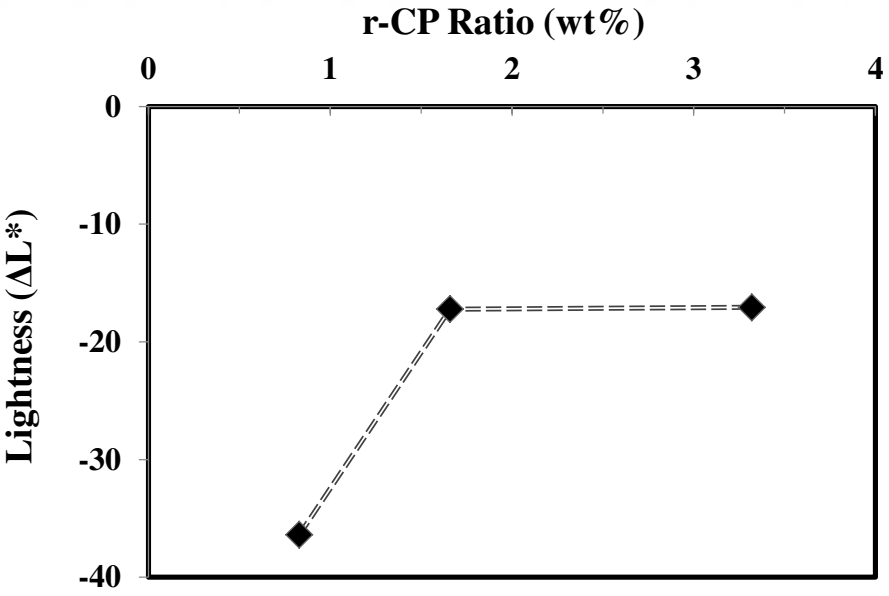

Figure 4.8 Lightness difference (ΔL*) of frc-PET filaments

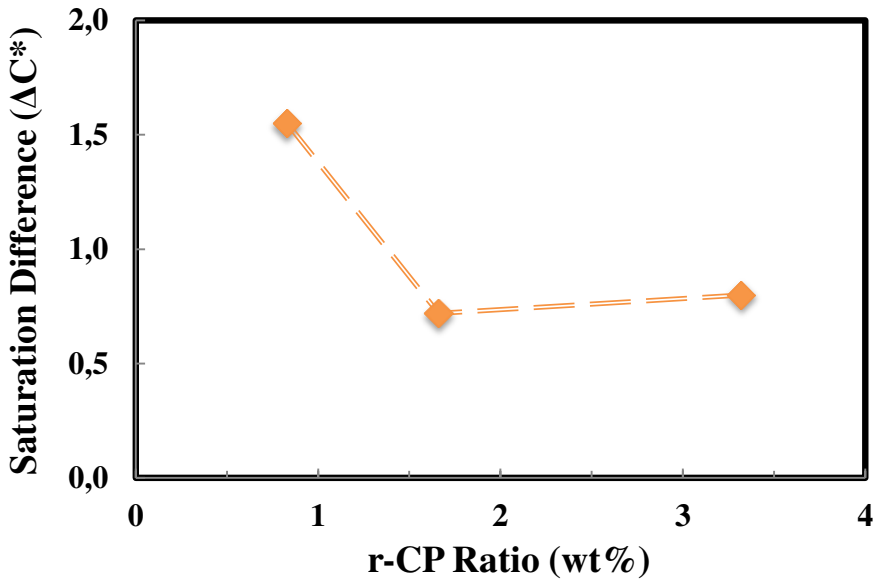

Figure 4.9 Colour saturation difference (ΔC*) of frc-PET filaments

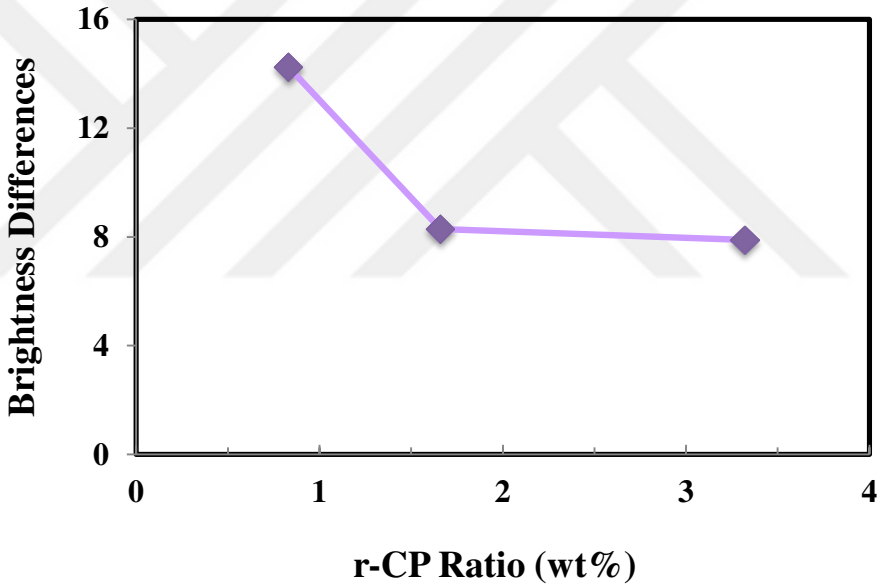

Figure 4.10 Brightness difference of frc-PET filaments

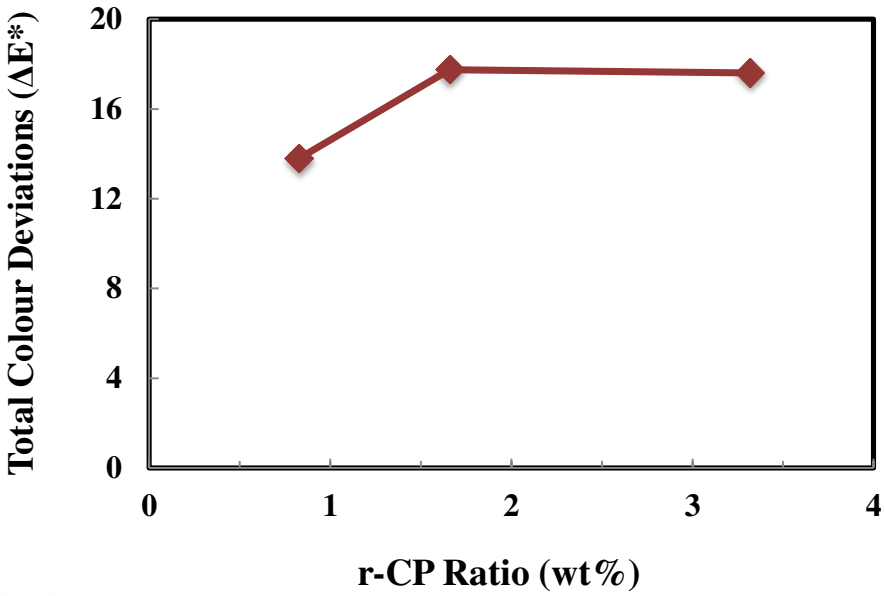

Figure 4.11 Total colour deviation (ΔE*) of frc-PET filaments

4.3.3 Effect of Fully Recycled and Coloured Masterbatch (frc-MB) Composites Ratio on Morphological Properties of Fully Recycled PET (frc-PET) Filaments

Cross-sectional (Figure 4.12) and longitudinal (Figure 4.13) views of frc-PET were taken to investigate the morphological changes. When cross-sectional images of the fibers were examined, large-diameter fibers were detected for all samples including the control sample (frc-PET-0). The reason for this was probably the drawing process in which some filaments were not drawn like others. When longitudional images of the fibers were examined, comparatively higher morphological disorders (thick places) were detected for the highest r-CP loaded sample of frc-PET-20 (Figure 4.13). The reason for this can be very high amount of r-CP loading which may induce r-CP particle clustering or aggregations in the polymeric matrix.

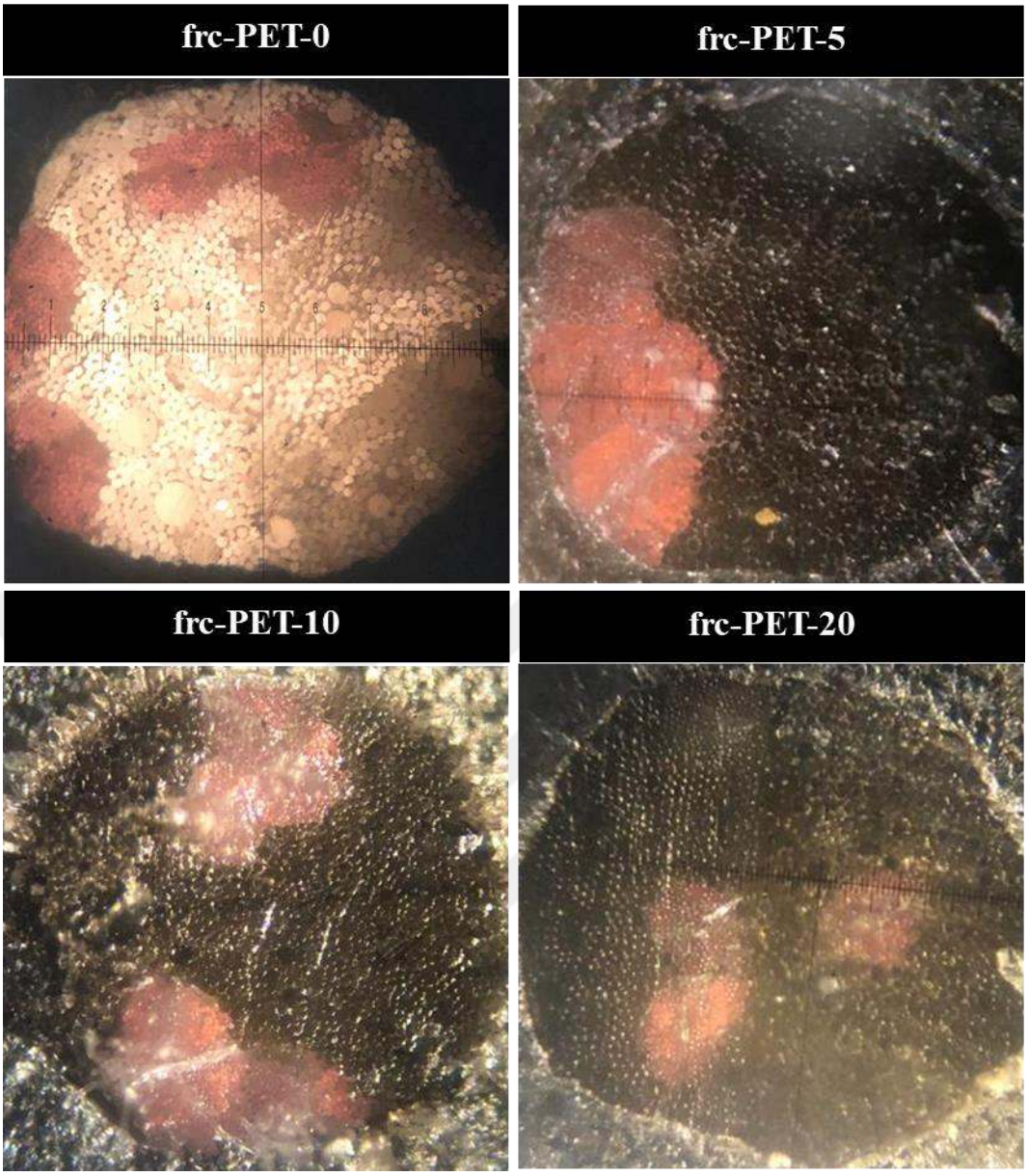

Figure 4.12 Cross-sectional views of frc-PET fibers

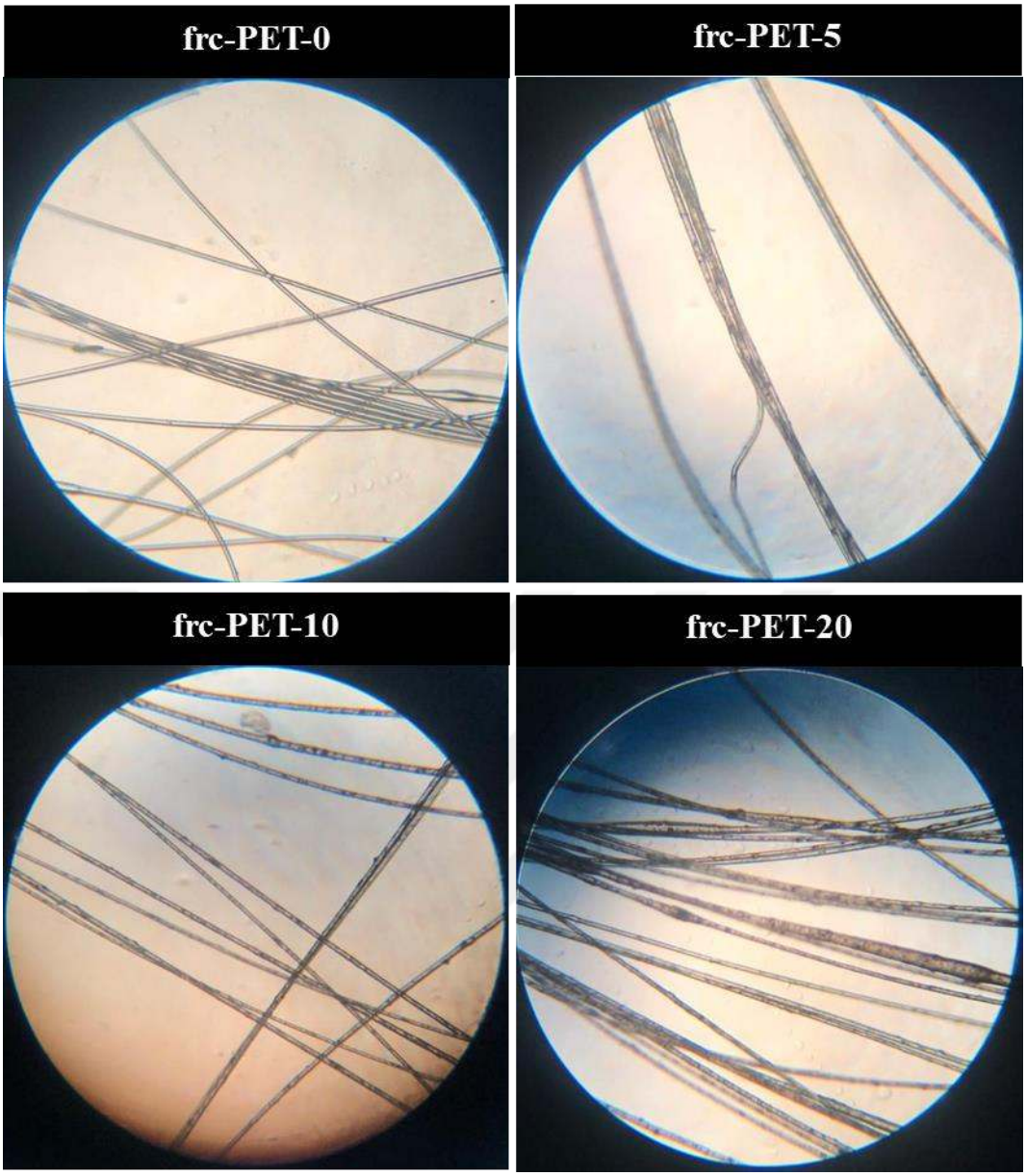

Figure 4.13 Longitudinal views of frc-PET fibers

4.3.4 Effect of Fully Recycled and Coloured Masterbatch (frc-MB) Composites Ratio on Mechanical Properties of Fully Recycled PET (frc-PET) Fibers

Tensile strength and elongation properties of the frc-PET fibers are given in Table 4.3. Our results showed that increasing the r-CP loading decreased the tensile strength and elongation values of the frc-PET fibers. Decreases in the tensile strength and elongation for 0.83 wt% and 1.66 wt% r-CP loaded samples were less but still existed. The worsening of these properties was more pronounced especially for the 3.32 wt% r-CP loaded frc-PET-20 fibers compared to control sample of frc-PET-0. This can be caused by the formation of r-CP aggregates and the increase of weakest spots along the fiber length. Also, particles added in PET polymer can cause a higher

concentration of stress which leads to the erlier failure of the PET fiber (Zhu et al., 2006). For this reason, the strength of the fibers decreased when a certain amount of additives added. Parallely, Jiang et al. (2016) also reported that when the masterbatch composite ratio increased, the strength of the fiber reduced.

Table 4.3 Linear densities and tensile mechanical properties of frc-PET fibers (standard deviation were given in between parenthesis)

Sample Code	frc-MB Ratio (wt%)	r-CP Ratio (wt%)	Linear Density (dtex)	Strength (cN/dtex)	Elongation (%)
frc-PET-0	0	0	3.4	2.57 (±0.24)	76.7 (±12.3)
frc-PET-5	5	0.83	3.6	2.52 (±0.24)	74.2 (±12.3)
frc-PET-10	10	1.66	3.5	2.40 (±0.17)	63.6 (±7.4)
frc-PET-20	20	3.32	3.1	1.91 (±0.37)	56.3 (±18.5)

CHAPTER 5

CONCLUSIONS

5.1 Investigation of the Formations of Useful By Products from Degraded Polyethylene Terephtalate (PET) Waste

In this study, formations of useful by products from degraded polyethylene terephtalate (PET) waste were investigated (Chapter 3). For this purpose, thermal, molecular, structural and chemical analyzes of the degraded PET (*d*-PET) were compared with virgin fiber grade PET, r-PET flake, and r-PET granules. According to obtained results, while r-PET flake had the highest intrinsic viscosity (IV) value of 0.81 dl/g, *d*-PET had the lowest IV value of 0.12 dl/g. The reason for this situation was explained as the effect of several recycling cycles under harsh conditions which affected the IV properties of polymers and decreased the IV of the polymers. The molecular weight (M_w) of the *d*-PET reduced dramatically when it was degraded. Because, *d*-PET was thermally processed many times in which the PET can be can be subjected to mechanical forces at high heat several times and can be oxidized during recycling if it was directly contacted to oxygen during recycling.

According to the thermal characterization, T_{mi} (initial melting temperature), T_{mp} (peak melting temperature), T_{mf} (final melting temperature), and T_g (glass transition temperature) temperatures of r-PET flakes, r-PET granule, and *d*-PET were lower than those of virgin fiber grade PET. This can be caused by several recycling cycles applied to PET before it degrades, since each recycling cycle can induce molecular chain damages. Also, *d*-PET had the lowest decomposition temperatures at 1%, 10%, and 50% weight reduction compared to other samples and total weight loss at 650 °C was the highest for. This can be caused by oxidation and various mechanical forces applied on the polymer at high heat during repeated recycling processes.

In experiments carried out with *d*-PET in atmospheric controlled high temperature furnaces an optimum process parameter was decided for the carbonization parameter. The optimum parameters was *d*-PET size of 10 mm, carbonization temperature (T_c) of 500 °C, heating rate (HR) of 10 °C/min, residence time in carbonization (t_r) of 1 h, gas flow rate (FR) of 100 L/h, and at N_2 atmosphere. When the material size increased, the amount of carbonized material increased and chemical yield decreased. This was due to the better dissipation of heat in small sized materials which induced easier gasification. Comparisions of O_2 and N_2 gas purgings revealed that O_2 partially induced oxidation and decomposition upon heating. 50 L/h N_2 gas flow rate gave more brownish by-products compared to 100 L/h N_2 gas flow rate. This was a sign of low blanketing with N_2 which was supposed to sweep away the O_2 from the heating zone of the furnace. Also, when the flow rate of the gas increased, the amount of carbonized material decreased and chemical yield increased. When the residence time in carbonization increased, the amount of carbonized material reduced and chemical yield increased. When total yields were compared, there were not significant differences between 1 hour and 2 hours. Increasing the heating rate increased both carbonized materials and chemical yields. It was probably caused by the higher rate of gasification at higher heating rate which took more time to reach the temperature of carbonization. The carbonization temperature increase did not have much effect on the amount of carbonized material obtained after carbonization. However, the amount of chemicals obtained after carbonization reduced when the temperature was raised from 500 °C to 600 °C.

Chemicals obtained from the *d*-PET carbonization process under N_2 atmosphere were found to be benzoic acid. According to Energy Dispersive - X-Ray Spectroscopy (ED-XRF) results, *d*-PET contained Si, Ca, Ti, S, Sb, Cl, K, Fe, P, Al, and Cu elements. Our results showed that the carbonization of the *d*-PET yielded higher carbon (C) percentage.

Carbonized materials obtained as a result of the carbonization process were milled at different milling time, different milling speeds and 2 different cycles. According to the results of this analysis, long milling time and high milling speeds reduced the particle size. Nano sized carbonized powders were successfully obtained at the end.

5.2 Investigation of Physical and Mechanical Properties of Fully Recycled filaments coloured with Carbon Powder Obtained from Degraded PET (*d*-PET)

In this study, physical and mechanical properties of fully recycled filaments coloured with carbon powder obtained from degraded PET (*d*-PET) were investigated (Chapter 4). In the literature, there was no study conducted on the pyrolysis or carbonization of the *d*-PET. Also, studies related with the pyrolysis of PET bottle wastes were limited and only focused on the formation of the oil or chemical, gas and carbonized materials (Sophonrat, 2019). These studies do not concentrate on the usage of these by-products in a useful medium. In this regard, our studies which were presented at Chapter 3 initially focused on the formation of the chemicals and carbonized materials from *d*-PET which is the waste of the waste. Therefore, we concentrated our efforts to use the recycled carbon powder (r-CP) obtained from the carbonized materials of *d*-PET in forming a fully recycled colour masterbatch (frc-MB) composites. This study also includes the formation of fully recycled and coloured PET fibers or filaments (frc-PET) containing only frc-MB composites and r-PET flakes. In this regard, initially ratios of the r-CP in frc-CMB were varied during the formation of frc-MBs and their colour analyses were carried out to determine the optimum r-CP addition. Secondly, frc-PET filaments were obtained at different loading of the frc-MB to r-PET matrix polymer. After frc-PET filaments were successfully formed, their colour and mechanical properties were investigated with respect to varying ratios of frc-MB in fibers.

Our colour daviations results of test plates of frc-MBs showed that there was no serious colour difference between test plates of frc-MB composites containing 16.6 wt% (frc-MB-16.6) and frc-MB composites containing 30 wt% (frc-MB-30). Also, brightness of frc-MB-16.6 was found to be very close to that of frc-MB-30.

The investigation of the effect of frc-MB composites ratio on colour properties revealed that the colour strength difference increased gradually for frc-PET filaments containing 5 wt% (frc-PET-5) to frc-PET filaments containing 10 wt% (frc-PET-10) and then remained almost the same for frc-PET filaments containing 0 wt% (frc-PET-20). Lightness difference results (ΔL^*) of frc-PET-10 and frc-PET-20 which found to be close to each other, were closer to zero more than that of frc-PET-5. When saturation difference (ΔC^*) results were compared, it was found that frc-PET-

5 had higher saturation differences than frc-PET-10 and frc-PET-20. It was expected to obtain lower numbers for higher r-CP loading which can change the colour saturation and make it duller. Brighthtness difference results also supported these findings since the lowest loading of r-CPs gave the highest brightness difference value meaning that brightness decreased compared to higher loading levels. According to the total colour deviation (ΔE*) results, it was found that there was a very small difference in between frc-PET-10 and frc-PET-20. The colour analyses results showed that, the saturation of the filaments at r-CP ratio of 1.66 wt% was already occurred.

After the investigation of the effect of frc-MB composites ratio on morphological properties of frc-PET fibers, large-diameter fibers were detected for all samples including the control sample (frc-PET-0). The reason for this was probably the drawing process in which some filaments were not drawn like other samples. When longitudional images of the fibers were examined, comparatively higher morphological disorders (thick places) were detected for the highest r-CP loaded sample of frc-PET-20. The reason for this can be very high amount of r-CP loading which may induce r-CP particle clustering or aggregations in the polymeric matrix.

The effect of adding varying amounts of r-CP on tensile mechanical properties of frc-PET fibers was also investigated. Our results showed that increasing the r-CP loading decreased the tensile strength and elongation values of the frc-PET fibers. Decreases in the tensile strength and elongation for 0.83 wt% and 1.66 wt% r-CP loaded samples were less but still existed. The worsening of these properties was more pronounced especially for the 3.32 wt% r-CP loaded frc-PET-20 fibers compared to control sample of frc-PET-0. This can be caused by the formation of more r-CP aggregates and the increase of weakest spots along the fiber length at frc-PET-20 fibers.

In conclusion, we successfully developed and characterized fully recycled and coloured masterbatches and filaments with only using recycled and degraded PET materials and products.

REFERENCES

Acar, K. (2009). Fluoresans Renkler İçeren Boyama Reçetesi Tahmin Algoritmalarında Başarının Artırılmasına Yönelik Yeni Bir Yöntem. (Doktora Tezi). Marmara Üniversitesi, İstanbul.

Achilias, D. S., Redhwi, H. H., Siddiqui, M. N., Nikolaidis, A. K., Bikiaris, D. N., & Karayannidis, G. P. (2010). Glycolytic Depolymerization of PET Waste in a Microwave Reactor, *Journal of Applied Polymer Science*. **118(5)**, 3066-3073.

Açıkgöz, Ç. (2001). Keten Tohumunun Alternatif Enerji Kaynağı Olarak İncelenmesi. (Doktora Tezi). Anadolu Üniversitesi, Eskişehir.

Al-Sabagh, A. M., Yehia, F. Z., Eshaq, G., Rabie, A. M., & ElMetwally, A. E. (2016), Greener Routes for Recycling of Polyethylene Terephthalate. *Egyptian Journal of Petroleum*. **25(1)**, 53-64.

Al-Salem, S. M., Lettieri, P., & Baeyens, J. (2009). Recycling and Recovery Routes of Plastic Solid Waste (PSW): A Review, *Waste Management*. **29(10)**, 2625-2643.

Altun, S. (2012). Prediction of Textile Waste Profile and Recycling Opportunities in Turk, *Fibres & Textiles in Eastern Europe*. 20, **5 (94)**: 16-20.

Altun, Ş., & Ulcay, Y. (2003). Polietilen Teraftalat (PET) Polimerinde Ekstruder İçerisinde Önemli Olan Bozunmalar, *Pamukkale Üniversitesi Mühendislik Bilimleri Dergisi*. **9(1)**, 89-93.

ASTM D3265-17a. (2017) Standard Test Method for Carbon Black—Tint Strength, ASTM International. West Conshohocken, PA, www.astm.org.

ASTM D3418-15, (2015) Standard Test Method for Transition Temperatures and Enthalpies of Fusion and Crystallization of Polymers by Differential Scanning Calorimetry, ASTM International. West Conshohocken, PA, www.astm.org.

ASTM D3822 / D3822M-14 (2020), Standard Test Method for Tensile Properties of Single Textile Fibers, ASTM International. West Conshohocken, PA, www.astm.org.

ASTM D4603-18, (2018) Standard Test Method for Determining Inherent Viscosity of Poly(Ethylene Terephthalate) (PET) by Glass Capillary Viscometer, ASTM International. West Conshohocken, PA, www.astm.org.

ASTM E1252-98(2013)e1, Standard Practice for General Techniques for Obtaining Infrared Spectra for Qualitative Analysis, ASTM International. West Conshohocken, PA, www.astm.org.

ASTM E1508-12a(2019), Standard Guide for Quantitative Analysis by Energy-Dispersive Spectroscopy, ASTM International, West Conshohocken, PA, 2019, www.astm.org.

ASTM E2550-17, (2017) Standard Test Method for Thermal Stability by Thermogravimetry, ASTM International, West Conshohocken, PA, www.astm.org.

Awaja, F., & Pavel, D. (2005). Recycling of PET, *European Polymer Journal*. **41(7)**, 1453-1477.

Aydın, H. (2004). PVC Üretimi ve Katkı Maddeleri. (Bitirme Tezi). Osmangazi Üniversitesi, Eskişehir.

Bratek, W., Świątkowski, A., Pakuła, M., Biniak, S., Bystrzejewski, M., & Szmigielski, R. (2013). Characteristics of Activated Carbon Prepared from Waste PET by Carbon Dioxide Activation, *Journal of Analytical and Applied Pyrolysis*. **100**, 192-198.

Brydson, J. A. (1999). *Plastics materials*, Elsevier. Oxford: Butterworth-Heinemann.

Büyükaslan, E., Jevsnik, S., & Kalaoglu, F. (2015). A Sustainable Approach to Collect Post-Consumer Textile Waste in Developing Countries, *Marmara Fen Bilimleri Dergisi*. **27**, 107-111.

Camlibel, N. O. (Ed.). (2018). *Polyester: Production, Characterization and Innovative Applications*. BoD–Books on Demand.

Chattopadhyay, J., Pathak, T. S., Srivastava, R., & Singh, A. C. (2016). Catalytic Co-pyrolysis of Paper Biomass and Plastic Mixtures (HDPE (High Density Polyethylene), PP (Polypropylene) and PET (Polyethylene Terephthalate)) and Product Analysis, *Energy.* **103**, 513-521.

Coats, A. W., & Redfern, J. P. (1963). Thermogravimetric Analysis. A review, *Analyst*. **88(1053)**, 906-924.

Çelikgöğüs, Ç. Y., & Karaduman, A. T. D. (2010). *Polistiren atıkların ısıl-katalitik pirolizi* (Doktora Tezi), Ankara Üniversitesi, Ankara.

Çepelioğullar, Ö., & Pütün, A. E. (2013). Utilization of Two Different Types of Plastic Wastes from Daily and Industrial Life, *Journal of Selcuk University Natural and Applied Science*. **2(2)**, 694-706.

Çuhadar, Ç. (2005). Production and Characterization of Activated Carbon from Hazelnut Shell and Hazelnut Husk. (Master's Thesis). Middle East Technical University, Ankara.

Doğan-Sağlamtimur, N., Bilgil, A., Çalişkan, Ö., Vural, T., Aykanat, T., & Yolcu, F. (2017). Ömrünü Tamamlamiş Lastik ve Polietilen Tereftalat (PET) Şişe Atiklarinin Pirolizinin Tasarlanan Yeni Bir Reaktörde Kiyaslanmasi, *Niğde Ömer Halisdemir Üniversitesi Mühendislik Bilimleri Dergisi*. **6(1)**, 21-27.

Esfandiari, A., Kaghazchi, T., & Soleimani, M. (2012). Preparation and Evaluation of Activated Carbons Obtained by Physical Activation of Polyethyleneterephthalate (PET) wastes, *Journal of the Taiwan Institute of*

Chemical Engineers. **43(4)**, 631-637.

Eyerer, P. (2010). *Plastics: Classification, characterization, and economic data, In Polymers-Opportunities and Risks I.* Springer, Berlin, Heidelberg.

Faix, O. (1992). *Fourier transform infrared spectroscopy, In Methods in lignin chemistry*. Springer, Berlin, Heidelberg.

Foisal, A. B. M. (2017). Spectrophotometric Evaluation of Re-dyed Polyester Yarn, *SEU Journal of Science and Engineering.* **(12)**, (26-29).

Heikkinen, J. M., Hordijk, J. D., de Jong, W., & Spliethoff, H. (2004). Thermogravimetry as a Tool to Classify Waste Components to be used for Energy Generation, *Journal of Analytical and Applied Pyrolysis*. **71(2)**, 883-900.

Hoornweg, D., & Bhada-Tata, P. (2012). What a Waste: A Global Review of Solid Waste Management. *Urban Development Series Knowledge Papers,* (15).

İlkılıç, C., & Aydın, H. (2011). Fuel Production From Waste Vehicle Tires by Catalytic Pyrolysis and its application in a Diesel Engine, *Fuel Processing Technology*. **92(5)**, 1129-1135.

İpek, F. (2018). Tekstil renklerinin görsel renk yönetim sistemi ile değerlendirilmesi. (Yüksek Lisans Tezi). Pamukkale Üniversitesi, Denizli

Jankauskaite, V., Macijauskas, G., & Lygaitis, R. (2008). Polyethylene Terephthalate Waste Recycling and Application Possibilities: A Review. *Mater Sci (Medžiagotyra)*, **14(2)**, 119-127.

Jiang, Z., Ma, P., Guo, Z., Jia, Z., Pu, C., & Xiao, C. (2016). Effect of Coupling Agent on structure and Properties of Micro–Nano Composite Fibers Based on PET, *Journal of Applied Polymer Science.* **133(34)**.

Jiang, Z., Guo, Z., Zhang, Z., Qi, Y., Pu, C., Wang, Q., & Xiao, C. (2019). Preparation and Properties of Bottle-Recycled Polyethylene Terephthalate (PET) Filaments, *Textile Research Journal.* **89(7)**, 1207-1214.

Jung, M. R., Horgen, F. D., Orski, S. V., Rodriguez, V., Beers, K. L., Balazs, G. H., & Lynch, J. M. (2018). Validation of ATR FT-IR to Identify Polymers of Plastic Marine Debris, Including those Ingested by Marine Organisms, *Marine Pollution Bulletin*. **127,** 704-716.

Kalnicky, D. J., & Singhvi, R. (2001). Field Portable XRF Analysis of Environmental Samples, *Journal of hazardous materials*. **83(1-2)**, 93-122.

Kaplan Z., et al. (2019) "Tekstil Sektöründe Geri Dönüşüm ve Sürdürülebilirlik." *17. National 3.International the Recent Progress Symposium on Textile Technology and Chemistry.*129-131.

Kaplan, Z. "Geri Dönüşüm Polyester Malzemeden Oluşturulmuş Tamamıyla Geri Dönüştürülebilir Yumuşak Tuşeli ve Yüksek Dökümlü Kumaş ve Üretim Yöntemi." TR Patent No: 2020/02147. 13 Feb. 2020.

Kar, Y. (2011). Catalytic pyrolysis of car tire waste using expanded perlite, *Waste Management*. **31(8)**, 1772-1782.

Kar, Y. (2008). Çörekotu (Nigella sativa L.) Tohumunun Doğal Antioksidan ve Alternatif Enerji Kaynağı Olarak Incelenmesi (Doktora Tezi). Selçuk Üniversitesi, Konya.

Karayannidis, G. P., & Achilias, D. S. (2007). Chemical Recycling of Poly (Ethylene Terephthalate), *Macromolecular Materials and Engineering*. **292(2)**, 128-146.

Kaza, Silpa, et al. (2018) "What a waste 2.0: A Global Snapshot of Solid Waste Management to 2050." *The World Bank*.

Lee, J., Lee, T., Tsang, Y. F., Oh, J. I., & Kwon, E. E. (2017). Enhanced Energy Recovery from Polyethylene Terephthalate via Pyrolysis in CO2 Atmosphere While Suppressing Acidic Chemical Species, *Energy Conversion and Management*, **148,** 456-460.

Lindström, F. (2018). Chemical and Physical Changes in PET Fibres due to Exhaust Dyeing: Issues in Thermo-Mechanical Recycling of Dyed PET Textiles. (Master's Thesis). University of Boras, Sweden.

Liu, X., & Yu, W. (2006). Evaluating the Thermal Stability of High Performance Fibers by TGA, *Journal of Applied Polymer Science*. **99(3)**, 937-944.

Mansfield, E., Tyner, K. M., Poling, C. M., & Blacklock, J. L. (2014). Determination of Nanoparticle Surface Coatings and Nanoparticle Purity Using Microscale Thermogravimetric Analysis, *Analytical Chemistry*. **86(3)**, 1478-1484.

Loganathan, S., Valapa, R. B., Mishra, R. K., Pugazhenthi, G., & Thomas, S. (2017). *Thermogravimetric Analysis for Characterization of Nanomaterials. In Thermal and Rheological Measurement Techniques for Nanomaterials Characterization.* Elsevier.

Malik, N., Kumar, P., Shrivastava, S., & Ghosh, S. B. (2017). An Overview on PET Waste Recycling for Application in Packaging, *International Journal of Plastics Technology*. **21(1)**, 1-24.

Mangut, M., and Nevin K.. (2008) *Tekstil lifleri*. Ekin Kitabevi.

Master Organic Chemistry. Intl: www.masterorganicchemistry.com. 09.01.2020.

SEM-EDX. Materials Evaluation and Engineering. Intl.: www.mee-inc.com., 07.12.2020.

McGuire, R. G. (1992). Reporting of Objective Color Measurements, *HortScience*. *27*(12), 1254-1255.

Navarro, R., Ferrandiz, S., Lopez, J., & Segui, V. J. (2008). The Influence of Polyethylene in the Mechanical Recycling of Polyethylene Terephtalate, *Journal of Materials Processing Technology*. *195*(1-3), 110-116.

Nikles, D. E., & Farahat, M. S. (2005). New Motivation for the Depolymerization Products Derived from Poly (Ethylene Terephthalate)(PET) waste: A review, *Macromolecular Materials and Engineering*. *290*(1), 13-30.

Niksiar, A., Faramarzi, A. H., & Sohrabi, M. (2015). Kinetic Study of Polyethylene Terephthalate (PET) Pyrolysis in a Spouted Bed Reactor. *Journal of Analytical and Applied Pyrolysis*, **113**, 419-425.

Oromiehie, A., & Mamizadeh, A. (2004). Recycling PET Beverage Bottles and Improving Properties, *Polymer International*. **53(6)**, 728-732.

Pivnenko, K., Eriksen, M. K., Martín-Fernández, J. A., Eriksson, E., & Astrup, T. F. (2016). Recycling of Plastic Waste: Presence of Phthalates in Plastics from Households and Industry, *Waste Management*. **54**, 44-52.

Sanches, N. B., Dias, M. L., & Pacheco, E. B. A. V. (2005). Comparative Techniques for Molecular Weight Evaluation of Poly (Ethylene Terephthalate)(PET), *Polymer Testing*. ***24*(6)**, 688-693.

Scott, D. S., Czernik, S. R., Piskorz, J., & Radlein, D. S. A. (1990). Fast Pyrolysis of Plastic Wastes. *Energy & Fuels*, **4(4)**, 407-411.

Sevencan, F., & Vaizoğlu, S. A. (2007). PET ve Geri Dönüşümü. *TSK Koruyucu Hekimlik Bülteni*, *6*(4), 307-312.

Shah, J., Jan, M. R., & Mabood, F. (2009). Recovery of Value-Added Products from the Catalytic Pyrolysis of Waste Tyre, *Energy Conversion and Management*. *50*(4), 991-994.

S Sharuddin, S. D. A., Abnisa, F., Daud, W. M. A. W., & Aroua, M. K. (2016). A Review on Pyrolysis of Plastic Wastes. *Energy Conversion and Management*, ***115***, 308-326.

Starlinger. recoStar Product Line. Intl.: www.starlinger.com, 21.11.2020.

Statista. Distribution of Polyethylene Terephthalate (PET) Consumption Worldwide in 2016, by End-use. Intl.: www.statista.com. 21.11.2020.

Sophonrat, N. (2019). Pyrolysis of Mixed Plastics and Paper to Produce Fuels and Other Chemicals (Doctoral Dissertation), KTH Royal Institute of Technology,

Sweden.

Sulyman, M., Haponiuk, J., & Formela, K. (2016). Utilization of Recycled Polyethylene Terephthalate (PET) in Engineering Materials: A Review. *International Journal of Environmental Science and Development*, **7(2)**, 100.

Tayyar, A. E., & Üstün, S. (2010). Geri Kazanılmış PET'in Kullanımı, *Pamukkale University Journal of Engineering Sciences*. **16(1).**

Terakado, O., & Hirasawa, M. (2005). Effect of Metal Oxides on the Pyrolysis Residues Of Poly (Ethylene Terephthalate): Formation of Carbonaceous Submicron, Nano-Scale Filaments and Mesoporous Compounds, *Journal of Analytical and Applied Pyrolysis.* **73(2)**, 248-256.

Green Solutions LLC, Thurston County Waste Composition Study (2008 – 2009), South Prairie, Washington.

Tortora, Phylis G., and Billie J. Collier. (1997). *Understanding textiles*. Prentice-Hall, Englewood Cliffs, New Jersey, United States.

Uzun, B. B., & Yaman, E. (2014). Atık Lastiklerin Katalitik Pirolizi Üzerine Bir İnceleme. *ISEM2014*, 995-1004.

Xrite. Tolerancing Part 3: Color Space vs. Color Tolerance, Intl.: www.xrite.com.11.01.2021.

Yeşil, Y. (2010). Melanj Elyaf Karışımlarında Renk Değerlerinin Yeni Bir Algoritma Geliştirilerek Tahmin Edilmesi. (Doktora Tezi), Çukurova Üniveristesi, Adana.

Zhu, Y. G., Li, Z. Q., Zhang, D., & Tanimoto, T. (2006). PET/SiO2 Nanocomposites Prepared by Cryomilling. *Journal of Polymer Science Part B: Polymer Physics*, **44(8)**, 1161-1167.